PROBE OXIDATIVE DAMAGE IN DNA CHARGE TRANSFR PROCESS

A Thesis
Presented to
The Academic Faculty

By

Huachuan Cao

In Partial Fulfillment
Of the Requirements for the Degree
Doctor of Philosophy in Chemistry

Georgia Institute of Technology

December, 2004

PROBE OXIDATIVE DAMAGE IN DNA CHARGE TRANSFR PROCESS

Approved by:

Dr. Gary B. Schuster, Chairman
School of Chemistry & Biochemistry
Georgia Institute of Technology

Dr. Suzanne B. Shuker
School of Chemistry & Biochemistry
Georgia Institute of Technology

Dr. Nicolas V. Hud
School of Chemistryl & Biochemistry
Georgia Institute of Technology

Dr. Uzi Landman
School of Physics
Georgia Institute of Technology

Dr. Andrew Lyon
School of Chemistry & Biochemistry
Georgia Institute of Technology

Date Approved: December 2004

This thesis is dedicated to

my beloved grandmother, parents and sister

for their everlasting love,

inspiration,

support,

and for always being there for me.

Words alone can not express the appreciation that I hold for you.

ACKNOWLEDGEMENT

The research outlined in the thesis would not be possible without help and inspiration from many people at Georgia Tech. First and foremost, I would like to extend a cordially thank you to Dr. Gary B. Schuster for giving me the opportunity to explore an exciting field. He gave tremendous support and advice on my study and research during years in this group. Additionally, his passion and earnest for chemistry and science is an inspiration to all, especially me. I would also like to thank past and present members in Schuster Group, a group of intelligent and motivated people, for helping me carry out my experiments and teaching me the things I did not know before. Special thanks to Dr. Valerie Sartor for her generous help in learning basic PAGE experimental skill; Dr Ibrahim Abodu, Dr. Anthony Dotse and Dr. Jie Li for sharing their expertise in overcoming the problem encountered in my first organic synthesis project, which kept me on the ground when I was driven insane; Dr. Edna Boone for her patient and generous help in PAGE and instruments. Her diligence set a high bar to push me work harder and struggle through the graduate school; Dr Chusheng Liu for the constructive discussion and insightful advice for life time goal and occasionally inviting me to his family dinner and taking a bite of those delicious dumplings homemade by his wife; Dr. Nadia Boguslavsky and Dr Sriram Kanvah for oligonucleotide synthesis; All the other individuals in the group made my graduate life enjoyable and provided me with scientific clarity on numerous occasions. Despite their excellent tutelage, I could not be where I am now.

My current and previous thesis committee should also be acknowledged. Dr. Kathleen Seley and Dr. Laren Tolbert served on my Master Thesis committee. They are of great help to revise my first “achievement” in English writing and guide for Ph.D. project. I also extend my appreciation to Dr. Nicolas Hud, Dr. Donald Doyle and Dr. Suzanne Shuker and Dr. Uzi Landman for donating their time and effort in serving on my PhD thesis committee, providing suggestions and trying to make me a better scientist. They all had a hand in helping me reach this point. I thank them all for their great advices.

During my time at the institute, I have befriended a great many people. A number of theses individuals have guided me through numerous emotional and scientific jungles. However, I will only highlight some here. Zhiguo Ren and Yu Li are the great friends I have known since my first year in chemistry department. They are awesome partners to get through those restless nights before midterm, literature exams, projects’ due date and finals and gave me endless support when I was frustrated with the stresses from classes, projects and research and when I suffered from endless wait for my visa in China. Hao Wu, Zhongtang Cai and Eunjoo Oh were great roommates to kill the time and share the gourmet together, hence permitting me to forget about science every now and then. I also want to express my appreciation to Dr. Haiying Li for his support and encouragement. My gratitude also extends to Lezah Roberts, Thabby Ndlebe, Nathan Schlientz, Gozde Guler, Chiko Umeweni, Rochelle Fisher, Dr. Abraham Joy and Dr. Sriram Kanvah who are sincere friends to share not only researches but also the fun of life in this country with dramatic different cultures. They were great friends with whom to hang out, explore Atlanta and as emotional and scientific soundboards. Additional thanks are extended to

Rick Redic, Prolay Das and Frank Onyemauwa. All pushed me toward graduation in various ways.

Another anchor throughout my graduate career was my family. The unconditional love of my mother, father, and sister was the momentum for my flagging emotional journey when I did not feel like continuing at Georgia Tech and was feeling discouraged. I would not have made it this far without you all.

TABLE OF CONTENTS

LIST OF TABLES

PART I

PART II

LIST OF FIGURES

PART I

APPENDIX A

APPENDIX B

LIST OF SYMBOLS AND ABRREVIATIONS

A	Adenine
AQ	Anthraquinone
AQ26DS	Anthraquinone 2, 6-disulfonate
BET	Back electron transfer
Boc-ON	2-(tert-butoxycarbonyloxyimino)-2-phenylacetonitrile
C	Cytosine
CD	Circular dichroism
C_2GlySp^{4+}	N', N'-Diethyl(sperminecarbonyl)glycinamide, hydrofluoroacetate
C_8GlySp^{4+}	N', N'-Dioctyl(sperminecarbonyl)glycinamide, hydrofluoroacetate
$C_{18}GlySp^{4+}$	N', N'-Dioctadecyl(sperminecarbonyl)glycinamide, hydrofluoroacetate
CT DNA	Calf-thymus DNA
DCC	Dicyclohexylcarbodiimide
DCU	Dicyclohexylurea
DMT	Dimethoxytrityl
DNA	Deoxyribonucleic acid
EDTA	Ethylenediaminetetraacetic acid
EDC	1-ethyl-3-(3-dimethylaminopropyl)carbodiimide
EDU	1-ethyl-3-(3-dimethylaminopropyl)urea
ESI-MS	Electrospray ionization mass spectrometry
FAB-MS	Fast atomic bombardment mass spectrometry

FPG	Formamidopyrimidine glycosolase
G	Guanine
G_m	8-Methylguanine, 8-MeG
G_{br}	8-Bromoguanine, 8-BrG
IE	Ion Exchange
IP	Ionization Potential
K_{BET}	Back electron transfer rate constant
K_{hop}	Charge hopping/migrating rate constant
K_{trap}	Charge trapping/quenching rate constant
MALDI-TOF	Matrix-assisted laser desporption ionization time-of-flight mass spectroscopy
NMR	Nuclear magnetic resonance
OD	Optical density
8-oxoG	7,8-Dihydro-8-oxodeoxyguanosine
PAGE	Polyacrylamide gel electrophoresis
T	Thymine
T_m	Melting temperature
TEAA	Triethylammonium acetate
UV-vis	Ultraviolet-visible spectroscopy

SUMMARY

As a hydrophilic biopolymer, a DNA molecule is surrounded by water molecules in aqueous solution. The charge hopping mechanism indicates the competition between cation quenching by water molecules and cation migration and trapping at guanine bases partially determines the distance and efficiency of charge transport in DNA. Lipid, with hydrophilic head group and hydrophobic tail group, can effectively bind DNA to induce hydrophobic environment around the DNA helix and exclude or reduce the water contact with bases in the DNA duplex. Therefore, the effect of water molecules on charge transport can be studied by comparison between nature DNA and DNA-lipid complexes. We synthesized several DNA-binding lipids in this research. The preliminary results show no significant difference in GG damage between pure DNA and DNA- N'-N'-dioctylglycinamide complex which is attribute to no or little association between N'-N'-dioctylglycinamide and DNA under UV irradiation conditions indicated by fluorescence quenching experiment.

We further synthesized N', N'-Diethyl(sperminecarbonyl)glycinamide, hydrofluoroacetate (C_2GlySp^{4+}) N', N'-Dioctadecyl(sperminecarbonyl)glycinamide, hydrofluoroacetate (C_8GlySp^{4+}) and N', N'-Dioctyl(sperminecarbonyl)glycinamide, hydrofluoroacetate ($C_{18}GlySp^{4+}$) which posses improved DNA binding affinity due to their multi-charged spermine head-groups. Among those, C_8GlySp^{4+} and C_2GlySp^{4+} can form stable complex with DNA oligomer in aqueous solution, characterized by time dependent UV and CD spectra. C_2GlySp^{4+} showed the similar inhibition on oxidative damage in GG steps as spermine while C_8GlySp^{4+} showed much more significant effect at the same concentration. All the lipids bear the same binding headgroup, spermine. It

has been shown that the major driving force for the binding is electrostatic interaction. Consequently all lipids and spermine should afford the similar binding affinity towards DNA duplex, we attributed the observation to the longer length of dialkyl group in C_8GlySp^{4+}, which can more effectively shield the DNA duplex from the water molecules than either spermine or C_2GlySp^{4+}. A kinetic model based on phonon-assist polaron hopping mechanism was proposed to rationalize the experimental results.

The finding may give insight on the protection of DNA oxidative damage by reducing the access of the water molecule to DNA duplex. The final results may have potential impact on the application of DNA as conducting biopolymer and protection of DNA in biological system.

The mechanism of long range charge transfer in DNA has be studied extensively from the view point of mutagenesis and carcinogenesis induced by carcinogenic agents, ionizing radiation, photosensitization with endogenous photosensitizes and high-intensity laser irradiation. Guanine is primarily oxidized base among DNA nucleobases due to its low oxidation potential, compared to C, A and T. One-electron oxidation in various systems creates a positive charged hole in DNA, which migrates through the DNA π stack and ends up at a guanine (G) base. Many studies have shown that the reaction of a guanine radical cation with water or active oxygen species occurs primarily at G_n (n=2, 3) sequences. Noticeably 5'-G of 5'-GG-3' sequences is selectively oxidized in B-form DNA in reaction systems using a variety of oxidizing agents. Recently experimental and theoretical studies have attributed this effect to the low oxidation potential of G_n (n=2, 3) sequences.

In second part of this research work, we showed that substitution of G with G_m in DNA sequence traps the migration of radical cation, while substitution with G_{br}, with an E_{ox} above G, does not. However, both G_m and G_{br} affect the relative reactivity of the guanine in G_n steps. Furthermore, the smaller effect of G_3 sequence on efficiency of oxidative cleavage than G_m indicates the contradiction with theoretically calculated E_{ox} results, which does not consider the flexible structure of DNA in aqueous solution and counter ion effects. Those calculations are questionable because non-canonical structures and surrounding environments of DNA can contribute significantly to the modulation of charge migration in DNA. All these finding shows that the efficiency of charge transfer is controlled by E_{ox} of the base and that steric effect play an important role in determining the relative reactivity of G in G_n sequences.

CHATER I

INTRODUCTION

The mechanism of long range charge transfer in DNA has be studied extensively from the view point of mutagenesis and carcinogenesis induced by carcinogenic agents, ionizing radiation, photosensitization with endogenous photosensitizes and high-intensity laser irradiation. Guanine is primarily oxidized base among DNA nucleobases due to its low oxidation potential, compared to C, A and T. One-electron oxidation in various systems creates a positive charged hole in DNA, which migrates through the DNA π stack via multi-step hops in long distance and ends up at guanine (G) bases. Many studies have shown that the reaction of a guanine radical cation with water or active oxygen species occurs primarily at G_n (n=2, 3) sequences. Noticeably 5'-G of 5'-GG-3' sequences is selectively oxidized in B-form DNA in reaction systems using a variety of oxidizing agents.

In first part of thesis, we study the DNA radical cation quenching reaction with water, a factor that governs oxidative damage in DNA charge transport process, by inducing hydrophobic environment around DNA upon binding of synthetic lipid compounds. In second part of research work, we substituted G in XG (X= G, A, T) and GGG sequence with G_m and G_{br} whose oxidation potential brackets that of normal G to investigate the thermodynamic and steric effect on charge transport and trapping in DNA. Those studies may help to reveal the crucial factors controlling oxidative damage pattern in DNA and afford a possible approach to protect such adverse effect in charge transport.

PART I

STUDY ON CHARGE TRANSFER IN DNA-LIPID COMPLEXES

CHAPTER II

INTRODUCTION AND BACKGROUND

DNA π Stack Helix Structure

In order to understand the charge transfer in DNA, the fundamental knowledge about DNA duplex helix structure is essential. DNA, deoxyribonucleic acid, is the carrier of human's genetic information. It is a very stable polymeric bio-molecule, consisting of nucleotide monomer units linked together by phosphate backbone. Four different bases, adenine (A), guanine (G), cytosine (C) and thymine (T), can form base pair through hydrogen bonding, which holds the DNA duplex and forms double helix structure.

Each nucleotide has common structure of a sugar (deoxyribose) and one phosphate groups (Figure I-1). The difference between nucleotide lies in the nitrogenous heterocyclic bases. Adenine and guanine are pyrimidines while thymine and cytosine are purines. The glycosidic link is between carbon atom 1 of the sugar and nitrogen atom at the position 9 and 1, respectively, of the purine and pyrimidine rings. The linkage is β, i.e. above the plane of the ring. Phosphate group is linked at 5' position of sugar. The phosphoric acid –OH groups are both ionized at physiological pH since one of the –OH groups has a pK_a of around 2 and the second one has pK_a of around 7, which means they are highly hydrophilic and DNA is highly negative charged in aqueous solution under such condition. Those negative charges are neutralized by positively charged proteins, metal ions and polyamines.[1] The sugar moiety with hydroxyl groups is also highly

hydrophilic. The bases are essentially hydrophobic but at the edge of each there is hydrogen-bonding potentiality which affords the foundation of DNA duplex secondary structure. Polynucleotide chains are linked through sugar-phosphate-sugar backbone, in which the phosphate bridges between the 3'-OH of sugar moiety on one nucleotide to the 5'-OH of sugar moiety on the next, with a base attached to each sugar residue on the 1' position.

DNA duplex structure was held together by complementary base pairing, i.e. hydrogen bonds between bases (Figure I-2). These base pairs, A:T and G:C, are well-known as Watson and Crick base pairs. In aqueous solution, hydrophobic forces cause the bases collapse together and stacked on top of each other, known as base stacking, which further stabilizes the duplex and form helix structure (Figure I-3).

As depicted in Figure I-2, three hydrogen bonds hold the deoxyguanosine nucleotide to deoxycytidine nucleotide, whereas the other pair, A:T pair, is held by two hydrogen bonds. Thus, G:C hydrogen bonding is stronger by approximate 50%. Because of this additional strength and also because of base stacking interaction, regions of DNA that are rich in G:C bonds are much more resistant to denaturation, or "melting", than A:T rich regions.

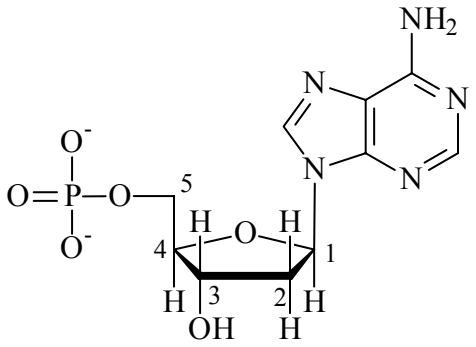

Adenosine 5'-monophosphate (AMP)

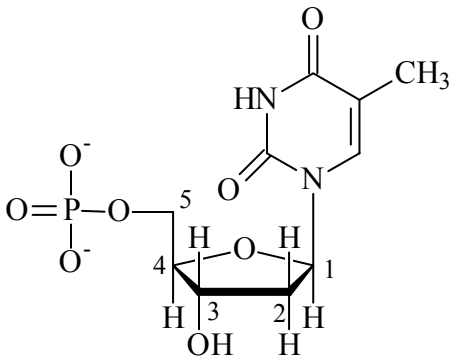

Thymine 5'-monophosphate (TMP)

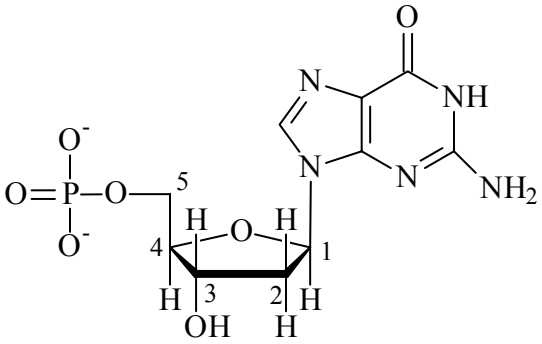

Guanosine 5'-monophosphate (GMP)

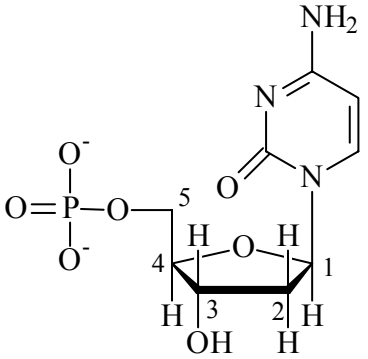

Cytidine 5'-monophosoate (CMP)

Figure I-1 The four nucleotide monomers of DNA

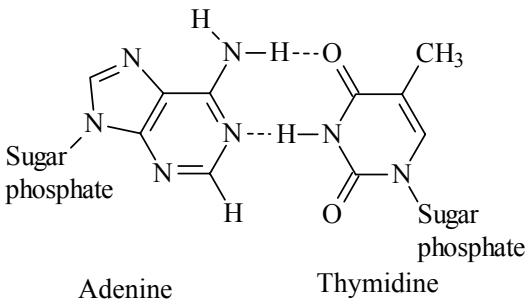

Adenine Thymidine

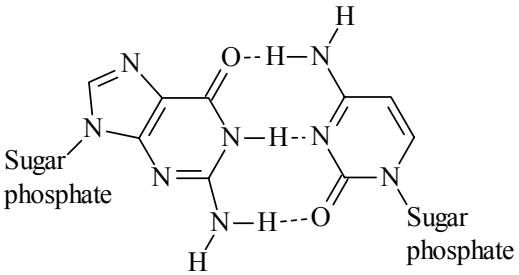

Guanine Cytosine

Figure I-2 Hydrogen bonding between Watson-Crick base pairing

Double-stranded DNA exists in more than one form. The right-handed B form is most commonly found under physiologic condition (low salt, high degree of hydration). DNA-RNA hybrid and double-stranded RNA are always found in A-form structure. Several other kinds of secondary structures are also possible under special circumstances, including left-handed Z form structure which is commonly seen in G/C rich sequence and sequence containing 8-methyl guanine and 5-methyl cytosine. A single turn of B-form DNA about the axis of the molecule contains 10 base pairs with spanning distance of 3.4 nm. The width of the double helix in B-form is 2 nm.[1]

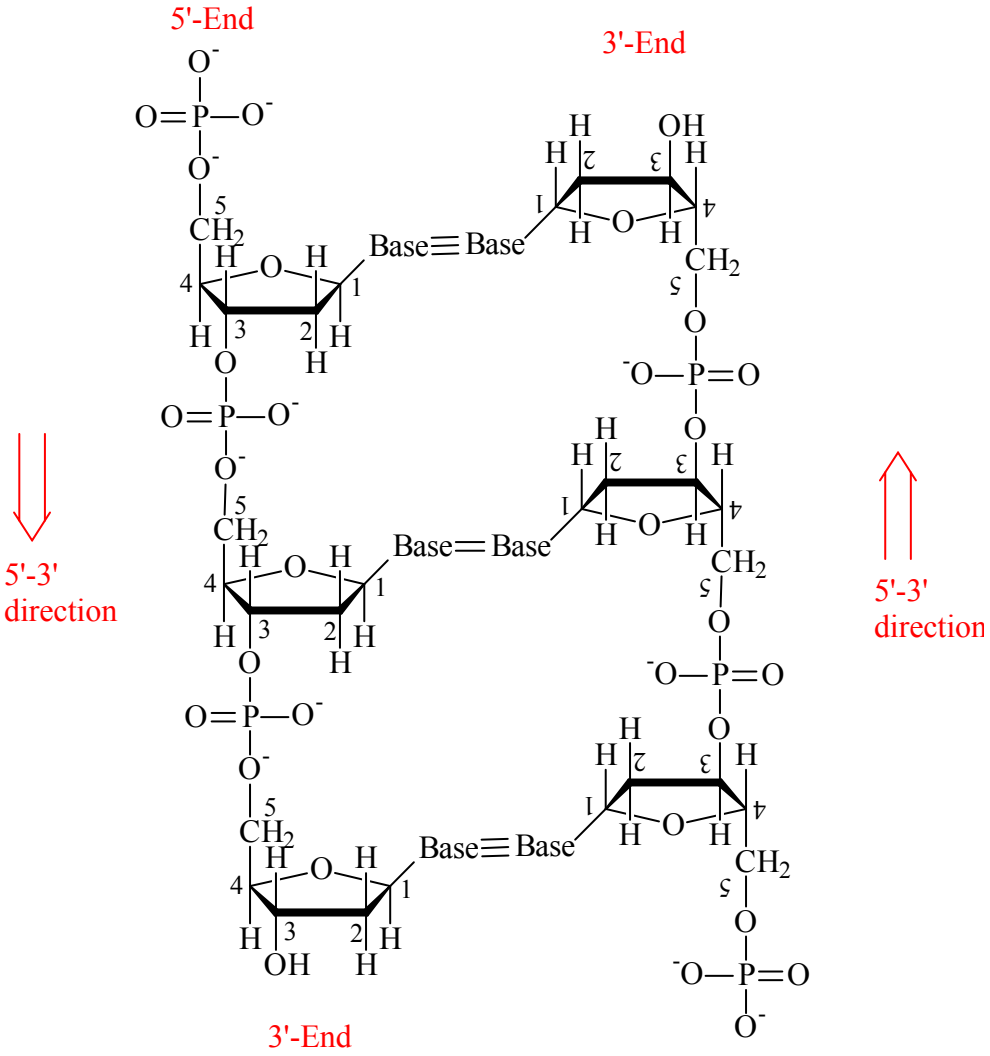

Figure I-3 Two anti-parallel polynucleotide strands of DNA

Genetic information is hidden in DNA sequences. The damage or modification to DNA bases may cause genetic mutation in semi-conservative replication processes of DNA. For instance, it's well known that mutation on guanine，like 8-oxo-7, 8-dihydro-2'-deoxyguanosine (8-oxoG) among other oxidation products, leads to low fidelity in replication and enhances the probability of adenosine incorporation. Thus the mutation from G:C base pairs into T:A base pairs occurs. Oxidative agents such as riboflavin, cationic anthraquinone derivatives or active oxygen species generated by ionizing radiation and endogenous oxidation process react with deoxyguanosine (dG) residue in DNA to form 8-oxodeoxyguanosine.[2,3] Therefore, the oxidative stress becomes an important mutagenic or carcinogenic lesion in *vivo* and is associated with as many as half of all human cancers.[4]

Table I-1 Parameters of polynucleotide helices [1]

	A Form	B Form	Z Form
Direction of helix rotation	Right	Right	Left
# of Residue per turn	11	10	12 (6 dimmers)
Rotation per residue	33	36	-60 per dimmer
Rise in helix per residue	0.255 nm	0.34 nm	0.37 nm

Hydrophilic DNA Duplex

DNA duplex consists of base, sugar and phosphate backbone (Figure I-3). The negative charges on phosphate, which are neutralized by positive ions in aqueous solution, make DNA a hydrophilic structure. It has been shown that DNA is well hydrated in aqueous solution where nine to ten water molecules are associated with each nucleotide in the first hydration shell. Well-ordered water molecule is believed to be an integral part of DNA structure and mediates interaction between DNA and binding species, for instance, proteins and lipids. Counter ions can form an ionic atmosphere around the negatively charged DNA cylinders rather than bind directly to singular charges.

Hydration is very important for the conformation of nucleic acids. The strength of these aqueous interactions is far greater than those for proteins due to their highly ionic character.[5] The DNA double helix can take up a number of conformations (*e.g.* A-DNA, B-DNA, C-DNA, D-DNA and the left handed Z-DNA). B-DNA requires the greatest hydration and requires about 30%, by weight, water to maintain its native conformation in the crystalline state. Partial dehydration converts it to A-DNA by decreasing the free energy required for A-DNA deformation and twisting, which is usefully employed by encouraging supercoiling but eventually leads to denaturation.[6] Hydration is greater and more strongly held around the phosphate groups that run along the inner edges of the major grooves. The water molecules are not permanently situated however, due to the rather diffuse electron distribution of the phosphate groups. Hydration is more ordered and more persistent around the bases with their more directional hydrogen-bonding ability and restricted space. Water molecules are held relatively strongly with residence

times for the first hydration shell being about 0.5 - 1 ns. Because of the regular structure of DNA, hydrating water is held in a cooperative manner along the double helix in both the major and minor grooves which aids both the annealing and unwinding of the double helix.

Nucleic acids have a number of groups that can hydrogen bond to water. The bases in DNA, even involved in hydrogen-bonded pairing, are capable of one further hydrogen-bonding link to water within the major or minor grooves in B-DNA, except for the hydrogen-bonded ring nitrogen atoms (pyrimidine N^3 and purine N^1). Thus, in B-DNA, guanine hydrogen bond to a water molecule from both the minor groove 2-amino- and major groove 6-keto-groups with further single hydration on the free ring nitrogen atoms (minor groove N^3 and major groove N^7). Cytosine hydrogen bond to a water molecule from both the major groove 4-amino- and minor groove 2-keto-groups. Adenine hydrogen bond to a water molecule from the major groove 6-amino-group with further single hydration on the free ring nitrogen atoms (minor groove N^3 and major groove N^7). Thymine hydrogen bond to a water molecule from both the minor groove 2-keto- and major groove 4-keto-groups. Phosphate hydration in the major groove is thermodynamically stronger but exchanges faster. There are six (from crystal structures)[7] or seven (from molecular dynamics)[8] hydration sites per phosphate, not including hydration of the linking oxygen atoms to the deoxyribose or ribose residues. The deoxyribose oxygen atoms can hydrogen bond to one water molecule each. The total for all these hydrations, in a G/C duplex, would be about 26-27 but about 14 of these water molecules are shared. There are a number of ways in which these water molecules can be arranged with B-DNA possessing 22 possible primary hydration sites per base pair in a

G/C duplex but only occupying 19 of them.[8] The DNA structure depends on how these sites are occupied; water providing the zip, holding the two strands together. It should be noted that about 2% of the hydrating water molecule sites may be transiently replaced by cations.

There may be a spine of hydration running down the bottom of the B-DNA minor groove particularly where there is the A=T duplex,[9] known to favor B-DNA. Water molecules hydrogen-bond by donating two hydrogen bonds, bridging between thymine 2-keto(s) and/ or adenine ring N^3(s) in sequential opposite strands (*i.e.* not paired bases). This water is fully hydrogen bonded by accepting two further hydrogen-bonds from secondary hydration water, so fixing the primary hydration water more firmly in place such that they exchange slower (0.9 ns) than any other water hydrating the DNA. The primary hydration may occur regularly down the minor groove connecting the strands but any cooperative effect is through the secondary hydration. This secondary hydration is more strongly held than in the G:C duplex giving rise to greater apparent hydration. Such a spine of hydration may be important in stabilizing the B-DNA.[10] The A:T base pairing produces the narrower minor groove and more pronounced spine of hydration, whereas the G:C base pairing produces a wider minor groove with more extensive primary hydration, due in part to the 50% greater hydration sites. Such solvent interactions are key to the hydration environment, and hence its recognition, around the nucleic acids and directly contributes to the DNA conformation. B-DNA possessing higher phosphate hydration, less exposed sugar residues and smaller hydrophobic surface, is stabilized at high water activity, whereas A-DNA, with its shared inter-phosphate water bridges, is more stable at low water activity.

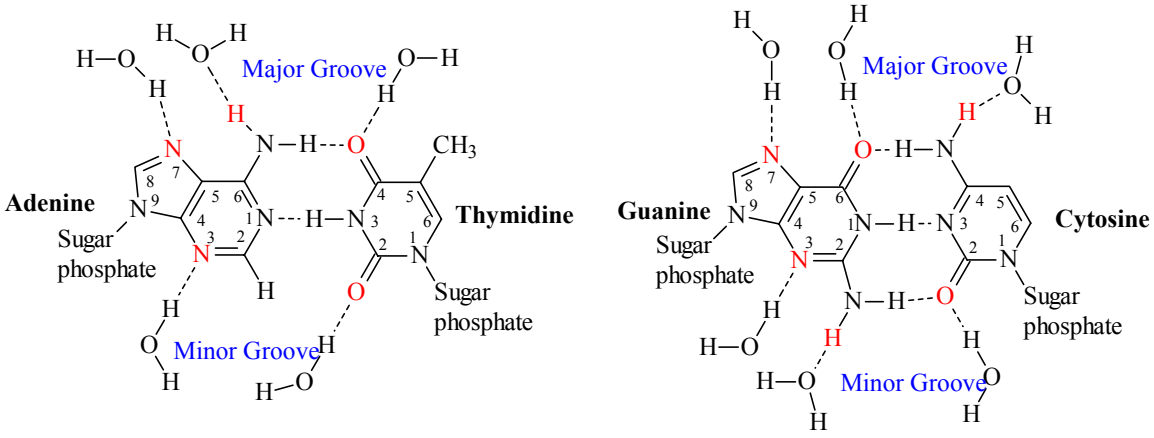

Figure I-4 Hydrogen bonding sites on nucleic acid base pairs

Most of studies in charge transfer in DNA are in aqueous solution with Na^+ or Mg^{2+} as the counter ion.[11, 12] Effect of those ions on charge transfer in DNA has been previously studied and shown significant influence on modulating DNA conformation as well as oxidation potential on single base.[13] In the study in Schuster's group, to exclude the binding of positive ion, an d(5`-AAA-3'), $(A)_3$, track's phosphate backbone was modified with methylated phosphates where negative charges on phosphates were eliminated.[13] A significant reduction on distal GG damage was observed in the UV light induced charge transport experiment because no counterions populates across the $(A)_3$ bridge as indicated by molecular dynamic simulation. Furthermore, quantum calculations for the $(A)_3$ bridge yielded vertical ionization potential, 5.90 eV, for the (native) unmodified backbone, where 50% of the hole delocalized over the A bases and 20% over the complementary thymines and the rest distributed mainly over the sugar-phosphate backbone and some on the water molecules. The same $(A)_3$ phosphornated bridge, no Na^+ on the $(A)_3$ strand but including a hydration shell, has the vIP value of 6.16 eV. The

hole is distributed 40% on the $(A)_3$ and 25% on the complementary $(T)_3$. The increased ionization potential of the phosphonated $(A)_3$ bridge, together with its counterion-starved local environment, is predicted to reduce the probability for transfer of a hole into it. Thus, the higher energy bridge inhibits the transport and bounces back the charged hole.[13] Those findings prompt us to include water molecules and counterions in DNA coherent environments when we investigate the mechanism of charge transport in DNA.

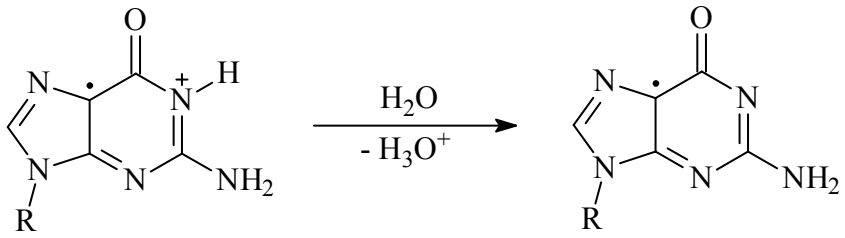

Figure I-5 Quenching of guanine radical cation by proton transfer

It is noteworthy that the hole migration and trap at guanine in DNA can be quenched by water (Figure I-5).[11] A study on charge transport in G:C mismatched DNA duplex, by Giese and coworkers, revealed that this effect was so significant that it diminished the charge transport through the mismatch site, which is more accessible to surrounding water molecules.[14] In aqueous solution there is always competition between the migration of charge (K_{CT}) along the DNA helix and the irreversible quenching of charge by water (K_{H2O}) and oxygen at most reactive sites, which partially determines the efficiency and distance of positive hole migration. It is of interest to build up a hydrophobic environment around DNA and examine the charge transport process in DNA without or with less interference from surrounding water molecules. This study can

not only give us the insight on the mechanism of charge migration in DNA helix and subsequent oxidative damage at oxidative labile sites, but also provide experimental support for the research on utilize DNA oligomers as new conducting nanoelectronic material[15] in which the oxidative damage and radical quenching in DNA would be an important factor determining the conductivity of DNA polymer.

Lipid Binding to DNA

A lipid is a kind of amphiphilic molecule with both a hydrophilic, "water loving" polar head, and a hydrophobic, "water hating" non-polar tail, functional group. It can self assemble and form ordered structures, thermodynamically stable in favor of enthalpy change, in aqueous solution. Soaps and detergents are single-chain amphiphiles that form spherical micelles where polar heads hidden the non-polar tail against water. Many nature, like phosphate lipid in cell membrane, and synthetic lipids used in gene transfer and drug delivery are bi-chain (two tail groups) structures. They tend to form lipid bilayers, in which two polar surfaces shield the non-polar interior, because the bulky tail groups prohibit the formation of micelles. The common bilayer structure includes open bilayered lamellae and self-closed liposomes (Figure II-6).[16]

Lipids are widely used to improving the efficiency of DNA transfection process through the hydrophobic membrane of a cell, in which DNA is encapsulated as lipid-DNA complex (lipoplex). Currently, the majority of studies reported only synthesis and activity of novel cationic lipid gene delivery system. However, there are only a few studies on the structure and structure-activity relationship of DNA-lipid complex. Early

studies proposed the formation of aggregation because of electrostatic attractive force and encapsulation of condensed DNA.[17] Recently, electron microscopic observations show different images. Both cryoelectron microscopy (cryo-EM) and Freeze-Fracture microscopy shows similar aggregates surrounded by a halo of fibers of approximately 6.5 nm diameter which matches the diameter of DNA and a bilayer.[18, 19] These structures, obtained from different cationic lipid and DNA of various lengths, were given various name, such as spaghetti, medusas and sea urchins. Negative stain and metal-shadowing electron microscopy, however, shows the different anisotropic elongated DNA coated by lipid.[20] It is still unknown if these different observations are due to various DNA and lipid system or preparation methods because of little knowledge about thermodynamics and kinetics of DNA-lipid complex. The question regarding which kind of structure is more effective in transfection is also under investigation. Therefore it is hard to relate the efficiency of a specific gene transfer vector with the structure of complex formed between this vector and DNA. This poses a problem on selecting candidate molecule to study in this research.

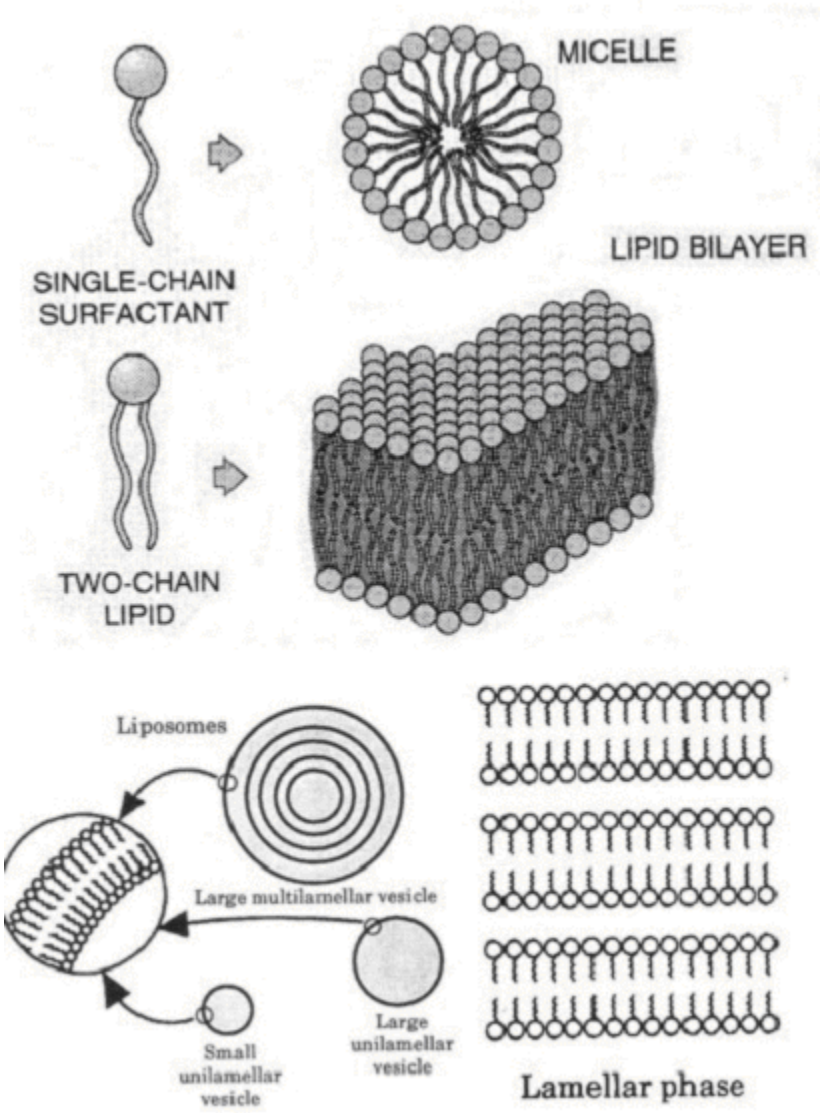

Figure I-6 Schematic Structure of Micelle, Liposomes and Lamellar Bilayer.[16]

The binding of lipid molecule to DNA does not necessarily dehydrate the DNA complex completely. Even though few studies directly show the preservation of water molecule in lipid-DNA complex, the observation of 6.5 nm periodicity in electron microscopy as well as in small angle X-ray scattering (SAXS) measurement is consistent with a lipid bilayer thickness of 4 nm and hydrated (one water shell) DNA helix of 2.5 nm.[18, 21] If the dehydration happens, a smaller periodicity of 4-5 nm would be observed because of the lack of water layer and consequently tilted frozen hydrocarbon chain. Rädler and coworker also proposed existence of highly immobilized water located in the interfacial region between DNA double strands and lipid lamellae and formed the bifurcated bridge between DNA backbone and lipid headgroups.[22] If this fact holds for all DNA-lipid complex, we may consider carrying out experiment in non-aqueous organic media to completely eliminate the effect of water molecule. Furthermore, this has to be done with the preservation of DNA secondary double-helix structure. Studies have shown that this is possible by substituting counter cations of phosphate anions in DNA with cationic amphiphiles.[23, 24]

Different from water molecules, some experiments prove that the counterions were entirely released from both lipid and DNA upon formation of lipid-DNA aggregate at isoelectronic point, where positive(lipid)/negative(DNA) charge ratio is 1:1. This was due to electrostatic demands and favorable entropic contribution to free energy.[25] This characteristic of DNA-lipid complex extends us a chance to elucidate effect of counterions on modulation of charge transfer in DNA.

Introduction to Charge Transport in DNA

Oxidative damage in DNA probably presents the most extensive lesions to mutagenesis, carcinogenesis and a number of degenerative diseases.[26,27] Even though the damage may stem from diverse biological pathways in different biological system, there are three known major chemical sources leading to the oxidative damage in DNA. First, singlet oxygen or hydroxyl radical generated from an excited photonuclease as reactive intermediate;[28] second, hydrogen atom abstraction from an intermediate free radical; at last, the loss of an electron from aromatic bases to form an intermediate radical cation. All three processes are most common mechanism to damage DNA via photosensitization. The last pathway, in particular, was studied extensively in past decade since it was noticed that the nucleobases as far as 200 Å away from the initial site of charge injection, the removal of an electron, was damaged through charge transport (CT) process.[29]

The interest in the charge transport in DNA are not only limited for its biological consequence, but also for the potential implication as microelectronic device.[30] It has been reported that desiccated DNA, as long as 600 nm in length, are very efficient conductor.[31] Therefore, we can envision the application of DNA as quantum wire in mesoscopic device. However, the other researchers presented the contrary experiment implying that DNA is insulator or semiconductor and conduct charge similar to regular protein.[32-36] The unnatural condition required by those experiments may account for wide range of conducting properties. The impassionate debates around electronic property of DNA leads to several important questions: How does the charge migrate along DNA duplex? What are the dominate factors and their roles in this charge transport process?

The occurrence of electron transfer over long distance in DNA duplex in aqueous buffer solution was well-established a decade ago.[37-40] Recent extensive experimental and theoretical researches on the radical cation transport in DNA duplex from several laboratories have proposed several mechanisms. It is generally accepted that radical cation migrate through DNA by a series of hops instead of instant tunneling through well-stacked DNA bases,[41] especially for long distance charge transfer process. The several hopping mechanisms including hole resting model,[42-44] A/G-hopping model [11,45], phonon assistant polaron hopping model [3, 12, 46] and conformation gated hopping model [47], among the others, have emerged and been enthusiastically debated. DNA dynamics, which could occur in the time scale of charge transport, was also incorporated into molecular simulation to elucidate the effect of DNA sub-environment (water and counterions molecule) on modulating the oxidation potential and charge distribution across the bases[13] and the thermally induced fluctuation on achieving the optimal alignment for charge migration through DNA π stacking.[48,49]

Photoinduced charge transfer in anthraquinone DNA conjugate

Several different species can cause the oxidative damage in DNA. Most photonucleases and hydroxyl radical are two common species that cleave DNA with no or little sequence selectivity. The former target the hydrogen atom of the sugar and deoxyribose moiety and the latter directly abstracts a hydrogen atom from the DNA deoxyribose-phosphate backbone. Some nucleases, for instance riboflavin[50], organometallic compounds[51], naphtalimide derivatives[52, 53] and certain anthraquinone

derivatives[54] can selectively damage GG sequence, particularly 5'-G in GG sequence. It oxidizes the covalently-linked neighboring base to the radical cation that migrates through the DNA helix before it gets trapped at GG sequence, the one with the lowest oxidation potential. This preferential cleavage is the characteristic observation from the intra-strand charge migration, trapped and oxidation of DNA oligomer.

The anthraquinone derivatives, which cause the light-induced oxidative damage at GG site near to the attached site or far from its attachment as long as 200 nm, were developed in Schuster's group and have been widely applied in the study of charge transport process in DNA. The quinone complexes bind to DNA by intercalation or fit into minor groove. The photoexcitation leads to the selective damage at 5'-G of GG sequences, which is revealed as the strand cleavage only upon alkali treatment.[3] The nonselective and spontaneous cleavage occurs when the tethered anthraquinone chromophore was irradiated. The damage underwent the hydrogen abstraction from deoxyribose moiety pathway. [55]

The application of anthraquinone photosensitizer in the study of the charge transport in DNA has several key advantages over the other photosensitizers. The reduced quinone, gaining an electron to oxidize the DNA after the photo-irradiation, is recyclable through recombination with the base radical cation in back electron transfer (BET) process to regenerate the starting materials. Therefore, the anthraquinones demonstrate the ability to recyclization through reduced and oxidized form, a characteristic not evident in other photosensitizers. The excited singlet AQ undergoes intersystem crossing (ISC) rapidly to triplet excited states, which avoids the quick back electron transfer process to quench the radical cation reaction.(PII Figure I-1)

The quinone is a good oxidant at its excited state. The charge injection can occurs no matter which base it is attached to. Free anthraquinone associate with DNA duplex through either randomly intercalation or minor groove binding. The length of tether between covalently linked quinone and DNA restricts such binding mode can not occur. It has been proposed that covalent-linked AQ is end-capped over the terminal bases,[56] which affords the ability to inject the radical cation through either base at the terminal sites.

Third, there is little side reaction or by product observed in photo excitation process, which is, on the contrary, evident in other photosensitizers. The anthraquinone derivatives only damage the DNA once they absorbs UV light at 350 nm region, which is about 100 nm away from the major absorption region of DNA.

Finally, there is no evidence in inter strand conjugation between anthraquinone and DNA helix as shown in the other organometallic photosensitizer.[57] This is critical to provide reliable experimental data on intra-strand charge transfer study especially when the experiments are carried out at high concentration.

In our study, anthraquinone (AQ) was covalently linked to DNA oligomer to form AQ-DNA conjugate. The synthesis of AQ is shown in Figure II-1, a modified method originated by Mori *et.al*.[58] Generally, the synthesis of the AQ-oligomeric conjugate involves the attachment of the 3'-end of the DNA oligomer base to a commercial bead support. Chain grows at the 5'-end, one monomer at a time. Finally the AQ chromophore is covalently linked within the final steps of the solid phase synthesis of the oligomer. The length of the tether between AQ and oligomer confine the secondary binding mode of the AQ to DNA duplex. The aromatic planar structure makes it possible for AQ to

intercalate into DNA bases. However, the short ethyl linker will not allow this conformation. It is possible that the AQ positions over both strands of the duplex and injects the charge into either strand when it is excited by UV light. The subsequent oxidative cleavage will occurs on both strands at the sites sensitive to charge transfer damage.

References

1. Mathews, C. K., Holde, K. E., *Biochemistry, 2nd Ed*., Benjamin-Cummings Publishing Co. Inc., 1996, 98-102.

2. Ito, K. *J. Biol. Chem.* 1993, 268: 13221-13227.

3. Ly, D., Kan, Y., Armitage, B., Schuster, G., *J. Am. Chem. Soc.* 1996, 118, 8747-8748.

4. Beckman, K. B.; Ames, B. N. *J. Biol. Chem.* 1997, 272, 19633-19636

5. Makarov, V., Pettitt B. M.; Feig M. *Acc. Chem. Res.* 2002, 35, 376-384

6. Mayer, C.; Timsit, Y. *Cell. Mol. Biol.* 2001, 47 815-822

7. Schneider B.; Patel K.; Berman, H. M. *Biophys. J.* 1998, 75 2422-2434

8 Auffinger, P.; E. Westhof, E. *J. Mol. Biol* .2001*,* 300, 1113-1131

9. Denisov, V. P.; Carlström, G.; K. Venu K.; Halle, B. *J. Mol. Biol.* 1997, 268, 118-136

10. Feig, M.; Pettitt B. M., *J. Mol. Biol.* 1999, 286, 1075-1095

11. Giese, B, *Acc. Chem. Res.* 200, 33, 631-636.

12. Schuster, G. B. *Acc. Chem. Res.* 2000, 33, 253-260.

13. Barnett, R. N., Cleveland, C. L., Joy, A., Landman, U., Schuster, G. B. *Science* 2001, 294: 567-571.

14. Giese, B.; Wessely, S. *Angew. Chem. Int. Ed*. 2000, 39, 3490

15. Fink, H.-W. *Cell Mol. Life Sci.* 2001, 58, 1

16. Lasic, D. D. 1997. *Liposomes in Gene Delivery*, CRC Press.

17. Felgner, P. L., Gadek, T. R., Holm, M.; Roman, R., Chan, H. S.; Wenz, M., Northrop, J. P., Ringold, M., Danilesen, H., *Proc. Natl. Acad. Sci. USA* 1987, 84: 7413-7417.

18. Gustaffson, J.; Almgrem, M.; Karlsson, G.; Arvidson, G. *Biochim. Biophys. Acta* 1995, 1235, 305-317

19. Sternberg, B. S.; F; Huang, L. *FEBS Lett.*1994, 356: 361-366.

20. Gershon, H., Ghirlando, R., Guttman, S. B., Minsky, A., *Biochemistry* 1993, 32, 7143-7151.

21. Lasic DD, Strey H, Stuart MCA, Podgornik R, Frederik PM, *J. Amer. Chem. Soc.* 1997, 119 (4), 832-833

22. Pohle, W; Selle C.; Gauger, D. R.; Zantl, R.; Artzner, F.; Rädler, J. O, *Phys. Chem. Chem. Phys.* 2000, 2, 4642-4650

23. Tanaka, K.; Okahata, Y. *J. Amer. Chem. Soc.* 1996, 118, 10679-10683

24. Wong, F. M. P.; Reimer, D. L.; Bally, M. B. *Biochemistry 1996*, 35, 5756 -5763

25. Wagner, K.; Harries D.; May, S.; Kahl, V.; Rädler, J. O; Ben-Shaul A. *Langmuir* 2000, 16, 303-306

26. Demple, B.; Harrison, L. *Annu. Rev. Biochem.* 1994, 63, 915-948

27. Loft, S.; Poulsen, H. E.; *J. Mol. Med.* 1996, 74, 297-312

28. MacGregor, R. B. J. *Anal. Biochem.* 1992, 204, 324

29. Beratan, D. N.; Priyadarshy, S.; Risser, S. M. *Chem. Biol.* 1997, 4, 3-4

30. Di Ventra, M.; Zwolak, M. *DNA Electronics*: Nalwa, H. S., Ed.; American Scientific Publishers: Stevenson Ranch, CA;

31. Fink, H. W.; Schonenberger, C. *Nature*1999, 398, 407-410

32. Porath, D.; Bezryadin, A.: De Vries, S.; Dekker, C. *Nature* 2000, 403, 635-638

33. Cai, L. T.; Tabata, H.; Kawai, T. *Appl. Phys. Lett.* 2000, 77, 3105-3106

34. Yoo, K. H.; Ha, D. H.; Lee, J. O. *Phys. Rev. Lett,* 87, 198102.

35. Storm, A. J.; van Noort, J.; de Vries, SS.; Dekker, C. *Appl. Phys. Lett.* 2001, 79, 3881-3883

36. de Pablo, P. K.; Moreno-Herrero, F.; Colchero, F.; Gómez Herrero, J.; Herrero, P.; Baró, M.; Ordejón, P.; Soler, J. M.; Artacheo, E. *Phys. Rev. Lett.* 2000, 85, 4992-4995.

37 Arkin, M. R.; Stemp, E. D.; Holmlin, R. E., Barton, J. K.; Horman, A.; Olson, E. J. C.; Barbara, P. F. *Science* 1996, 273, 475-480

38 Lincoln, P.; Tuite, E.; Norden, B.*, J. Am. Chem. Soc.* 1997, 119, 1454-1455

39 Pratt, F.; Hou, C. C.; Foote, C. S. *J. Am. Chem. Soc.* 1997, 119, 5051-5052

40 Kasai, H.; Yamaizumi, Z.; Berger, M.; Cadet, J. *J. Am. Chem. Soc* 1992, 114, 9692-9694

41. Turro, N. J.; Barton, J. K. *Biol. Inorg. Chem.* 1998, 3, 201

42. Jortner, J. Bixon, M. Langenbacher, T., Micheal-Beyerle, M. E. *Proc. Natl. Acad. Sci. USA* 1998, 95, 12759.

43. Bixon, M.; Jortner, J., *J. Phys. Chem. B.* 2000, 104, 3906.

44. Bixon M.; Giese, B.; Wessely S.; Langenbacher T.; Micheal-Beyerle M. E.; Jortner J. *Proc. Natl. Acad. Sci. USA* 1999, 96, 111713

45. Giese B.; *Top. Curr. Chem.* 2003, 236, 27

46. Liu, C-S; Hernandez, R.; Schuster, G. B. *J. Am. Chem. Soc.* 2004 126, 2877-2884

47. O'Neill, M. A.; Barton, J. K. J. Am. Chem. Soc. 2004, ASAP

48. D'Orsogna, M. R.; Rudnick, *J. Phys. Rev. E* 2002, 66 artno041904

49. Bruinsma, R.; Cruner, G.; D; Orsogna, M. R.; Rudnick, *J. Phys. Rev. Lett.* 2000, 85, 4393-4396

50. Kawanishi, S.; Yamamoto, K.; Inoue, S.; Ito, K. *J. Biol. Chem.* 1993, 268, 13221-13227.

51. Holmlin, R. E., Hall, D. B., Barton, J. K. *Nature*1996, 382, 731-735

52. Yamamoto, M., Tsuchida, A., Nakatani, K., Sugiyam, H., Takayama, M., Saito, I. *J. Am. Chem. Soc.* 1995, 117: 6406-6407.

53. Saito, I.; Takayama, M.; Kawanishi, S. *J. Am. Chem. Soc.* 1995, 117, 5590-5591.

54. Armitage, B.; Yu, C.; Devadoss, C.; Schuster, G. *J. Am. Chem. Soc.* 1994, 116, 9847-9859.

55. Breslin, D. T.; Schuster, G. B. *J. Am. Chem. Soc.* 1996, 118, 2311-2319

56. Sartor, V.; Henderson, P. T.; Schuster, G. B. *J. Am. Chem. Soc.* 1999, 121, 11027-11033.

57. Fahlman, R. P.; Sharma R. D.; Sen D. *J. Am. Chem. Soc.* 2002, 124, 12477-12485

58. Mori, K.; Subasinghe, C.; Cohen, J. S. *FEBS Letters* 1998, 248, 213-218.

59. Dias, R. S.; Lindman, B.; Miguel, M. G. *J. Phys. Chem. B* 2002, 106, 12600-12607

CHAPTER III

EXPERIMENTAL SECTION

General Methods

^{1}H and ^{13}C NMR spectra were recorded on a Varian 300 MHz Spectrometer. Radioactively labeled isotope [γ-^{32}P] ATP was purchased from Amersham Bioscience. Synthetic oligonucleotides (gel filtration grade) were obtained either commercially from Dr. Nadia Boguslavsky of Georgia Institute of Technology or were synthesized on an Applied Biosystem DNA synthesizer and were, therein, purified by a Hitachi 7000 reverse-phase HPLC system. Terminally-linked anthraquinone oligonucleotides were synthesized in the second way mentioned above and purified within the same manner as the native oligodeoxynucleotides. All native oligomer were PAGE purified to ensure the purity before photo-irradiation experiments. The mass of each oligonucleotide was determined by matrix assisted laser desorption ionization time-of-flight (MALDI-TOF) or electrospray ionization (ESI) mass spectrometry. The extinction coefficients of the oligonucleotides were calculated using nearest-neighbor values, and the absorbance was measured at 260 nm using a Hewlett-Packard Spectrometer. Anthraquinone-modified oligonucleotide solution concentrations were determined in same way except that an anthraquinone was replaced with adenine in the extinction coefficient determination. UV melting and cooling curves were recorded on a Cary 1E spectrophotometer equipped with a multi-cell block, temperature controller and sample transport accessory. The buffer used for all DNA experiments (PAGE, CD, UV denaturation) was 10 mM sodium

phosphate at pH 7.0. Graphics of the phosphoimagines and autoradiograms of the electrophoretic gels were obtained by Fuji 2340 BAS-Image System.

Synthesis and purification of DNA oligomer

Oligodeoxynucleotides was synthesized by a standard, solid-phase β-cyanoethyl phosphoramidite chemistry on ABI expedite DNA synthesizer. The cartridge containing 3'-terminal base on solid resin was purchased from Glen Research. The coupling of each base was monitored with trityl coupling yield. The cartridge was removed from the instrument and washed with 5 ml 30% concentrated ammonium hydroxide twice. The solution was incubated at 60 ^{o}C for at least 8 hours to ensure the complete deprotection of DMT group before it was dried on Labconco Centrivap concentrator under vacuum at 56 ^{o}C over 12 hours, connected with a Labconco cold trap. The resulting yellow solid was re-dissolved in the 3-5 mL deionized water and filtered through Gelman 0.45 μm acrodisc filter to remove the insoluble impurity from the resin. The sample was purified on Hitachi 7000 HPLC system with Varian Dynamax 250x21.4 mm reverse phase C18 column using 0-25% gradient water/acetonitrile (A: 5% acetonitrile in water, B: 50% acetonitrile in water) with 0.05 M triethylammonium acetate (TEAA). The collected DNA effluent was dried on Labconco centrivap concentrator under vacuum at 56 ^{o}C over 8 hours and reconstituted in 1-2 mL deionized water for the desalting procedure.

A Waters Spec-Pak filter cartridge was washed with 10 mL deionized water, 10 mL 20% acetonitrile before the DNA solution was loaded. The DNA solution was pushed through the filter slowly to ensure the majority of DNA sustain on the filter. 10 ml

deionized water was used to wash off the excess ions slowly. Finally, DNA was washed out from the cartridge with 10 mL acetonitrile solution and subsequently dried on Labconco centrivap concentrator. Hewlett-Packard Ultra-violet spectrometer determined the concentration of purified DNA solution at the wavelength of 260 nm.

Anthraquinone-oligonucleotide Conjugate Synthesis

DNA sequence synthesis was performed on the solid phase synthesis following standard conditions, using cyanophosphoramidite monomer. The resin was thoroughly washed before the conjugate was ready to be coupled to the AQ monomer. The cartridge (containing resin) was removed from the synthesizer. The AQ-phosphoramidite monomer was dissolved in 500 uL of dry CH_3CN solution containing 0.1 M tetrazole. The monomer was taken into the cartridge by a syringe. Once the coupling was complete, the monomer solution was removed from the cartridge by pressure injection. The cartridge was placed back onto the synthesizer and the automated sequence was allowed to resume. The coupling efficiency was quantified by measuring the UV-absorption and the trityl cation released and comparing it to that of the pervious and subsequent step.

Removal of the oligomer from the solid support and subsequent purification by reverse phase HPLC proceed as usual. The dried and purified conjugates showed a light yellow color. Analytical HPLC, UV-vis and MALDI-TOF were used to determine the purity and identity of the conjugate.

Page Purification and Radiolabeling of DNA oligomer

The T4 Polynucleotide Kinase, PNK buffer and [γ-^{32}P]-dATP were purchased from Amersham pharmacia and used as received. Piperidine and buffer ingredients were purchases from Aldrich-Sigma and used without further purification.

DNA oligomers were radiolabeled at 5'-end using [γ-^{32}P] ATP and T4 Polynucleotide kinase. 5.0 uM DNA samples were incubated with 1.0 uL [γ-^{32}P] ATP, 2 uL PNK buffer and 1 uL T4 Polynucleotide Kinase in the total volume of 20.0 uL at 37 ^{o}C for 45 min. The labeled DNA sample was suspended in denaturing loading buffer dye and purified on 20% denaturing polyacrylamide gel. The labeled product was located with in the gel by autoradiography. The band corresponding to labeled DNA samples was excised from the gel and eluted in 800.0 uL elution buffer (0.5 M NH_4OAc, 10.0 mM $Mg(OAc)_2$, 1.0 mM EDTA and 0.1% SDS) at 37 oC for 4.0 hours. The supernatant from the samples was extracted with thin tip pipette and centrifuged at 12,000 g for 3 minutes on Thermo Forma Microcentrifuge. Radiolabeled DNA was precipitated from the supernatant solution by the addition of 1.0 uL glycogen and 700.0 uL cold absolute alcohol. The resulting solution was vortexed to homogenous solution and put on the dry ice for 45 minutes before it was spun for 30 minutes on microcentrifuge at 12,000 g. The supernatant was removed from centrifuge tube carefully without disturbing the DNA precipitate at the bottom. The resulting DNA pellet was washed twice with 80% ethanol at room temperature and spun to dryness with a Savant Speed Vac Plus for 45 minutes. The dried sample was reconstituted in deionized water for hybridization.

Cleavage Analysis by UV Irradiation and PAGE

The samples for irradiation were prepared by hybridizing a mixture of "cold" (unlabeled) and radiolabeled oligonucleotide (5 uM) to a total volume of 20 ul each in 10 mM sodium phosphate at pH 7.0. Hybridization was achieved by heating the sample up to 90 ºC for 5 minutes, followed by slow cooling to room temperature over the course of 6 hrs or overnight. A small aliquot of concentrated lipid solution (2 mM) was added, if necessary, to make the samples with proper lipid concentration. Deionized water and NaPi buffer were used to adjust the volume of all samples such that all had the same DNA duplex and buffer concentration. Samples were irradiated in microcentrifuge tubes in a Rayonet photoreactor (Southern New England Ultraviolet Company, Barnsford, CT) equipped with 8X350 nm lamps.

After irradiation, the sample were precipitated once with cold absolute ethanol at the presence of 1 ul glycogen, washed twice with 80% ethanol and dried as described as above. Each sample was treated with 100 uL piperidine (1 M) and incubated at 90 ºC for 30 minutes. After the evaporation of piperidine in Savant Speed Vac with medium temperature setting, nanopure water (2x20 uL) was added to each sample and drying process was repeated to ensure the complete removal of piperidine. Samples (3000 cpm), suspended in denaturing formamide-loading buffer, were electrophoresed on a 20 % 19:1 acrylamide:bisacryamide gel containing 7 M urea. The gels were dried on HOEFER Scientific Slab Gel Dryer SE1160 over 2 hours and the cleavage sites were visualized by autoradiography.

Photocleavage by Singlet Oxygen from Rose Bengal

The samples for irradiation were prepared by hybridizing a mixture of "cold" (unlabeled) and radiolabeled oligonucleotide (5 uM) in 10 mM sodium phosphate at pH 7.0. Hybridization was achieved by heating the sample up to 90 ºC for 5 minutes, followed by slow cooling to room temperature over the course of 6 hours or overnight. A small amount of concentrated lipid solution was added to DNA duplex samples to make the solution with the proper charge ratio between DNA and lipid. The resulting mixture was incubated at room temperature for 30 minute. Before the irradiation, an indicated amount of Rose Bengal (5 mM) solution was added to DNA-lipid complex solution. The irradiation with low energy visible ($\lambda > 400$ nm) light was performed using an Oriel 250 W Hg/Xe Lamp equipped with specific transmission cutoff-filter which block all the light with wavelength shorter than 490 nm. Visible light was focused approximately 15 cm from 50 uL sample solution containing in 120 uL ultra micro-centrifuge tubes. These Perkin-Elmer MicroAmp reaction tubes do not absorb light at wavelength above 390 nm. The instrument setup was kept in darkness to minimize the effect of scattering light. The specific concentration and buffers used per irradiation are indicated in each figured captions.

Post irradiation samples were proportioned and reserved for FPG enzyme or piperidine treatments. The samples subject to piperidine treatment was precipitated as described above and vacuum, spun-dried. A 100 µL of piperidine (1 M) was added to each sample which was subsequently vortexed and heated at 90 ^{o}C for 3 minutes. The samples were dried in the Savant over 1.5 hours at medium heat after pulsed for 10

seconds by Savant Speed Vac Plus. The dried samples were co-evaporated with 20 uL nanopure water twice to ensure the complete removal of piperidine. The final samples were dissolved in 5.0 uL of denaturing formamide-loading buffer and loaded on 20% polyacrylamide sequencing gel to separate the photocleavage products, which was detected by autoradiography.

FPG Enzymatic Digestion of Photo-oxidized DNA

1 uL FPG enzyme and 10 μL standard buffer solution containing 50 mM TrisHCl (pH=7.5), 2 mM EDTA, 70 mM NaCl were incubated with 5 μM DNA at 37 ºC for 2 hours. FPG enzyme was killed by heating at 70 ºC for 45 min and followed by ethanol precipitation at -20 ºC. The samples were dried and analyzed by 20% polyacrylamide sequencing gel as described above.

UV Thermal Denaturation

2.5 μM solutions of various oligonucleotide duplexes in 10 mM phosphate buffer, at pH 7.0, were prepared. The data was collected on a Varian Cary 3C-1E UV-Visible spectrometer equipped with temperature-regulated 6-cell sample block-holder. The samples were placed in quartz cuvettes (1.5 ml capacity. 1.0 cm path length) and sealed with tape to prevent the evaporation of water during heating/cooling cycles. Melting curves were obtained by monitoring the UV absorbance at 260 nm as the temperature was ramped from 90 ºC to 20 ºC at a rate of 0.5 ºC /min with 3 minute interval at the each

ending temperature for the complete equilibrium. Four ramps were performed to ensure consistent results. Data were exported to origin 3.78 where the absorbance at 260 nm was plotted against temperature for each sample and corresponding derivative curves were obtained. The melting temperatures (T_m) were determined as the maxima of the first derivative plots of absorbance versus temperature. Data obtained for cooling process was found to be same as that obtained from heating ramp with error value of ±0.5 ^oC.

DNA Conformation Identification by Circular Dichroism Spectrometry

The CD spectra were recorded on Jasco-720 instrument at room temperature. 5 scan accumulations were collected for each sample at the scanning speed of 200 nm/min over 200 to 400 nm range. The spectral resolution and bandwidth were 0.2 nm and 1.0 nm, respectively. The solution was prepared containing 2.5 μM DNA duplex in 10 mM sodium phosphate buffer at pH 7.0. After hybridization of DNA duplex, an appropriate amount of lipid solution was added to each DNA sample and the resulting solution was incubated at room temperature for 30 minutes prior to the CD measurement to allow the equilibrium of DNA-lipid complexes. The pre-hybridized samples in 1.0 cm path-length quartz cells were measured in a chamber flushed with dry N_2 gas to prevent the moisture condensation on the surface of quartz cells. For time dependant study, a timer was set to measure the spectra at defined intervals.

Time Dependant UV Study

The solutions were prepared containing 2.5 μM DNA duplex in 10 mM sodium phosphate buffer at pH 7.0. UV spectra were monitored from 200 nm to 500 nm region every 30 min, up to 20 hours, after the addition of the proper amount of lipid into DNA duplex solution. The data were exported and process in Origin 4.0 to obtain the overlapped UV spectra for DNA duplexes with different charge ratio of lipids.

Fluorescence Quenching of Ethidium Bromide

Fluorescence studies were carried out on SPEX 1681 Fluorolog spectrometer using 1 mL quartz cell with path length of 1 cm. The cell holder was maintained at room temperature. The excitation and emission slits were set at 0.25 mm. Sample containing 5 μM DNA and 10 μM EB in 10 mM sodium phosphate buffer at pH 7.0 was titrated with small aliquot (2 μL) of concentrated lipid (2 mM). After the addition of each aliquot of lipid, the mixture was stirred and incubated for 20 min to allow the complete formation of DNA-lipid complex before the next measurement. The solution was monitored on the UV spectrum to ensure no aggregation within the measured lipid concentration and time scale. Spectra were obtained with excitation at 530 nm (546 nm for N', N'-Dioctylglycinamide) and the emission was monitor from 550 to 750 nm. The intensity at 600 nm (595 nm for N', N'-Dioctylglycinamide) was used to plot the variation curve of fluorescence intensity versus the increment of ratio between lipid and DNA duplex.

Anthraquinone Phosphoramidite Synthesis

The Figure II-1 was followed for synthesis of anthraquinone phosphoramidite.

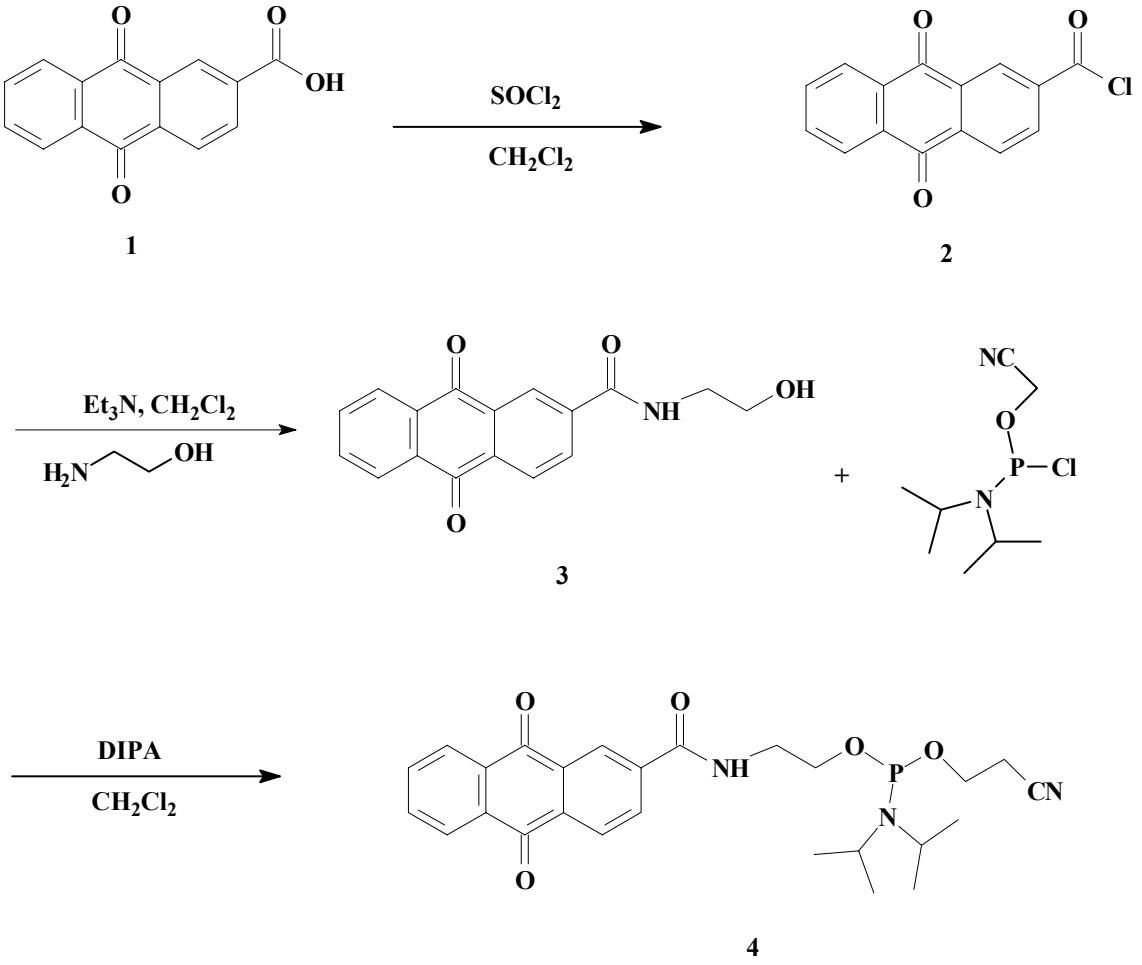

Figure II-1 Synthesis of anthraquinone phosphoramidite.

2-Carbonylanthraquinone chloride (2) A 5.5 mL thionyl chloride was added to 2.0 g (18.6 mmol) of anthraquinone-2-carboxyalic acid in a round bottom flask fitted with a water condenser leading to 1 M NaOH solution. The reaction mixture was heated at reflux for 5 hours while a yellow solid was formed. The solid was collected with a glass

frit and was rinsed several times with 5 mL cyclohexane to wash off excessive thionyl chloride. 2-charbonylanthraqunione chloride was obtained as pale yellow needles after air-dried overnight (1.98 g, 95% yield): Melting Pt: 146.5 ^{o}C (lit 147 ^{o}C)[1]

N-(2-hydroxyethyl)-2-anthraquinonecarboxamide (3) A solution of 687 mg (2.5 mmol) of anthraquinone-2-carbonyl chloride in 20 mL of dry methylene chloride was added dropwise to a solution of 0.61 ml (10 mmol) of 2-aminoethanol and 0.37 ml (2.7 mmol) of triethylamine in 90 ml of methylene chloride. The mixture, which became cloudy upon complete addition of the anthraquinone-2-carbonyl chloride solution, was stirred overnight at room temperature. The solution was filtered and a pale yellow solid was isolated. Recrystallization from hot isopropyl alcohol gave N-(2-hydroxyethyl)-2-anthraquinonecarboxyamide as a dull yellow powder (545 mg, 73% yield). M.P. 199-200 C; 1H NMR (300MHz, DMSO-d6) δ 3.40 (t, J=5.9 Hz, 2H), 3.56(t, J=5.9 Hz, 2H), 4.80(t, J=5.6 Hz, 1H), 7.93-7.99(m, 2H), 8.22-8.36(m, 4H), 8.66(d, J=1.7 Hz, 1H), 8.95(t, J=5.4 Hz, 1H);

N-(2-(O-methoxydiisopropylphosphityl)ethyl)-2- antraquinonecarbox-amide (4). N-(2-hydroxyethyl)-2-anthraqhinonecarboamide (259 mg, 0.878 mmol) was dissolved in dried CH_2Cl_2 (2 mL), followed by addition of DIEA (0.67 mL). The mixture was stirred under N_2 until everything dissolved. To this flask, diisoporpylmethylphosphoramidite (0.17 mL, 0.88 mmol) was added dropwise, yielding a clear orange-red solution upon complete addition, and the reaction was stirred at room temperature for additional 30 min. The mixture was poured into 5 ml of ethyl acetate containing 0.5 ml of triethylamine. The

organic layer was washed twice with 5 ml of 5% sodium bicarbonate, twice with 5 ml of brine and dried over sodium sulfate. Solvent was removed and then applied directly to silica gel column. Elution with CH_2Cl_2:EtOAc:Et_3N (45:45:10) give one major fraction with R_f 0.65 compared to the starting materials R_f 0.55. The solvent was removed under reduced pressure to give dark red oil which was used directly in the DNA synthesis. 1H NMR(300 Mhz, $CDCl_3$) δ 1.19 (dd, j=5.0 Hz, 1.8 Hz, 14 H), 3.46(d, J=13 Hz, 3H), 3.58-3.76(m, 5H), 3.88-3.94(m, 2H), 7.37(br, t, 1H), 7.81-7.84(m, 2H), 8.30-8.41(m, 4H), 8.64(d, J=1.5 Hz, 1H).

Synthesis of C_nGlySp^{4+} Lipids

Ornithine hydrochloride and other reagents for organic synthesis were purchased from Aldrich and Sigma (St. Louis, MO). Dioctadecylamine was purchased from Fluka (Milwaukee, WI). Homogeneity of synthetic products was assessed by thin-layer chromatography performed on 0.25 mm F254 silica gel 60 plates (VWR International). Mass spectra were recorded at the Mass Spectrometry Center by fast atomic bombardment mass spectrometry (FAB-MS) or electrospray ionization mass spectrometry (ESI-MS), using a VG Instruments 70SE and Micromass Quattro LC, respectively.

Figure II-2 and II-3 were followed in synthesis of Diethylamidolglycylspermine (C_2GlySp^{4+}),Dioctylamidoglycylspermine (C_2GlySp^{4+}) and Dioctadecylamidoglycyl-spermine (C_2GlySp^{4+}).[2-5]

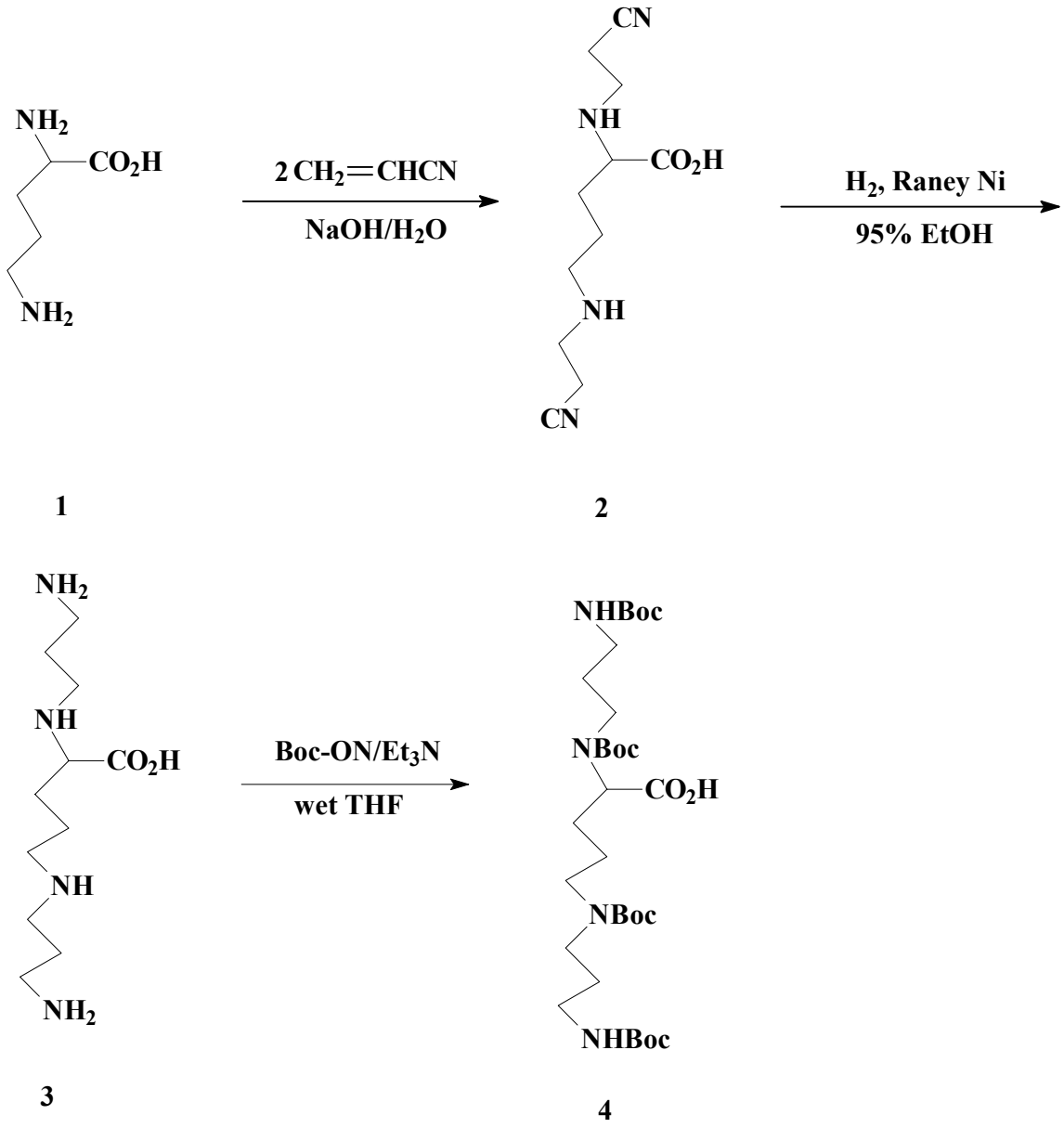

Figure II-2 Synthesis scheme for L-5-carboxylspermine headgroup

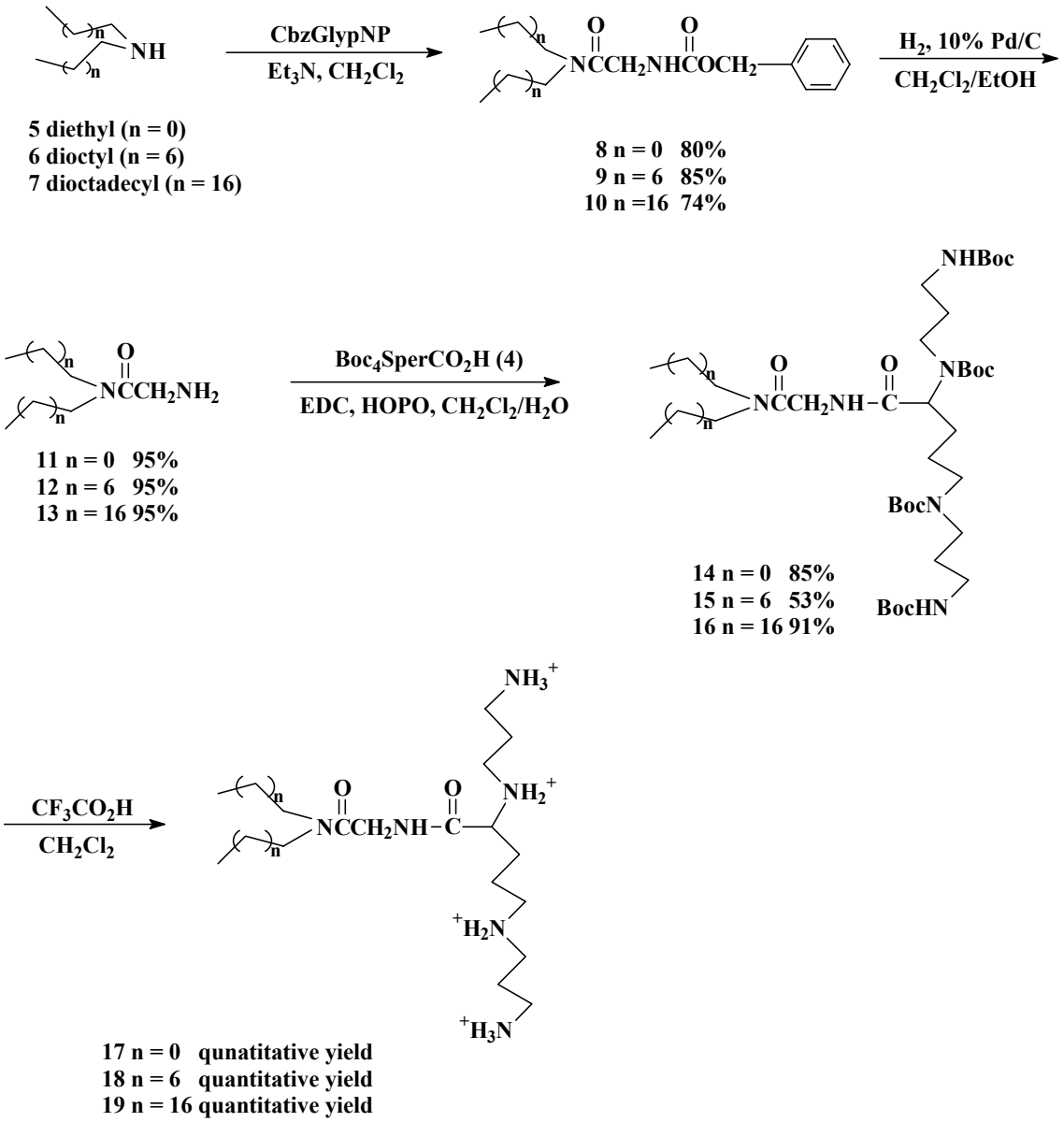

Figure II-3 Synthesis Scheme for diethylamidoglycylsperimine, dioctylamidoglycyl-spermine and dioctadecylamidoglycylspermine.

N^{α}, N^{σ}-diethylcyanide ornithine (2) Method 1. To a stirred solution of 0.5 g (2.97 mmol) L-ornithine hydrochloride dissolved in 12.5 ml MeOH were added 2.75 ml 25wt%(2.2 equiv. 6.53 mmol) tetramethylammonium hydroxide. After dissolution of ornithine salt, MeOH was evaporated. The mixture was then dissolved in 17.5 ml of dry dimethylformamide and the residual ammonium salt ($(CH_3)_4N^+Cl^-$) was filtrated, yielding ornithine as its free base. Following the addition of 6.52 ml acrylonitrile (2.2.euqiv., 6.53 mmol), the mixture was stirred for 16 hours in the dark to give 0.486 g crude product (brown solid). The crude product was never purified. No NMR spectrum reported. m/z 239.5 $(M+H)^+$

N^{α}, N^{σ}-diethylcyanide ornithine (2) Method 2. To L-ornithine hydrochloride salt (0.5 g, 2.97 mmol) dissolved in H_2O (5 ml) in an ice bath was added 1 M NaOH (6 mL) and then acrylonitrile (0.429 mL, 6.52 mmol). Followed by stirring in ice bath for 0.5 h, the reaction mixture was stirring under room temperature for another 15-17 hours. To this solution was added concentrated HCl (0.5 mL, 16.8 M) and ethyl alcohol (17.5 mL). The resulting mixture was left standing at R.T. for 10 hours. The white precipitate was collected by filtration, washed with ethyl alcohol (5 mL) and vacuum dried for 4h, yielding 325 mg crude product **2** (61% yield), white solid. This reactant was used without further purification. ^{1}H NMR ($CDCl_3$) σ 1.48 (m, 4H C**H_2**C**H_2**CHCOOH), 2.63 (m, 6H, 3xCH_2), 2.86 (2xt, J_1= 5.9, J_2=2.7 Hz, 4H, 2xCH_2CN), 3.07 (t, J=7.2 Hz, 1H, -C**H**COOH). m/z 239.4 $(M+H)^+$

5-Carboxyspermine (3). 0.275 g KOH (4.59 mmol) was dissolved in 3 mL 95% ethanol with vigorous stirring. 1.0 g crude N^{α}, N^{σ}-diethylcyanide ornithine was then added. The resulting mixture was placed under H_2 at 40 psi in Burgess-Parry hydrogenator, using 0.199 g Raney Nickel as catalyst.[2-4] After 22 hours, Raney Nickel was removed by filtration and the solvent was evaporated in vacuo, yielding 1.03 g of the crude 5-carboxyl-spermine potassium salt. Yellow oil; ^{1}H NMR ($CDCl_3$) σ 1.53 (m, 2H, C**H$_2$**CHCOOH) 1.65 (m, 6H, $CH_2CH_2CH_2$), 2.51 (m, 4H, 2xC**H$_2$**NH_2), 2.65 (m, 6H, C**H$_2$**NH), 3.09 (t, J=5.7 Hz, 1H, C**H**COOH). m/z 247.3 $(M+H)^+$

Tetra-butoxycarbonyl-5-carboxyspermine (4). To a solution of 5-Carboxylspermine (520 mg, 2.11 mmol) and TEA (0.443 mmol, 3.17 mmol) in mixture of H_2O(3 mL)/THF (6 mL) was added crystalline Boc-ON (2.31 g, 9.28mmol). After stirring for 2 hours the cloudy solution become clear. The mixture was stirred overnight at room temperature. After removing the solvent under reduced pressure, 2N HCl acidify solution to acidic pH=5. Added 15 mL ethylacetate to extract the product. Separated the organic phase and washed the aqueous phase with ethylacetate (2x15 mL). Combined organic phase was dried over $MgSO_4$ and solvent was removed in vacuo. Crude product was purified on silica gel chromatography using EtOAc/Hexane/TEA (1:3:16) to EtOAc/Hexane(1:5), yielding 0.927 g pure tetra-Boc-5-carboxyspermine. Light yellow solid; ^{1}H NMR ($CDCl_3$) σ 1.32 (s, 32H, $(CH_3)_3C$ from Boc), 1.40-1.90 (m, 8H, C**H$_2$**C**H$_2$**N), 2.90-3.20 (m, 10H, CH_2N), m/z 647.3 $(M+H)^+$

N', N'-Diethyl-N-(benzyloxycarbonyl)glycinamide (8). N-CBZ-glycine-p-nitrophenylester (1.58 g, 4.79 mmol) was added to a solution of 0.497 g diethylamine **(5)** (4.79 mmol) and triethylamine (0.484 g, 0.667 mL, 4.79 mmol) in 5 ml of CH_2Cl_2. After the resulting yellow mixture was refluxed for 24 hours, 20 ml ethyl ether Et_2O was added to mixture and extracted with 0.5 M Na_2CO_3 until the hydrolysis of unreacted ester was completed. The organic phase was washed by 1 M HCl (2x10 ml) and Brine (15mL), dried over $MgSO_4$ and evaporated to afford crude product. The crude product was applied on silica gel chromatography and eluted with 1-3% MeOH/CH_2Cl_2, yielding 1.05 g pure pale yellow solid 83% . ^{1}H NMR ($CDCl_3$) σ 1.15 (2xt, 6H, J= 7.2Hz, 2xCH_3), 3.21-3.43 (2xq, 4H, J = 7.2 Hz, $(CH_2)_2$N-), 4.00 (d, 2H, J= 4.2 Hz, COC**H$_2$**NH-), 5.12 (s, 2H, -OCH_2-), 5.85 (s, 1H, NH), 7.35 (m, 5H, C_6**H$_5$**-CH_2). m/z = 265.2 $(M+H)^+$

N', N'-Diethylglycinamide (11). A solution of 1.05 g N', N'-Diethyl-N-benzyloxycarbonyl)glycinamide **(8)** (3.98 mmol) in 8 mL of CH_2Cl_2/EtOH (v:v 1:1) containing 150 mg of 10% Pd/C was hydrogenated during 48 hours at atmospheric pressure. The reaction mixture was filtered through Celite that was further washed with CH_2Cl_2/EtOH (1:1). The N', N'-diethyl-glycinamide filtrate was evaporated, redissolved in CH_2Cl_2, and washed with 0.1 M NaOH. The organic phase was dried with $MgSO_4$ and evaporated under reduced pressure. Crude, grey solid, was purified on silica gel chromatography using 0-3% MeOH/CH_2Cl_2, yielding 0.502g pure product 97%, light yellow solid; ^{1}H NMR ($CDCl_3$) σ 1.09-1.20 (m, 6H, J = 6.9 Hz, 2xCH_3), 3.14-3.42 (2xq, 4H, J = 7.2 Hz , CH_3C**H$_2$**N-), 3.46 (s, 2H, -COC**H$_2$**N-). m/z = 131.1 $(M+H)^+$

N', N'-Diethyl[tetrakis(butoxycarbonyl)sperminecarbonyl]-glycinamide (14). To a solution of 42.3 mg N', N'-diethylglycinamide (0.325 mmol) in 2 ml CH_2Cl_2, were added water solution of Boc-5-carboxyl-spermine (200 mg, 0.309 mmol) and HOPO (35.1 mg, 0.310 mmol). The mixture was cooled down to 0 ºC in ice bath, and then EDC (66.3 mg, 0.340 mmol) was added. The resulting mixture was then stirred at 0-5 ºC for 3 hr before the ice bath was removed. 1 mL TEA was added. The resulting mixture was stirred at room temperature for another 24 hrs. 2 M HCl (2 mL) was added and the layer was partitioned. The organic phase was further washed sequentially with aqueous HCl (0.5 M, 2x5 mL), Brine (10 mL), $NaHCO_3$ (1M, 2x10 ml) and Brine (10 mL). It was then dried over $NaSO_4$, filtered and concentrated under reduced pressure to dryness. The crude was applied on silica gel chromatography and eluted with CH_2Cl_2/MeOH(0%-5%), yielding mg oil, 0.20g 85.1%. ^{1}H NMR ($CDCl_3$) σ 1.15 (m, 6H, 2xCH_3), 1.38-1.45 (m, 36H, 4x$(CH_3)_3$C-), 1.48-2.01 (m, 12H, 4xC**H$_2$**CH_2N-), 3.05-3.35 (m, 14H, CH_2C**H$_2$**N-), 3.24 (s, 1H, -NCOC**H**N-), 3.14-3.42 (2xq, 4H, J = 7.2 Hz , CH_3C**H$_2$**N-), 4.00 (s, 2H, $COCH_2$NH-). m/z = 759.9 $(M+H)^+$

N', N'-Diethyl(sperminecarbonyl)glycinamide, hydrofluoroacetate.(17) 200 mg Compound **(14)** (0.26 mmol) was dissolved in 2 ml CH_2Cl_2. Trifluoroacetic acid (1 mL) was added. The resulting mixture was stirred for 30 min. Then the solvent was removed in vacuo. Procedure was repeated if there is no complete removal of butoxycarbonyl group. 214 mg light yellow oil, quantitative yield. ^{1}H NMR (CD_3OD) σ 0.87 (t, 6H, J=6.0 Hz, 2xCH_3), 1.78-2.16 (m, 8H, C**H$_2$**CH_2N^+), 3.00-3.20 (m, 14H, C**H$_2$**N-, C**H$_2$**N^+), 4.00(t, 1H, J=6.6 Hz, C**H**N^+), 4.14(s, 2H, COC**H$_2$**NH-). m/z = 359.5 $(M+H)^+$

N', N'-Dioctyl-N-(benzyloxycarbonyl)glycinamide (9). N-CBZ-glycine-p-nitrophenylester (1.37 g, 4.14 mmol) was added to a solution of 1 g dioctylamine **(6)** (1.277 mL, 4.14 mmol) and triethylamine (0.419 g, 0.577 mL, 4.14 mmol) in 5 ml of CH_2Cl_2. After the resulting yellow mixture was refluxed for 24 hours, 20 ml ether Et_2O was added to mixture and extracted with 0.5 M Na_2CO_3 until the hydrolysis of unreacted ester was completed. The organic phase was washed by 1 M HCl (2x10 mL) and H_2O (15 mL), dried over $MgSO_4$ and evaporated to afford crude product. The crude product was applied on silica gel chromatography and eluted with 1-3% MeOH/CH_2Cl_2, yielding 1.513 g pure light yellow oil 84.4%. ^{1}H NMR ($CDCl_3$) σ 0.876 (m, 6H 2xCH_3), 1.27 (s, 20H, 2x$(CH_2)_5$), 1.519 (s, 4H, 2xC**H$_2$**CH_2N), 3.14-3.31 (2xt, 4H, J = 7.8 Hz, $(CH_2)_2$N-), 4.00 (d, 2H, J= 4.2, COC**H$_2$**NH-), 5.12 (s, 2H, -OCH_2), 5.84 (s, 1H, NH), 7.32 (m, 5H, C_6**H$_5$**-CH_2). m/z = 433.5 $(M+H)^+$

N', N'-Dioctylglycinamide (12). A solution of 911 mg N', N'-Dioctyl-N-benzyloxycarbonyl)glycinamide (9) (2.11 mmol) in 10 ml of CH_2Cl_2/EtOH (v:v 1:1) containing 200 mg of 10% Pd/C was hydrogenated during 48 hours at atmospheric pressure. The reaction mixture was filtered through Celite that was further washed with CH_2Cl_2/EtOH (1:1). The N', N'-dioctyl-glycinamide filtrate was evaporated, redissolved in CH_2Cl_2, and washed with 0.1 M NaOH. The organic phase was dried with $MgSO_4$ and evaporated under reduced pressure. Crude was purified on silica gel chromatography using 0-3% MeOH/CH_2Cl_2, yielding 531 mg pure product 95.2%. Light yellow oil; ^{1}H NMR ($CDCl_3$) σ 0.87 (m, 6H, 2xCH_3), 1.27 (s, 20H, 2x$(CH_2)_5$), 1.51 (s, 4H,

2xC**H$_2$**CH$_2$N-), 3.12-3.31 (2xt, 4H, J1 = 8.1 Hz , CH$_2$C**H$_2$**N-), 3.44 (s, 2H, -COC**H$_2$**N-). m/z = 298.4 $(M+H)^+$

N', N'-Dioctyl[tetrakis(butoxycarbonyl)sperminecarbonyl]glycinamide (15). To a solution of 100 mg N', N'-dioctylglycinamide (0.336 mmol) in 2 mL CH_2Cl_2, were added water solution of Boc-5-carboxylspermine (206.7 mg, 0.32 mmol) and HOPO (35.6 mg, 0.32 mmol). The mixture was cooled down to 0 ºC in ice bath, and then EDC (67.3 mg, 0.35 mmol) was added. The resulting mixture was then stirred at 0-5 ºC for 3 h before the ice bath was removed. Keep stirring at room temperature for another 36 hrs. 2 M HCl (2 mL) was added and the layer was partitioned. The organic phase was further washed sequentially with aqueous HCl (0.5M, 5 mL), Brine (10 ml), $NaHCO_3$ (1 M, 2x10 mL) and Brine (10 mL). It was then dried over $NaSO_4$, filtered and concentrated under reduced pressure to dryness. The crude was applied on silica gel chromatography and eluted with Hexane/EtOAc(5%-25%), yielding 157 mg light yellow oil, 53.1%. ^{1}H NMR ($CDCl_3$) σ 0.87(m, 6H, 2xCH_3), 1.27(s, 20H, 2x$(CH_2)5$), 1.38-1.45(m, 36H, 4x$(CH_3)_3$C-), 1.48-2.01(m, 12H, 6xC**H$_2$**CH$_2$N-), 3.05-3.35(m, 14H, CH$_2$C**H$_2$**N-), 3.24(s, 1H, -NCOC**H**N-), 4.00(s, 2H, COCH$_2$NH-). m/z = 927.8 $(M+H)^+$

N', N'-Dioctyl(sperminecarbonyl)glycinamide, hydrofluoroacetate.(18) 157 mg Compound **(15)** was dissolved in 2 ml CH_2Cl_2. Trifluoroacetic acid (1 ml) was added. The resulting mixture was stirred for 30 min. Then the solvent was removed in vacuo. Procedure was repeated if there is no complete removal of butoxycarbonyl group. 165mg yellow oil, quantitative yield. ^{1}H NMR (CD_3OD) σ 0.87 (t, 6H, J=6.5 Hz, 2xCH_3), 1.30

(bs, 20H, 2x$(CH_2)_5$), 1.45-1.70 (m, 4H, 2xC**H_2**CH_2N-), 1.78-2.16 (m, 8H, C**H_2**CH_2N^+), 3.00-3.20 (m, 14H, C**H_2**N-, C**H_2N^+**), 4.00 (t, 1H, C**H**N^+), 4.14 (s, 2H, COC**H_2**NH-). m/z = 527.8 $(M+H)^+$

N', N'-Dioctadecyl-N-(benzyloxycarbonyl)glycinamide (10). N-CBZ-glycine-p-nitrophenylester (1.00 g, 3.03 mmol) was added to a solution of 1g dioctadecylamine **(7)** (1.581 g, 3.03 mmol) and triethylamine (0.306 g, 0.421 mL, 3.03 mmol) in 4 ml of CH_2Cl_2. After the resulting yellow mixture was refluxed for 24 hours, 20 ml ether Et_2O was added to mixture and extracted with 0.5 M Na_2CO_3 until the hydrolysis of unreacted ester was completed. The organic phase was washed by 1 M HCl (2x10 ml) and H_2O (15 mL), dried over $MgSO_4$ and evaporated to afford crude product. The crude product was applied on silica gel chromatography and eluted with 1-3% MeOH/CH_2Cl_2, yielding 1.588 g pure light yellow solid (foam) 73.5% . ^{1}H NMR ($CDCl_3$) σ 0.877 (t, 6H, J= 6.6Hz, 2xCH_3), 1.26 (s, 60H, 2x$(CH_2)_{15}$), 1.522 (m, 4H, 2xC**H_2**CH_2N), 3.14-3.31 (2xt, 4H, J = 7.8 Hz, $(CH_2)_2$N-), 4.00 (d, 2H, J= 4.2 Hz, COC**H_2**NH-), 5.12 (s, 2H, -OCH_2), 5.84 (s, 1H, NH), 7.33 (m, 5H, C_6**H_5**-CH_2). m/z = 713.6 $(M+H)^+$

N', N'-Dioctadecylglycinamide (13). A solution of 1.35g N', N'-Dioctadecyl-N-benzyloxycarbonyl)glycinamide **(10)** (1.89 mmol) in 10ml of CH_2Cl_2/EtOH (v:v 1:1) containing 200 mg of 10% Pd/C was hydrogenated during 48 hours at atmospheric pressure. The reaction mixture was filtered through Celite that was further washed with CH_2Cl_2/EtOH (1:1). The N', N'-dioctadecyl-glycinamide filtrate was evaporated, redissolved in CH_2Cl_2, and washed with 0.1 M NaOH. The organic phase was dried with

$MgSO_4$ and evaporated under reduced pressure. Crude, grey solid, was purified on silica gel chromatography using 0-3% MeOH/CH_2Cl_2, yielding 1.037g pure product 94.6%. Light yellow solid; ^{1}H NMR ($CDCl_3$) σ 0.87(m, 6H, J = 6.6Hz, 2xCH_3), 1.25 (s, 60H, 2x$(CH_2)5$), 1.52 (s, 4H, 2x$C\mathbf{H_2}CH_2N$-), 3.14-3.32 (2xt, 4H, J = 7.0Hz , $CH_2C\mathbf{H_2}N$-), 3.76 (s, 2H, -$COC\mathbf{H_2}N$-). m/z = 579.6 $(M+H)^+$

N', N'-Dioctadecyl[tetrakis(butoxycarbonyl)sperminecarbonyl]-glycinamide (16). To a solution of 200mg N', N'-dioctadecylglycinamide (0.345 mmol) in 2 ml CH_2Cl_2, were added water solution of Boc-5-carboxyl-spermine (226.1 mg, 0.35 mmol) and HOPO (38.9 mg, 0.35 mmol). The mixture was cooled down to 0 ºC in ice bath, and then EDC (73.6 mg, 0.385 mmol) was added. The resulting mixture was then stirred at 0-5 ºC for 3 hr before the ice bath was removed. 1 mL TEA was added. The resulting mixture was stirred at room temperature for another 3 days. 2 M HCl (2 ml) was added and the layer was partitioned. The organic phase was further washed sequentially with aqueous HCl (0.5 M, 2x5 mL), Brine (10 ml), $NaHCO_3$ (1M, 2x10 mL) and Brine (10 mL). It was then dried over $NaSO_4$, filtered and concentrated under reduced pressure to dryness. The crude was applied on silica gel chromatography and eluted with CH_2Cl_2/MeOH(0%-5%), yielding 378 mg light yellow oil, 90.7%. ^{1}H NMR ($CDCl_3$) σ 0.87 (m, 6H, 2xCH_3), 1.27 (s, 20H, 2x$(CH_2)_5$), 1.38-1.45 (m, 36H, 4x$(CH_3)_3C$-), 1.48-2.01 (m, 12H, 6x$C\mathbf{H_2}CH_2N$-), 3.05-3.35 (m, 14H, $CH_2C\mathbf{H_2}N$-), 3.24 (s, 1H, -$NCOC\mathbf{H}N$-), 4.00 (s, 2H, $COCH_2NH$-). m/z = 1208.9 $(M+H)^+$

N', N'-Dioctadecyl(sperminecarbonyl)glycinamide, hydrofluoroacetate.(19) 378mg Compound **(16)** was dissolved in 2 mL CH_2Cl_2. Trifluoroacetic acid (1 mL) was added. The resulting mixture was stirred for 30 min. Then the solvent was removed in vacuo. Procedure was repeated if there is no complete removal of butoxycarbonyl group. 165mg yellow oil, quantitative yield. ^{1}H NMR (CD_3OD) σ 0.87 (t, 6H, J=6.0 Hz, 2xCH_3), 1.30 (bs, 60H, 2x$(CH_2)_5$), 1.45-1.70(m, 4H, 2x$C\mathbf{H_2}CH_2N$-), 1.78-2.16 (m, 8H, $C\mathbf{H_2}CH_2N^+$), 3.00-3.20 (m, 14H, $C\mathbf{H_2}$N-, $C\mathbf{H_2}N^+$), 4.00(t, 1H, J=6.6 Hz, $C\mathbf{H}N^+$), 4.14(s, 2H, $COC\mathbf{H_2}$NH-). m/z = 808.9 $(M+H)^+$

References

1. Rei, B. R., Chou, S. H., Cheng, J. W. *J. Mol. Biol*. 1992, 228, 1037-1041

2. Behr, J. P. *J. Chem. Soc., Commun.* 1989, 101-103

3. Bergeron, R. J.; Garlich, J. R. *Synthesis* 1984, 782-784

4. Remy J. S.; Sirlin, C; Vierling, P.; Behr, J. P. *Bioconjugate Chem*. 1994, 5 (6), 647-654

5. Siegel, C. S.; Lee, E. R.; Harris, D. J.; *US Patent 5912239*, 1997

CHAPTER IV

RESULTS AND DISCUSSIONS

Synthesis of Lipids

Many different types of cationic lipids have been synthesized and studied as gene transfection vector or drug delivery system since late 80's.[1, 2] However, most of early studies emphasis on the synthesis and transfection efficiency of novel cation lipid in vivo or in vitro experiment. The structures of the DNA-lipid complexes (lipoplex) were not well accessed in the literatures. Few researches have been done on the relationship between the transfection activity and DNA-lipid complex structures. Recent progress in DNA-lipid structure elucidation suggest three categories of complexes: one with a short-range lamellar structure composed of flat lipid bilayers and DNA packed between them;[3-10] another form in which DNA is encapsulated inside a lipid bilayer, forming cylindrical complexes that are closely package on a hexagonal network;[11] and finally the complexes where DNA attached to the outer surface of the positively charged liposome.[12] This presents the question of the kind of lipid to synthesize in order to meet our research goal.

We selected our target compound based on simplicity and gene transfer efficiency. The higher gene transfer efficiency implies higher binding affinity and formation of the stable hydrophobic layer around the DNA, which consequently compacts DNA and allows DNA-lipid complexes to approach and penetrate the hydrophobic cell membrane effectively. In this research we successfully synthesized four

different lipids, compound 12, 17, 18, 19 (Figure II-3), in which 19 is well known as DOGS with significant activity in transfection. The binding moiety is either glycyl amine (compound 11-13) or spermine group (compound 17-19). The spermine was known for high non-specific binding affinity toward DNA backbond and grooves. At neutral pH, spermine group is protonated with stronger electrostatic interaction towards negatively charge DNA helix.[13, 14] The dialkyl group was expected to act like a hydrophobic shield to reduce the exposure of DNA helix from water molecules. The longer alkyl chain's length should provide the stronger hydrophobic protecting effect. The glycyl spacer allows the free motion of long dialkyl group and minimized the steric hindrance when lipid binds to DNA duplex. The amide functional groups on glycyl also afford it the ability to anchor itself in the grooves of DNA via hydrogen bonds.

Even thought it is expected that compound 17, 18 and 19 are straightforward to synthesize considering their limited synthetic steps and relative simple structures. However compound 19 is a patented compound lack of information on detailed description of synthetic procedure. We met two major obstacles in our experiment. In synthesis of N^{α}, N^{σ}-diethylcyanide ornithine, the reaction always yielded brown solid which is only slightly soluble in MeOH and hard to separate by following the procedure reported in literature.[15-18] We could not identify the structure of impurity. At the beginning of synthesis, one equivalent amount of tetramethylammonium hydroxide was added to neutralize the HCl in L-ornithine hydrochloride via the formation of tetramethylammonium chloride salt which precipitated from MeOH and separated from the solution by filtration. Afterwards, the reaction proceeded with free L-ornithine. We speculated that the excess amount of tetramethylammonium triggered the polymerization

of acrylonitrile, which resulted in obtained brownish polymerized byproduct. By limiting the amount of tetramethylammonium in neutralizing the L-ornithine hydrochloride, the reaction afforded yellow solid with significant percentage of desired product, confirmed by Mass Spectrometry and NMR spectrum. However, we were not able to get product with higher purity. Revised procedure (Method 2) which proceeded without the utilization of tetramethylammonium hydroxide successfully yielded the pure target compound without further purification.

The second challenge came from the coupling of head group (5-carboxylsperimine) and tail group (dialkyl chain). Following the scheme in literature,[19-21] we first applied dicyclohexylcarbodiimide (DCC) as direct coupling agent. The byproduct dicyclohexylurea (DCU) was difficult to be separated from product even after two silica gel column chromatography with MeOH/CH_2Cl_2 and EtOAc/Hexane respectively. We were unable to identify the exact reason since various references showed that the simple filtration could effectively remove the DCU because of its poor solubility in most solvents. Consequently, we attempted the approach other than normal silica gel chromatography to separate the product and DCU. With four amino groups in spermine headgroup, the product can be easily ionized at near neutral pH.[15, 22] The difference in pKa between the product and DCU affords the feasibility to separate them using ion exchange (IE) column. By adjusting the pH of effluent it is possible to firstly elute the DCU, which is less likely to form cation at about neutral pH. On the other hand the ionized product at this pH would stay on cationic IE column because of electrostatic interaction with anionic resin, which can be subsequently flushed out using acidic solution. However, we could not achieve successful separation on IE Column either. The

recrystalization of the compound was attempted in petroleum ether, hexane/EtOAc. We could not get any solid precipitate from either solvent system. We ascribed this to the nature flexible structure of the compound. The long aliphatic chain moiety makes it less likely to sustain solid form. Finally, we decided to explore new coupling reagents. After looking into literatures several candidates were found (Figure 29).[23-28] 1-ethyl-3-(3-dimethylaminopropyl)-carbodiimide (EDC) is the most appealing one because its similarity to DCC and easy separation of byproduct 1-ethyl-3-(3-dimethylaminopropyl)-urea (EDU) that is water soluble at low pH. Most of EDC coupling reactions were carried out in the presence of additives to suppress the side reaction and reduce the racemization in peptide synthesis. Various additives were tested in peptide amide bond formation reaction, which showed HOPO and HOBt were superior in improving the yield and preservation of chiral integrity.[29] We successfully carried out the coupling reaction with EDC/HOPO as the coupling agent and obtained final products in satisfactory yield.

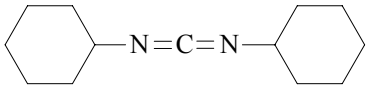

DCC (Dicyclohexylcarbodiimide)

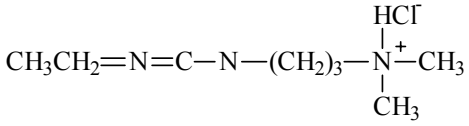

EDC (1-ethyl-3-(3-dimethylaminopropyl)-carbodiimide) hydrochlo

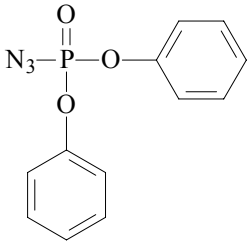

DPPA (Diphenylphosphoryl Azide)

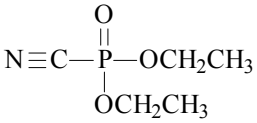

DEPC (Diethylphosporyl Cyanide) Diethyl Cyanophosponate

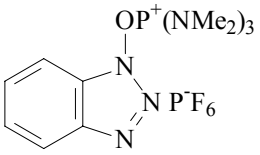

B.O.P. (1'-hexafluorophosphate Benzotriazolyl N-Oxytrisdimethyalamino Phosphonium)

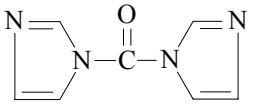

N, N'-Carbonyldiimidazole

Figure III-1 Several amide coupling agents

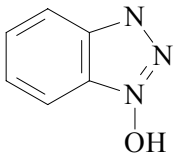

1-hydroxybenzotriazole (**HOBt**)

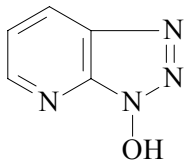

1-hydroxy-7-azabenzotriazole (**HOAt**)

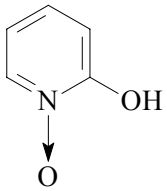

2-hydroxypyridine-N-oxide(**HOPO**)

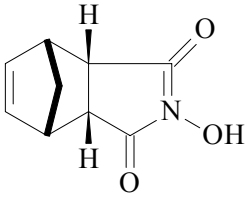

endo-N-hydroxy-5-norbornene-2,3-dicarboximide (**HON**

Figure III-2 Several EDC coupling reaction additives

Preliminary Study on N', N'-dioctylglycinamide Effect on Guanine Damage

N', N'-dioctylglycinamide is the first compound we synthesized. Effect of this compound on charge transfer in DNA was investigated using DNA (I) (Figure III-5) sequence. The result was shown in Figure III-3. No significant difference was seen except that land 5 and 7 show slightly more proximal and distal damage than normal DNA without adding any lipid compound (lane 3). Since this compound was not effective in gene transfection,[17] it is possible there is little binding interaction between this lipid and DNA duplex. No protection from the reaction with the water could be provided if there were no association between lipid and DNA. We further investigated binding between N', N'-dioctylglycinamide and DNA duplex using fluorescence quenching experiment.

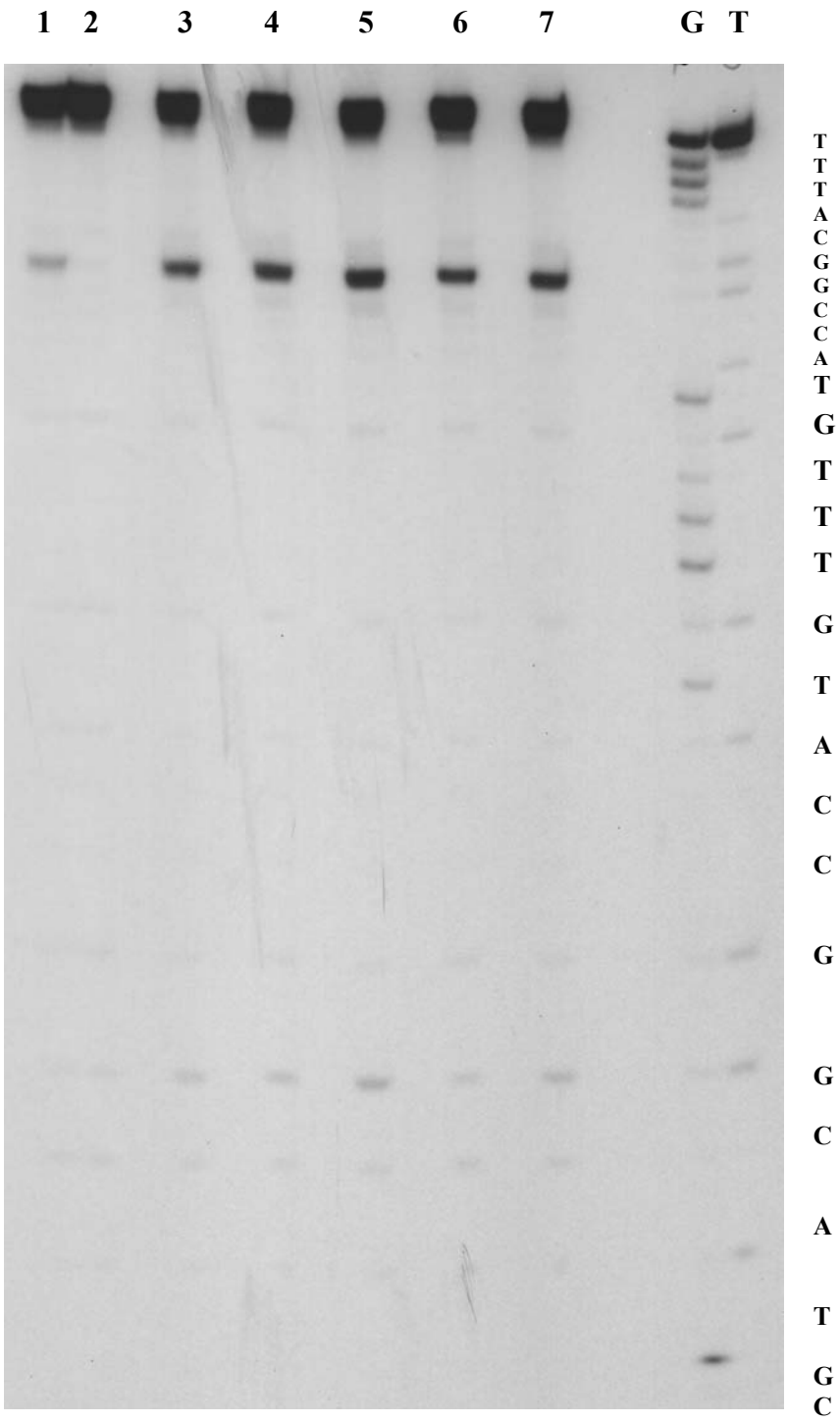

Figure III-3 Autoradiogram of a denaturing gel electrophoresis for 5'-32P-labeled DNA(I) with N', N'-dioctylglycinamide. light control (Lane 1), dark control (Lane 2), irradiation with lipid/DNA ratio at 2:1, 1:1, 1:2, 1:4, 1:8 (Lane 3, 4, 5, 6, 7). The last two Lanes are Maxam-Gilbert T and G sequencing lanes. All samples were irradiated at 350 nm for 5 min, followed by piperidine treatment at 90 °C for 30 min.

No effect of lipid on charge transport in DNA can be attributed to several reasons. One possibility can be no or little binding affinity of this particular lipid toward DNA duplex. One effective way to identify the binding interaction between DNA and lipid compound is to investigate the displacement of DNA bound ethidium bromide by target compound, which would subsequently quench the fluorescence if the ethidium bromide was expelled from the intercalation into DNA helix. [3, 19-21]

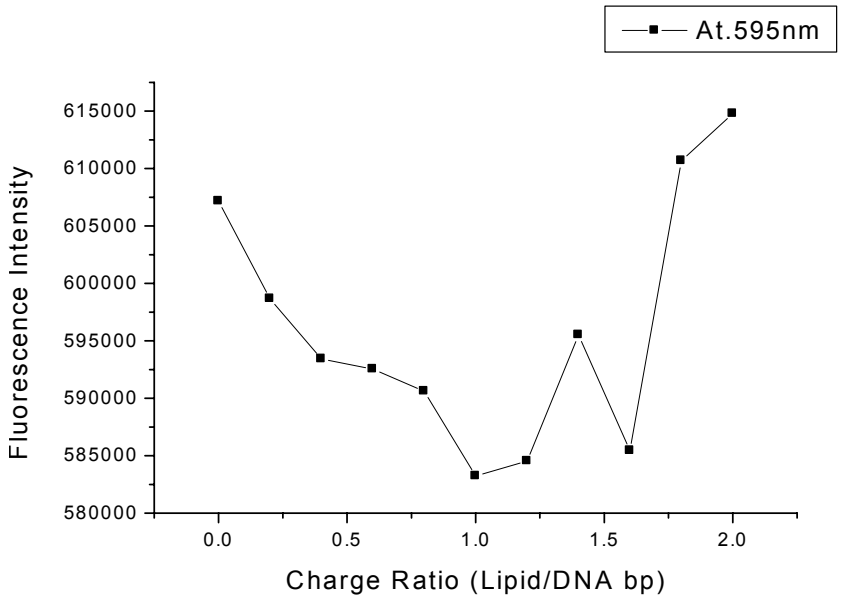

Figure III-4 Effects of N', N'-Dioctylglycinamide on the fluorescence of DNA-lipid complex. As a function of total positive charge (lipid) and negative charge (nucleotides), DNA concentration was kept at 5.0 μM with 10 μM EB.

The result from fluorescence experiment provides the answer to the question why there was little difference in UV irradiation experiment between DNA and DNA-lipid mixture. There was no significant decrease in fluorescence intensity with the addition of

N', N'-Dioctylglycinamide. Many studies reported the reduction of fluorescence intensity to about 20%-40% of original fluorescence intensity with the titration of lipid compound.[19-21] In our experiments, the slight variant is expected as the function of instrumental fluctuation and dilution of overall DNA-EB concentration while adding lipid solution. This compound failed to replace EB in DNA-EB complex to quench the fluorescence, which implied that the origin of PAGE experiment results stem from the lack of binding affinity of this particular molecule to DNA.

With the preliminary result we further synthesized three new lipids compounds, C_2GlySp^{4+}, C_8GlySp^{4+} and $C_{18}GlySp^{4+}$ with improved binding affinity towards DNA duplex so that we can move forward to perform more extensive studies to characterize the charge transport in DNA-lipid complexes.

Characterization of DNA-spermine and DNA-lipid Complexes

UV Absorption Spectra: The proof of AQ coupling with DNA oligomer

All non-AQ containing synthetic DNA oligomers were identified with Mass Spectrometry and subject to Maxam-Gilbert A/G and T sequencing in order to make sure the desired sequences were obtained. AQ-DNA conjugate can be further determined by screening the Ultra-violet absorption spectra at 350 nm besides the methods mentioned above. The DNA oligonucleotides are characterized by a strong absorbance at 260 nm shown in Figure III-6. The molar absorptivity is related to the base sequence in oligomers, which is ε_{260} = 246,500 $Lmole^{-1}cm^{-1}$ for DNA(I) and ε_{260} = 280,800 $Lmole^{-1}cm^{-1}$ for AQ-DNA(I). (Figure III-5) The AQ photosensitizer also has a significant absorbance at this particular wavelength, with ε_{260} = 55,600 $Lmole^{-1}cm^{-1}$. (Table III-1) The additional absorbance wavelength at 350 nm distinguished the AQ coupled DNA from non-AQ DNA oligomer. However, the extinction coefficient (ε_{334} = 6,900 Lmole-1cm-1) is much lower at this wavelength. The covalent-binding of anthraquinone to the DNA oligonucleotide can be confirmed by inspecting the UV-visible spectra at this wavelength as pointed by arrows in Figure III-6. The AQ are expected to associate with DNA terminus by end capping.[30, 31] Majima and coworkers also reported a similar association mode with respect to naphthalimide and phenothiazine derivatives attached to 5' and 3'-end of DNA duplex respectively.[32, 33] The short ethyl linker between AQ and 5' terminal base prohibits the intercalation into the DNA helix but allows the radical cation injection into either strand of the DNA duplex. The injection efficiency is dependent on G:C or

A:T pair but irrelevant to whether the AQ is attached to purine or pyrimidine of the pair.[34]

5′-AQ-AAATG CC GGTACAAACATGG CC GTACG-3′

3′-TTTAC **GG** CCATGTTTGTACC **GG** CATGC-5′

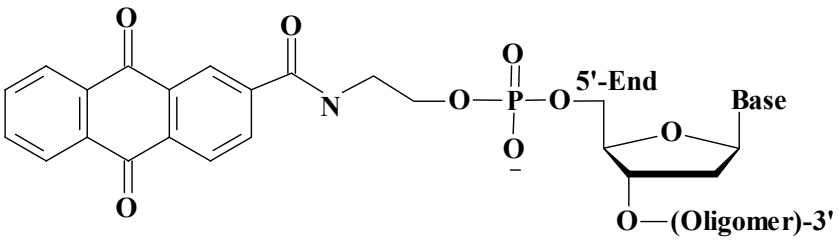

Figure III-5 DNA (I) sequence and 5'-linked anthraquinone photosensitizer.

Table III-1 Molar extinction coefficient of oligonucleotides and anthraquinone [35]

Wavelength (nm)	Molar Extinction Coefficient ($M^{-1}cm^{-1}$)				
	A	C	G	T	AQ
260 nm	15400	7400	11500	8700	18900

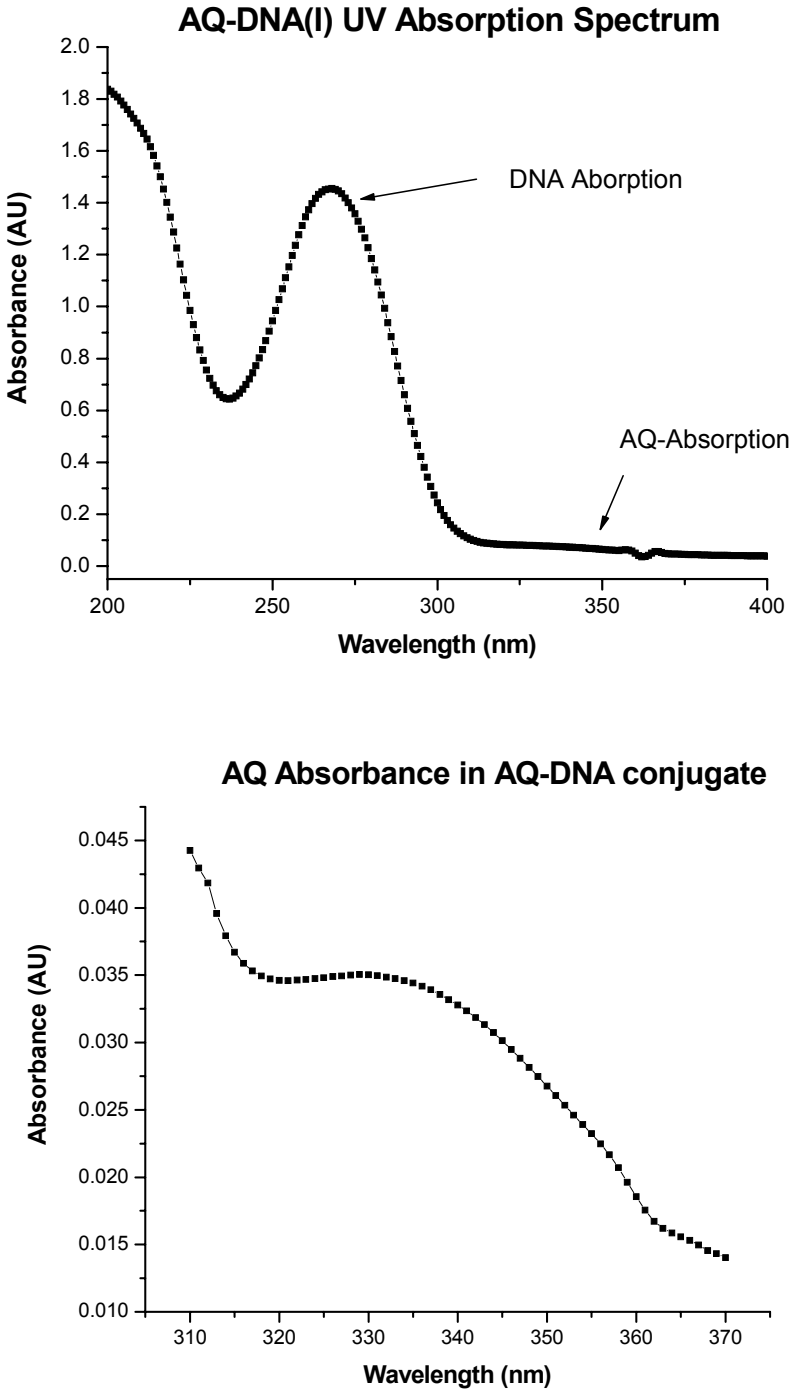

Figure III-6 AQ-DNA(I) Absorption Spectrum. The sample contains 5 μM DNA single strand. The enlargement of the absorbance spectrum between 350 nm and 370 nm was shown to indicate the covalent-binding of the chromophore to the oligomer.

Thermal denaturation: Stabilization of DNA duplex by lipids

Thermal denaturation behavior of DNA can reveal the stability and cooperativity of the oligonucleotides, in which two complimentary DNA sequences are subject to repeated heating and cooling cycles. The UV absorbance at 260 nm is monitored as the temperature ramps between 15 ^{o}C and 90 ^{o}C. DNA duplex will begin denaturation and re-naturation when the temperature is near its "melting" temperature (T_m), at which 50% of oligonucleotide and its complement are in duplex. The melting effect results in the increase in the UV absorption by about 40% due to the release of hyperchromicity in the base stacking with nearby bases. Once the duplex completely unraveled to two single strands, the increase in absorption is no longer evident. In the cooling cycle, the two single strands revert back to the duplex form and the cooperativity is measured. Because the stronger hydrogen bonds between G:C base pairs, one more hydrogen bond than that between A:T base pairs, (Figure I-2) DNA sequences with more G:C base pairs generally show higher melting temperature than those with the same length but less G:C base pairs. The melting behavior depends not only on the duplex itself, i.e. sequence and length, but also the salt concentration, solvation effect, modification and the present of other compounds with affinity to DNA duplex. The negatively charged phosphate groups in the DNA double helix are close together and will tend to repel one another unless they are neutralized. Since the concentration of salt (cations) in solution will affect the degree of neutralization, the stability of DNA double helices also depends on the salt concentration. In the cell, neutralization is achieved through salt ions, polyamines and special DNA-binding proteins.

Previous research established that some cationic surfactants/lipids have the ability to accelerate the re-naturation of DNA duplex and stabilize the formation of DNA helix.[36] Berg et al. showed that simple cationic detergents significantly enhanced the re-naturation rates by more than 2000-fold than the rate in 1 M NaCl at 68 ^{o}C in the presence of up to 106-fold excess of noncomplementary sequences, which is very similar to nuclear ribonucleoprotein A1 protein. They attributed the observation to their ability to bind to nucleic acid strands and present flexible, weakly interacting domains with a repeating structure.

We examined the thermal denaturation behavior of DNA (I) (Figure III-7) upon the addition of spermine and lipids. (Figure III-2) The addition of 1 to 4 equivalents (charge ratio) of spermine or lipids to solution containing DNA(I) shows an expected increase in observed T_m only when the concentration of additives is low, below 1:2 charge ratio in most cases. Only spermine and C_2GlySp^{4+} showed consistent increase in T_m even when the concentration of additive increased up to 1:4 charge ratio, i.e. 135 μM with 2.5 μM 27-base paired DNA duplex. The T_m of DNA(I)-spermine increases from 58.9 ^{o}C to 72.9 ^{o}C when the concentration of spermine rise from 0 to 4.0 charge ratio. C_2GlySp^{4+} lipid helped to stabilize the DNA by 11 ^{o}C, from 58.5 ^{o}C to 69.3 ^{o}C, under the same condition. On the other hand, C_8GlySp^{4+} lipid stabilized DNA duplex by 4 ^{o}C once the concentration increased from 1:0 to 1:2 charge ratio with DNA. (Figure III-10) But no melting behavior was obtained with higher concentration of C_8GlySp^{4+} lipid. In the case of DNA-$C_{18}GlySp^{4+}$ the denaturation transition was not observed once lipid concentration was higher than 2:1 charge ratio. These findings indicate that lipids stabilize the formation of DNA duplex at lower concentration but may denature the DNA

or destabilize the DNA duplex in aqueous solution at higher concentration. The latter effect may be related to hydrophobic tail group of lipids since the longer the alkyl chains are, the more significant the hydrophobic effect is. If the lipids packages DNA duplex inside a hydrophobic micelles, the resulting lipoplex can aggregate into water insoluble particle where no melting transition can be observed in our experiment.

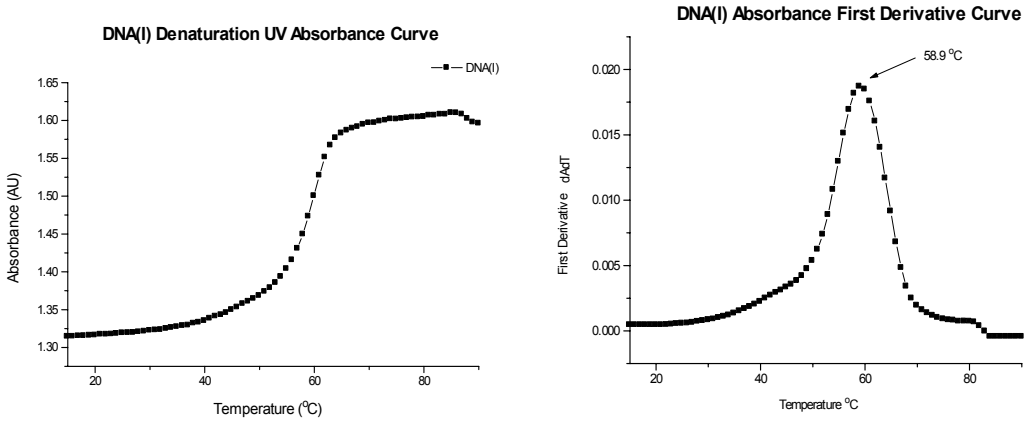

Figure III-7 DNA(I) denaturation UV absorbance curve and its first derivative curve. The sample contains 2.5 μM DNA(I) duplex in 10 mM sodium phosphate buffer at pH 7.0.

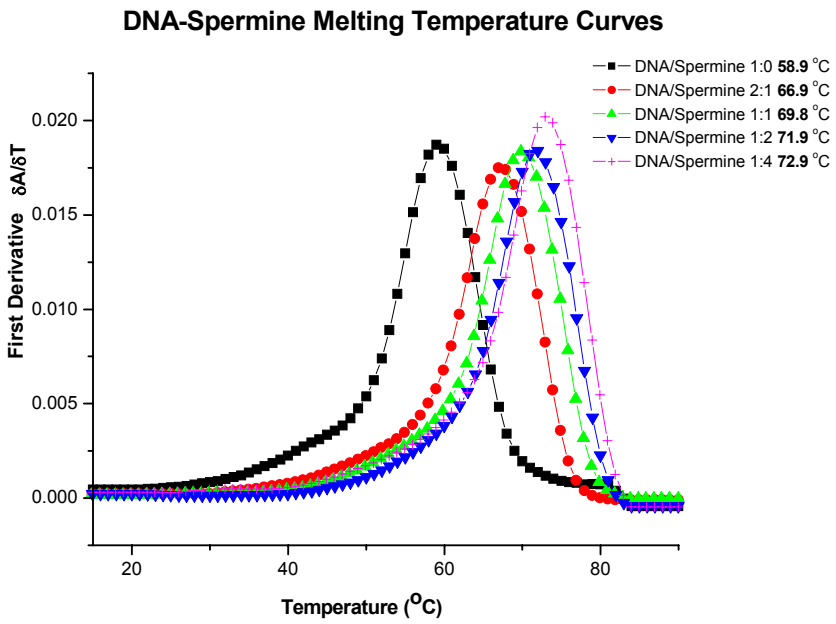

Figure III-8 Thermal denaturation of DNA(I) duplex with addition of spermine. Each sample contains 2.5 μM DNA duplex in 10 mM sodium phosphate buffer at pH 7.0 and the corresponding amount of spermine as indicated. The increase in melting temperature is a clear indication of stabilized DNA helix structure induced by spermine.

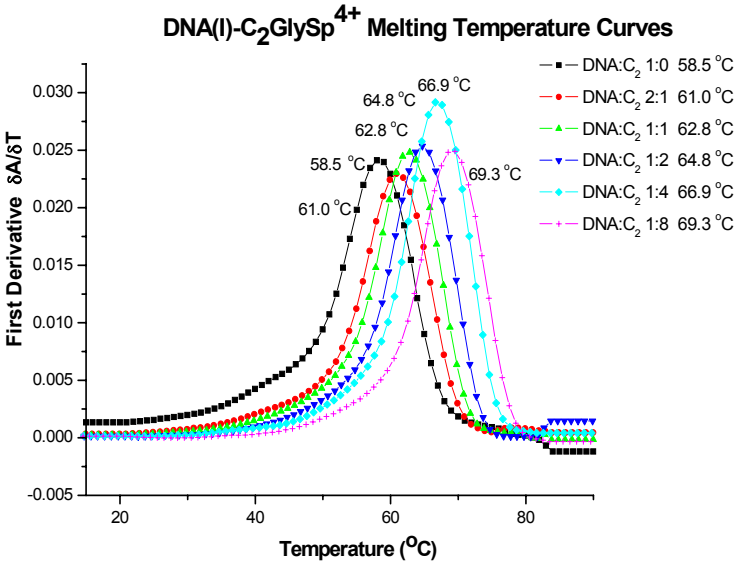

Figure III-9 Thermal denaturation of DNA(I) duplex with addition of C_2GlySp^{4+} lipid. Each sample contains 2.5 μM DNA duplex in 10 mM NaPi buffer (pH 7.0) and corresponding amount of C_2GlySp^{4+} as indicated. The curves are first derivative of absorbance against temperature.

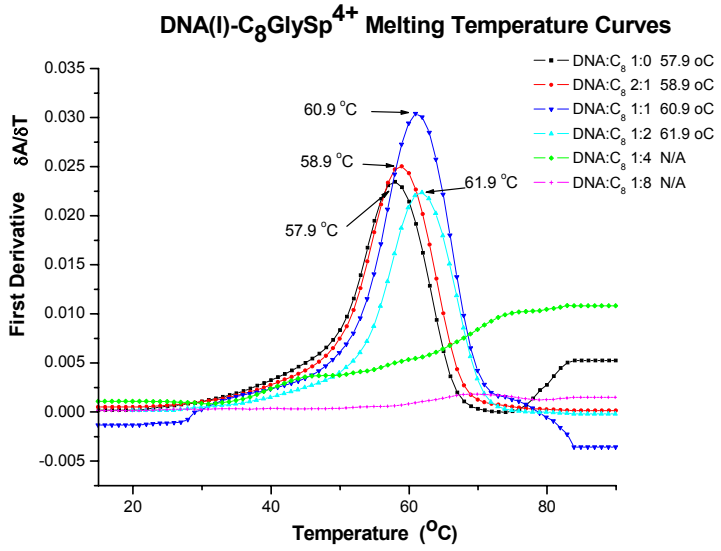

Figure III-10 Thermal denaturation of DNA(I) duplex with addition of C_8GlySp^{4+} lipid. Each sample contains 2.5 μM DNA duplex in 10 mM NaPi buffer (pH 7.0) and corresponding amount of C_8GlySp^{4+} as indicated. The increasing melting temperature is an indication of stabilized DNA helix structure induced by C_8GlySp^{4+} lipid. The flat curve for higher charge ratio indicated the no thermal transition of DNA duplex.

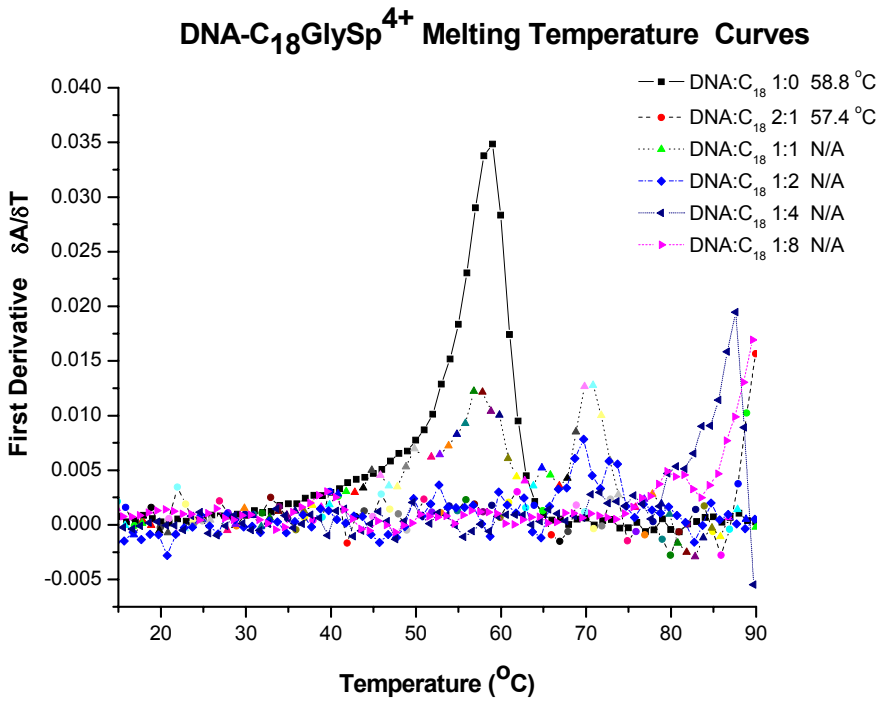

Figure III-11 Thermal denaturation of DNA(I) duplex with addition of $C_{18}GlySp^{4+}$ lipid. Each sample contains 2.5 μM DNA duplex in 10 mM NaPi buffer (pH 7.0) and corresponding amount of $C_{18}GlySp^{4+}$ as indicated. The increase in melting temperature is an indication of stabilized DNA helix structure induced by $C_{18}GlySp^{4+}$ lipid. The flat curve for higher charge ratio indicated no thermal transition of DNA duplex

Table III-2 T_m Data for DNA(I) with addition of various lipids at different concentrations

Lipid	*T_m (^oC)*				
	1:0	2:1	1:1	1:2	1:4
Spermine	58.9	66.9	69.8	71.9	72.9
C_2GlySp^{4+}	58.5	61.0	62.8	64.8	66.9
C_8GlySp^{4+}	57.9	58.9	60.9	61.9	N/A
$C_{18}GlySp^{4+}$	58.8	57.4	N/A	N/A	N/A

Note: All samples contain 2.5 μM DNA(I) duplex in 10 mM sodium phosphate buffer at pH 7.0. The ratio represents the charge ratio between DNA(I) duplex (54 negative charges) and lipids (4 positive charges)

Circular Dichroism: DNA conformation determination

Circular dichroism is an extremely useful tool in detecting the secondary structural alteration in DNA helical conformation because its spectra are very sensitive to any chirality change in optically active molecules. The chiral nature of the DNA helix gives rise to a strong CD signal which is seen to vary under certain condition, e.g. state of hydration, temperature, binding of macromolecules. Therefore, we can detect the secondary structure transition in DNA duplex by inspecting the corresponding CD spectra. Typical CD spectra for B-form DNA show one positive OD at 270 nm and one negative OD at 240 nm. Both are in ultraviolet wavelength because these are the regions where the electronic transition of purine and pyrimidine base in DNA occurs.

Native DNA (I) oligomer shows typical CD spectrum for B-form DNA. Not much change was observed for DNA-spermine and DNA-C_2GlySp^{4+} solution. However, it is evident that both peaks at 240 nm and 270 nm diminished with increasing C_8GlySp^{4+} and $C_{18}GlySp^{4+}$ concentration when DNA was hybridized with those lipids (Figure III 11-12) This indicates either a significant structural change in DNA helix or a significant lower DNA concentration in aqueous phase of the solution. It is well known that A-form DNA, as well as C-form DNA, which generally form under dehydrated condition or high salt concentration, possesses the different CD signal from B-form DNA.[37-40] If C_8GlySp^{4+} or $C_{18}GlySp^{4+}$ reduces the water accessibility as we expected and disturbs the hydration spine along the DNA grooves, it is likely that some of DNA helixes switch towards A-like or C-like conformation and yield overlapping spectrum with that from B-form DNA that shows diminished signal at both peak wavelength. Lipids were widely used as gene transfer factors and DNA condensing agents to facilitate the transfection through cell

membrane. The high concentration of lipids can not only condense DNA to compact form but also accelerate the formation of aggregate, which is unstable in aqueous solution.[10, 41] In such case, the concentration of DNA in aqueous phase decreases dramatically that eventually leads to the weaker signal in CD spectra in an alternative way.

Our further examination using UV spectrum eliminates the former possibility and supports the second explanation that DNA precipitates out from the aqueous solution during the hybridization process at the presence of lipids. (Figure III-14-18)

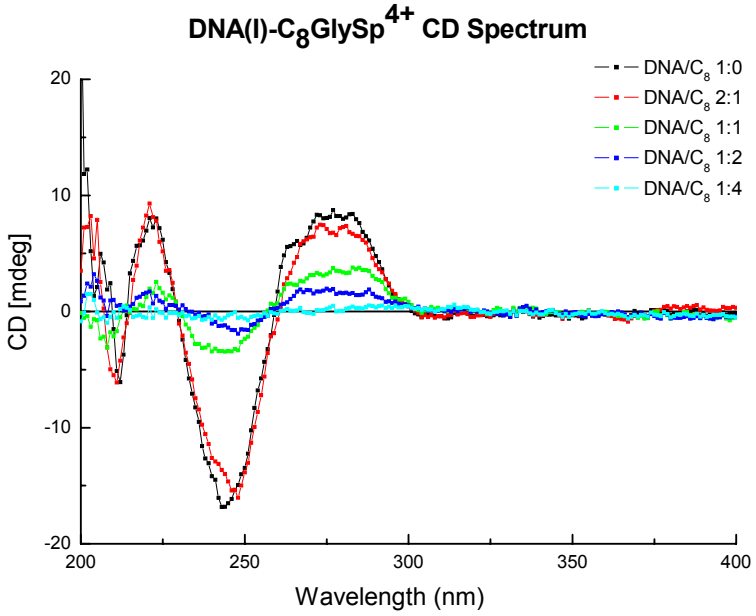

Figure III-12 CD spectra of DNA(I) solution) with various amount of C_8GlySp^{4+} lipid. 2.5 μM DNA(I) in 10 mM sodium phosphate, pH 7.0 after co-hybridization. The spectra were monitored from 200 nm to 400 nm and a drastic decrease in CD signal change was observed.

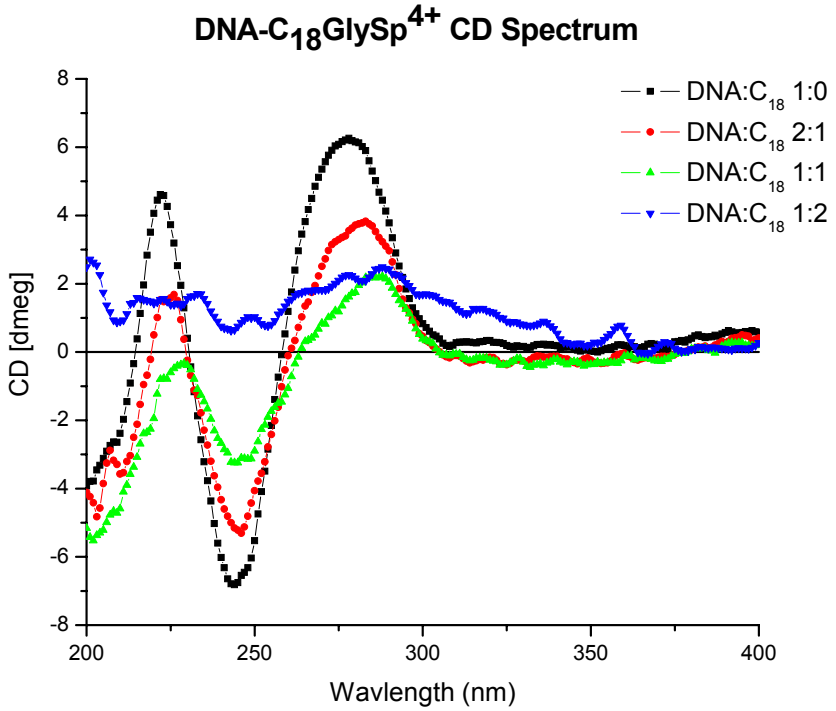

Figure III-13 CD spectra of DNA(I) solution with various amount of $C_{18}GlySp^{4+}$ lipid . 2.5 μM DNA(I) in 10 mM sodium phosphate, pH 7.0 after co-hybridization. The spectra were monitored from 200 nm to 400 nm and a drastic decrease in CD signal change was observed.

UV Time-Dependent Experiment: lipids induced aggregation

The melting temperature data were obtained from first derivative curves of absorbance-time UV data as shown in Figure III-7. The native DNA duplex yields well-defined transition stage and a relative sharp peak indicating the melting temperature. In order to get comparable results, all the samples consist of 2.5 μM DNA duplex in 10 mM sodium phosphate buffer. The only difference between samples lies in the type and concentration of lipids added into the solution. By inspecting the original UV data, those samples, from which no obvious transition was obtained, showed much lower UV absorbance during heating and cooling process. This is an indication of loss of DNA in

aqueous phase. Polyamines were widely used to condense long sequence DNA and genome to form condensate.[42] It is possible that oligomer-lipid complex grow into an aggregate form that is insoluble in aqueous phase due to hydrophobic effect when the concentration of lipid is above certain critical point. Therefore, UV absorbance dropped dramatically upon adding the large amount of lipid solution.

We further evaluated the stability of DNA-lipid complex by monitoring the UV spectrum over the long period of time. In this experiment DNA duplex was hybridized prior to the addition of lipid to prevent the possible effect on DNA hybridization process. The spermine and C_2GlySp^{4+} do not affect the UV spectra of DNA duplex even at high concentration as much as 1:4 charge ratio (135 μM). (Figure III-14) At a stark contrast, A remarkable enhance at the first three hours followed by a sharp decrease in absorbance was observed for both C_8GlySp^{4+} and $C_{18}GlySp^{4+}$ lipids at the high concentrations. At lower concentration, DNA-C_8GlySp^{4+} is stable at up to 1:2 charge ratio (67.5 μM) and DNA-$C_{18}GlySp^{4+}$ is stable at 1:1 charge ratio but with significant rise in UV signal, which is interpreted as light scattering from the small liposome and aggregate formed by excessive lipids.[43]

Those findings explained the experimental results from melting temperature and circular dichroism measurement. The dramatic decrease in UV absorbance indicates the lower concentration of DNA duplex in solution which, consequently, yields flat denaturation transition and lower CD signal.

$C_{18}GlySp^{4+}$ affects the stability of DNA duplex in aqueous solution most effectively while C_8GlySp^{4+} has less profound outcome. When the length of alkyl tail group was reduced to diethyl or none, in case of spermine, no effect was observed.

Considering the same DNA-binding head group possessed by all lipids and spermine, this trend clearly points out the root of destabilization lies in the dialkyl moiety in lipids' structure. $C_{18}GlySp^{4+}$, know as DOGS, is a very efficient gene transfection vector with high affinity to the DNA and ability to induce DNA into compact form.[1] In our experiment, its long didodecyl chains make it easily to form secondary bilayer or micelle structure to prevent the exposure to high polar water solution and stability itself. However, this effect also leads to the aggregation of DNA-$C_{18}GlySp^{4+}$ complex that is not very soluble in aqueous phase. Herein, the precipitation of aggregate was observed with loss of UV absorbance.

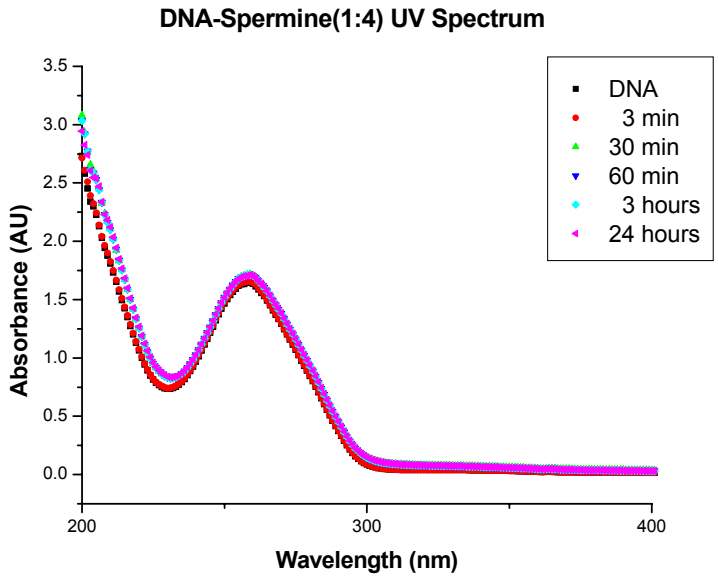

Figure III-14 UV spectra of DNA(I) solution after the addition of 1:4 charge ratio spermine. There are 2.5 μM DNA(I) and 135 μM spermine. The spectra were monitored over 24 hours and no significant change was observed.

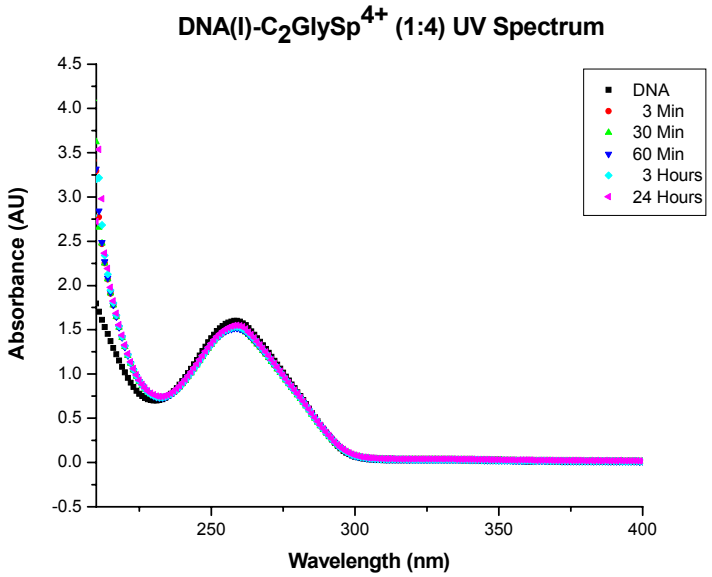

Figure III-15 UV spectra of DNA(I) solution after the addition of 1:4 charge ratio C_2GlySp^{4+} lipid. There are 2.5 μM DNA(I) and 135 μM C_2GlySp^{4+} The spectra were monitored over 24 hours and no significant change was observed.

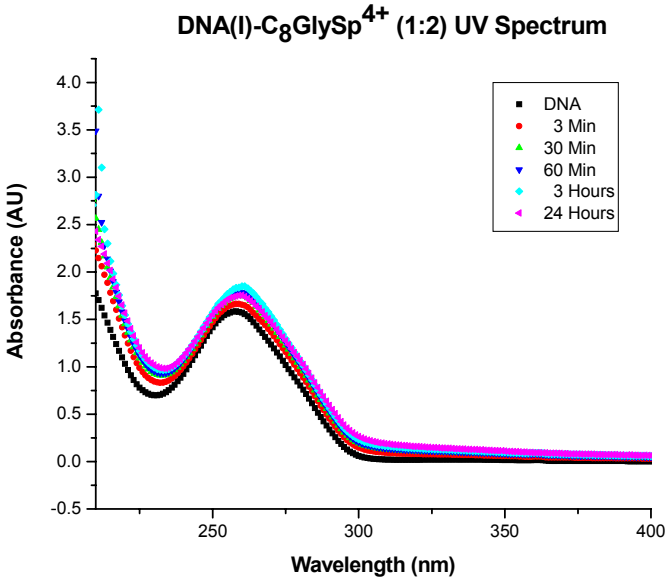

Figure III-16 UV spectrum of DNA(I) duplex solution after the addition of 1:2 charge ratio C_8GlySp^{4+} lipid. The sample contains 2.5 μM DNA(I) and 67.5 μM C_8GlySp^{4+} in 10 mM NaPi buffer at pH 7.0. The spectra were monitored over 24 hours and no significant change was observed.

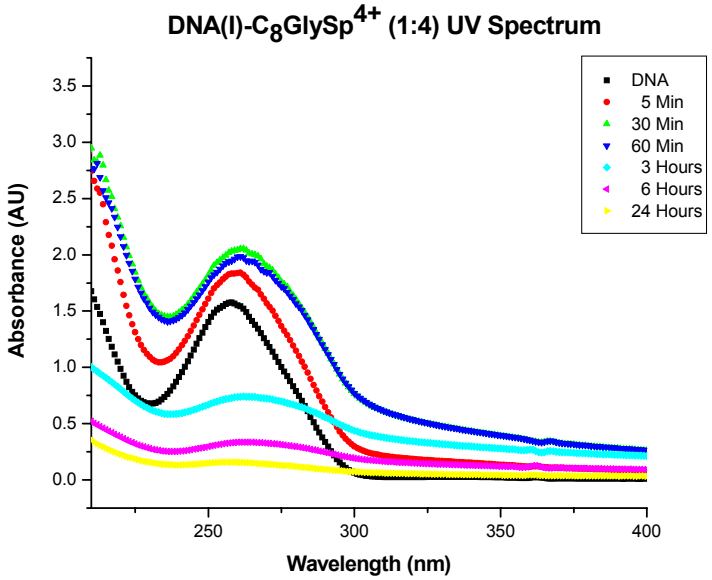

Figure III-17 UV spectra of DNA(I) duplex solution after the addition of 1:4 charge ratio C_8GlySp^{4+} lipid. The sample contains 2.5 μM DNA(I) and 135 μM C_8GlySp^{4+} in 10 mM NaPi buffer at pH 7.0. The spectra were monitored over 24 hours and a drastic decrease in UV absorbance was observed.

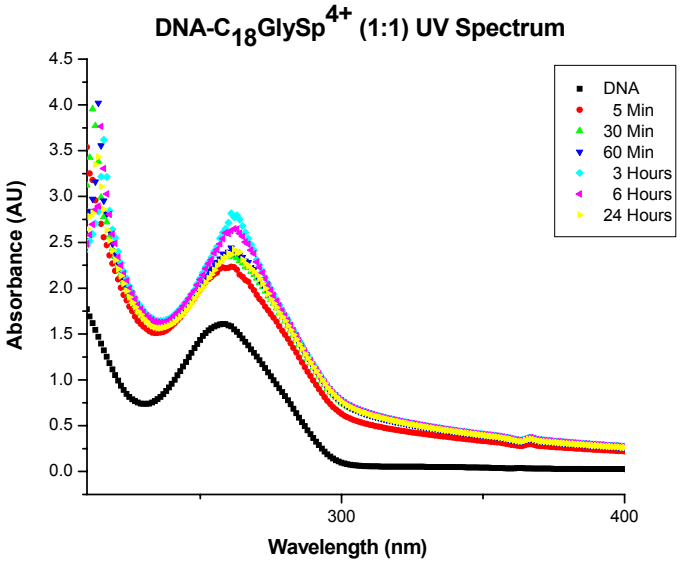

Figure III-18 UV spectra of DNA(I) duplex solution after the addition of 1:1 charge ratio $C_{18}GlySp^{4+}$ lipid. The sample contains 2.5 μM DNA(I) and 33.8 μM $C_{18}GlySp^{4+}$ in 10 mM NaPi buffer at pH 7.0.The spectra were monitored over 24 hours and a drastic decrease in UV absorbance was observed.

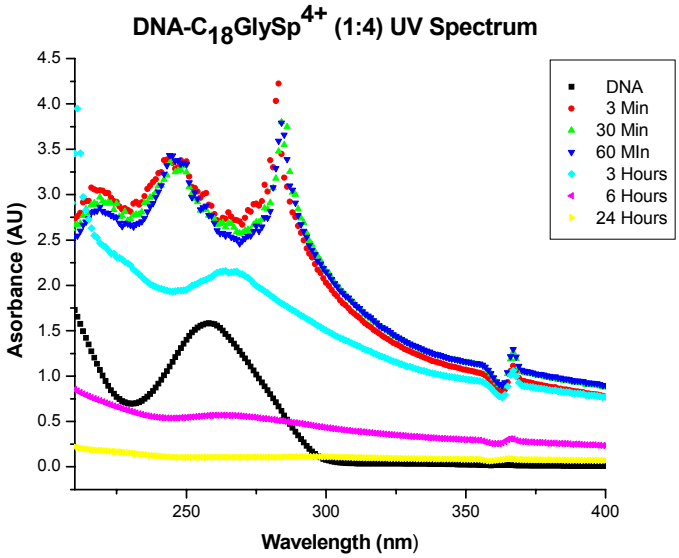

Figure III-19 UV spectra of DNA(I) duplex solution after the addition of 1:4 charge ratio $C_{18}GlySp^{4+}$ lipid. The sample contains 2.5 μM DNA(I) and 135 μM $C_{18}GlySp^{4+}$ in 10 mM NaPi buffer at pH 7.0.The spectra were monitored over 24 hours and a drastic decrease in UV absorbance was observed.

Time Dependent Circular Dichroism: monitor the structural alteration in DNA-lipid complexes

From previous CD experiments, it was observed that DNA-lipid complexes were not stable even at low concentration, i.e. the charge ratio of 1:2, if we hybridized the DNA in the presence of lipids. The decline in both CD and UV signal intensity demonstrated unstable DNA-lipid complexes in aqueous solution. However, UV spectra did not show significant change over the course of 24 hours provided the lipid was added after the hybridization of DNA duplexes. The different preparation method afforded the different stability of DNA-lipid complexes. The further experiment was carried out to investigate if there is the similar effect in CD spectrometry and if the complexes formed

in the latter approach possess any different structure from the regular native DNA duplexes.

CD spectra of DNA duplex solutions were monitored for over the period of 24 hours after the addition of spermine and lipid compounds.(Figure III-20-III-23) No significant change was observed for spermine, C_2GlySp^{4+} and C_8GlySp^{4+}, up to 1:4, 1:4 and 1:2 charge ratio respectively. With 1:3 charge ratio of C_8GlySp^{4+}, CD spectrum started to show the decrease at positive peak around 220 and 270 nm where the maximum of both peaks shifted toward blue region, whereas the negative peak at around 240 nm did not shift or decrease. This is a prominent indication of DNA's secondary structure transformation. This transformation is even more profound for the samples with $C_{18}GlySp^{4+}$, two positive maxima and one negative maximum started declining and blue shifting even at relative low concentration of lipid, which extended when we increased the concentration of $C_{18}GlySp^{4+}$. The observation from those CD experiment is complimentary to the data from time dependant UV measurement and confirmed that the concentration of lipid is critical to control the formation of stable DNA-lipid complex in aqueous solution without significantly disturbing DNA's secondary structure.

The conditions under which stable DNA-lipid complexes exist in aqueous solution were summarized in Table III-3. Those conditions only apply when we prepared the DNA-lipid complexes by adding lipid solution into pre-hybridized DNA duplex solutions. However, provided DNA duplexes were hybridized in the presence of lipids, the unstable complexes can form at even lower concentration of lipid. This was attributed to the slow hybridization process in which the DNA solution with lipids was heated up to 90 ^{o}C and cooled down slowly to room temperature. The slow process is more likely to

afford the thermodynamically stable complex structure, an aggregate form of DNA complexes which is not soluble in aqueous solution. On the other hand, kinetically favorable complexes were formed by adding lipid directly into DNA duplex solution. (Appendix Figure A-4) Furthermore, the binding of lipid to single strand DNA prior to the hybridization can slow the annealing of DNA duplex and impede the complete duplex formation.

Table III-3 Summary of DNA-lipid complexes' stability.

	Sp^{4+}				C_2GlySp^{4+}				C_8GlySp^{4+}				$C_{18}GlySp^{4+}$			
	2:1	1:1	1:2	1:4	2:1	1:1	1:2	1:4	2:1	1:1	1:2	1:4	2:1	1:1	1:2	1:4
T_m	+	+	+	+	+	+	+	+	+	+	+	-	+	+	-	-
UV	+	+	+	+	+	+	+	+	+	+	+	-	+	-	-	-
CD	+	+	+	+	+	+	+	+	+	+	+	-	-	-	N/A	N/A
SUM	+	+	+	+	+	+	+	+	+	+	+	-	+	-	-	-

Note: +: stable, positive results were obtained; -: unstable, negative results were obtained; N/A: not measured)

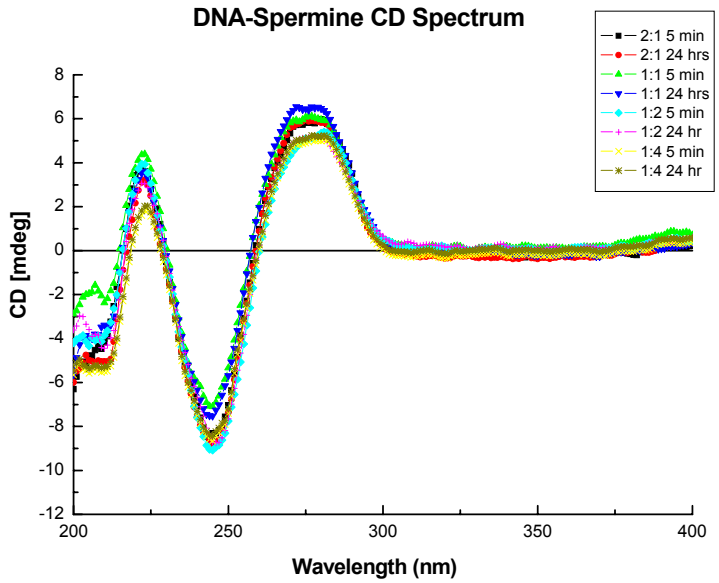

Figure III-20 CD spectra of DNA-spermine at various concentrations as indicated. Each sample contains 2.5 μM DNA(I) duplex in 10 mM sodium phosphate buffer. Spermine was added to the duplex solution prior to measuring CD spectra. The spectra were monitored over 24 hours.

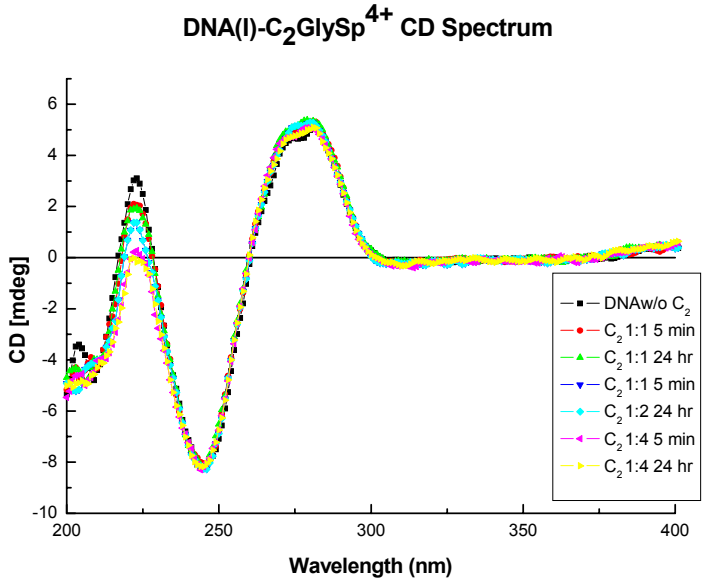

Figure III-21 CD spectra of DNA-C_2GlySp^{4+} at various concentrations as indicated. Each sample contains 2.5 μM DNA(I) duplex in 10 mM sodium phosphate buffer. C_2GlySp^{4+} lipid was added to the duplex solution prior to measuring CD spectra. The spectra were monitored over 24 Hours.

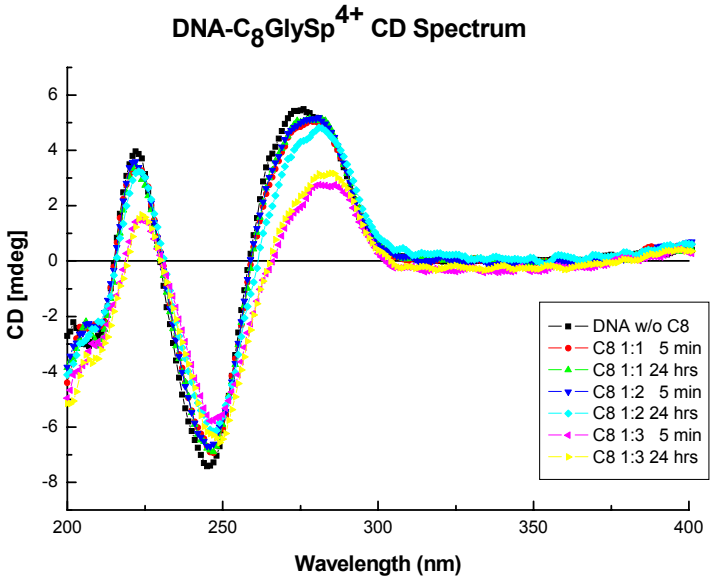

Figure III-22 CD spectra of DNA-C_8GlySp^{4+} at various concentrations as indicated. Each sample contains 2.5 μM DNA(I) duplex in 10 mM sodium phosphate buffer. C_8GlySp^{4+} lipid was added to the duplex solution prior to measuring CD spectra. The spectra were monitored over 24 hours.

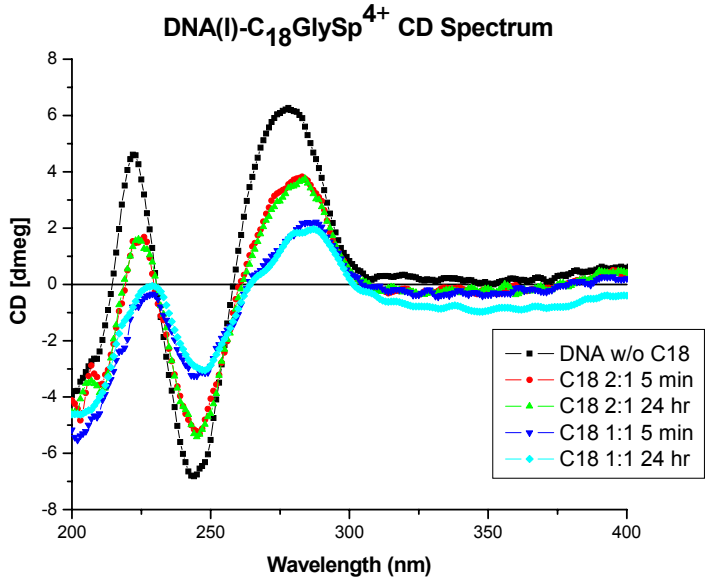

Figure III-23 CD spectra of DNA-$C_{18}GlySp^{4+}$ at various concentrations as indicated. Each sample contains 2.5 μM DNA(I) duplex in 10 mM sodium phosphate buffer. $C_{18}GlySp^{4+}$ lipid was added to the duplex solution prior to measuring CD spectra. The spectra were monitored over 24 hours.

Fluorescence quenching experiment: tight binding of lipids on DNA helix

The stable DNA-lipid complexes were achieved by controlling the proper sodium phosphate salt, lipid concentration and preparative method based on previous experiments, in which no significant change was observed in both UV and CD spectra for DNA-lipid complexes compared with native DNA duplexes. In order to quantify the effectiveness and affinity of lipids' binding to DNA we further assessed the fluorescence quenching ability of lipid on ethidium bromide (EB) intercalating in DNA double helix.

Ethidium bromide is a fluorescer with two absorbance peaks around 260 nm and 490 nm. (Figure III-24) Because its flat aromatic ring structure, it can intercalate into DNA base stacking with an equilibrium constant, K_b of approximately 10^4 M^{-1}.[44] Previous research by Henderson in Schuster's group showed that two distinctive binding mode were observed for some sequences, which is distinguished by two transition plateau at intermediate concentration of EB. However one specific binding mode dominates at either low or high concentration.[45]

Since the water is a major quenching species of fluorescence from ethidium bromide, EB will yield much stronger fluorescence once it intercalates into DNA helix which has a more hydrophobic environment. In addition, the intercalation restricts the conformational change in ethidium bromide ring structure, the excited ethidium bromide can not easily return to ground state via vibrational relaxation, which makes photo-emitting fluorescence the most feasible alternative route.[46]

UV spectrum of ethidium bromide and ethidium bromide bound DNA was shown in Figure III-24. The EB's spectrum shows two main transitions, a strong UV band with a

maximum below 300 nm, overlapping with the absorbance of DNA, and a weaker visible band with a maximum near 470 nm. The band at 470 nm are significantly shifted in EB-DNA(I) spectrum due to the electronic interaction between EB and the DNA helix.[47] The absorbance at 510 nm was the wavelength where we excited ethidium bromide with DNA solution and monitored the emission spectra between 540 nm and 750 nm. (Figure III-25, III-26) Both excitation and emission spectra showed dramatic increase in fluorescence intensity when DNA duplex was mixed with EB solution. A red shift in maximum is evident in excitation spectrum while a blue shift is observed in emission spectrum. To eliminate the possible effect of lipids on the excitation and emission of ethidium bromide, the fluorescence emission spectra of ethidium bromide were recorded in the presence of lipids. (Figure III-27) Neither the intensity nor the maximum variation in emission spectrum was observed, indicating no association and effect conveyed on ethidium bromide from lipids. This is reasonable considering the positive charge on both ethidium bromide and lipids where unfavorable electrostatic interactions prohibit the effective complex formation.

Figure III-28 shows the emission spectra of DNA-EB solution in 10 mM sodium phosphate buffer titrating with 2 mM C_8GlySp^{4+} lipid. After each aliquot of lipid was added, the solution was mixed well and incubated at room temperature for 15 minutes before the next measurement to allow the solution to reach equilibrium. It is noteworthy that the fluorescence intensity significantly dropped to almost 10% of DNA-EB without lipid once we slowly added up to two times charge ratio of the lipid. The emission band also shifted towards that of free ethidium bromide which indicated that the diminished emission band results from the exclusion of DNA-bound EB instead of precipitation of

DNA-EB-lipid complex from the solution because the latter would also show a decreasing emission band but in the absence of band shift.

The UV absorption spectra were recorded for each fluorescence measurement to ensure the stable solution we have in aqueous phase and less than significant scattering of light. (Appendix Figure A-2) This is proven to be necessary from our previous experiments to demonstrate the integrity and stability of the complex system.

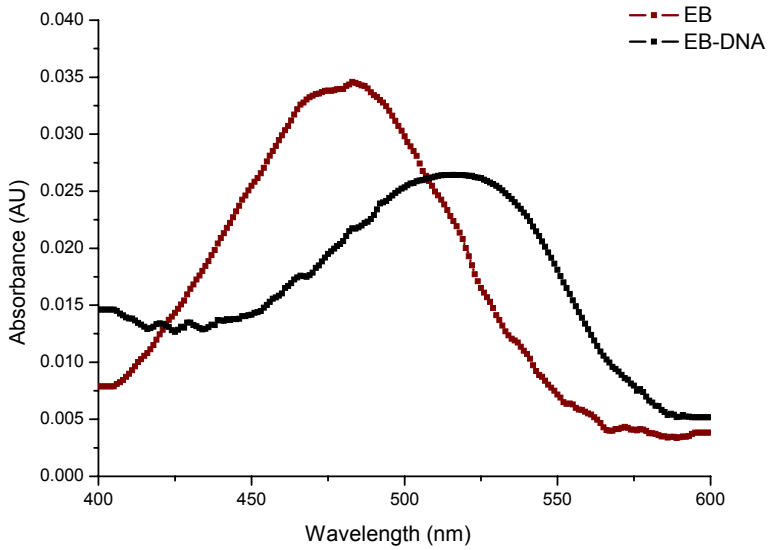

Figure III-24 UV Absorption Spectrum for Ethidium Bromide and EB-DNA(I) solution. The samples contains 2.5 μM DNA(I) and 5 μM EB in 10 mmol NaPi buffer, pH 7.0.

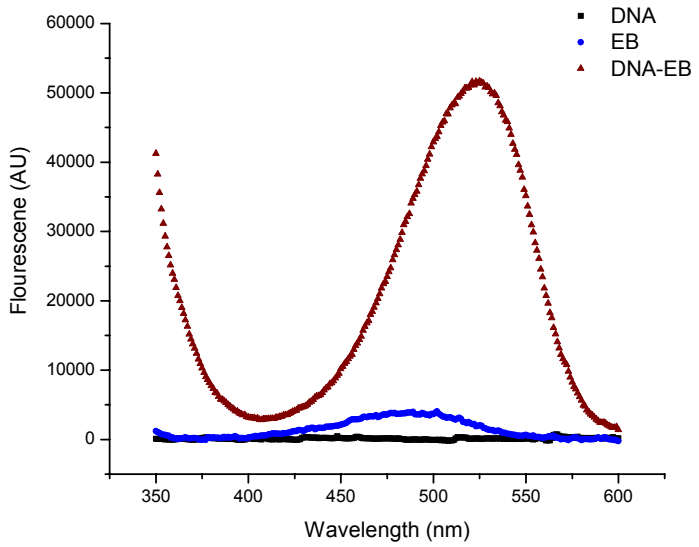

Figure III-25 Fluorescence excitation spectra of DNA, EB and DNA-EB. The samples contain 2.5 μM DNA(I) duplex, 5.0 μM EB and 2.5 μM DNA(I) duplex with 5.0 μM EB, respectively, in 10 mM sodium phosphate, pH 7.0

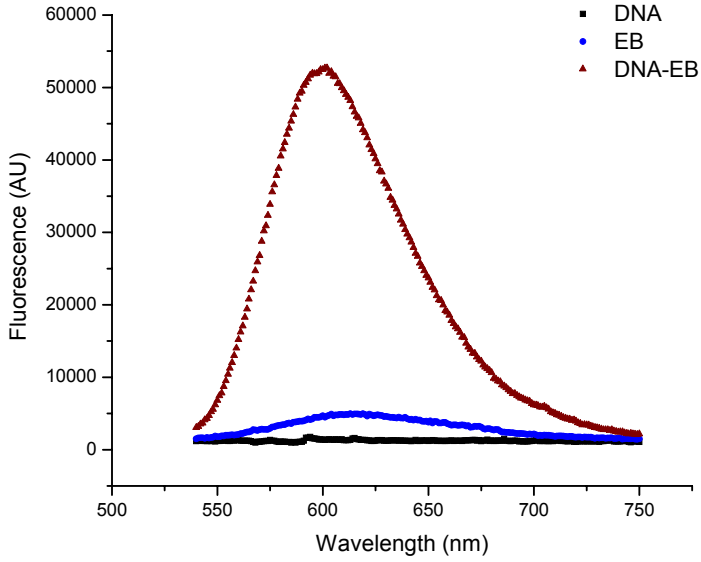

Figure III-26 Fluorescence emission spectra of DNA, EB and DNA-EB. The samples contain 2.5 μM DNA(I) duplex, pH 7.0, 5.0 μM EB and 2.5 μM DNA(I) duplex with 5.0 μM EB, respectively, in 10 mM sodium phosphate. Excitation wavelength is 510 nm.

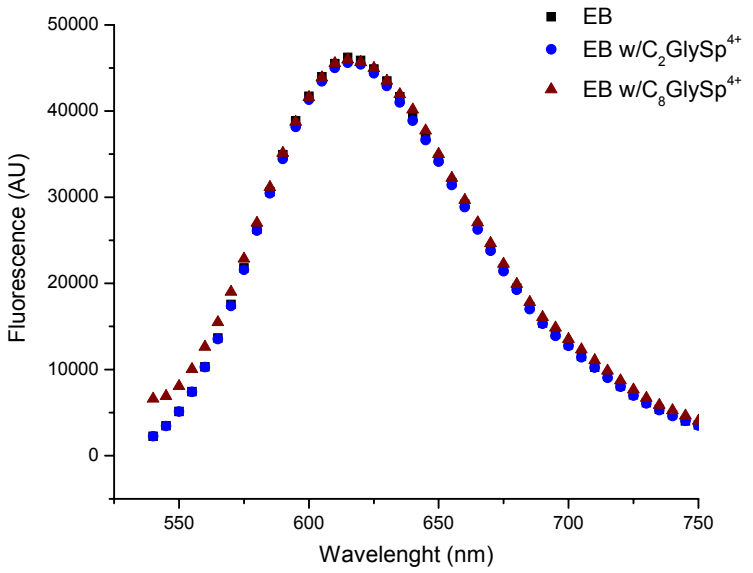

Figure III-27 Fluorescence emission spectra of EB with no lipid, C_2GlySp^{4+} and C_8GlySp^{4+}. Lipids' concentration is 33.8 μM. Excitation wavelength is 510 nm.

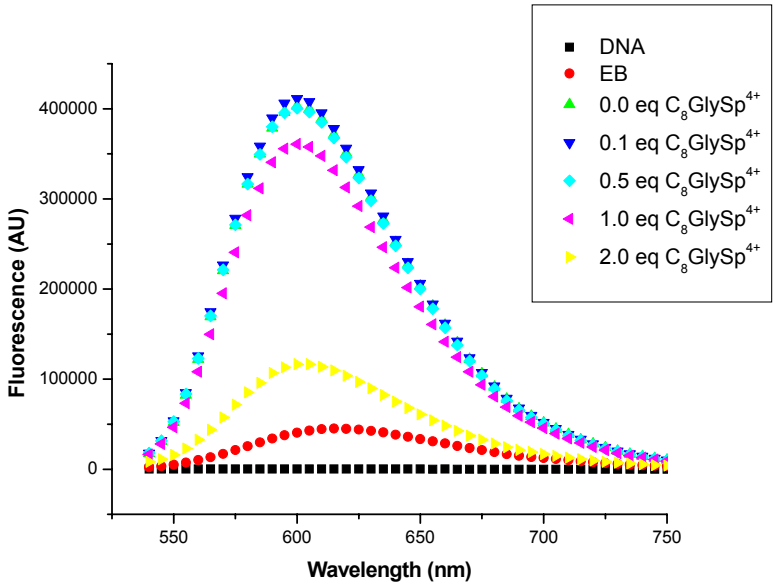

Figure III-28 Fluorescence emission spectra of EB quenching by C_8GlySp^{4+}. The sample contains 2.5 μM DNA(I) and 5 μM ethidium bromide. Excitation wavelength is 510 nm.

We examined the EB fluorescence quenching property with our synthetic lipids and two other surfactants. The results was normalized to DNA-EB complex without any additives and shown in Figure III-29. C_8GlySp^{4+} show most significant quenching ability among all the lipids and surfactants, followed by didodecyldimethylammonium (DDDA) and $C_{18}GlySp^{4+}$. C_2GlySp^{4+} and dodecyltrimethylammonium (DTMA) hardly showed any quenching ability if we consider the factor that we slightly diluted the solution by approximately 5% during our titration process. Nevertheless the fluorescence quenching effect of those two lipids is much less than the lipids with bulkier and longer alkyl chains. The observation is due to two equilibriums among DNA, EB and lipids. In original DNA-EB solution, there is equilibrium between DNA-EB complex and free EB with free DNA. By adding lipid, we disturb the equilibrium by binding lipids around DNA double helix and block the re-intercalation of free EB into DNA. The first equilibrium moves towards the side of free EB and free DNA. The second equilibrium between DNA-lipid and free DNA with free lipid favors the formation of stable DNA-lipid complex. If the second equilibrium has a higher association constant K_{a2} than the first one K_{a1}, the dissociation of DNA-EB becomes favorable and the equilibrium moves towards free EB and free DNA which binds to lipid in irreversible mode. Herein, we observed much less fluorescence intensity due to the dissociation of DNA-EB complexes.

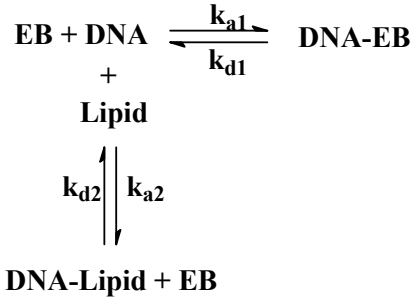

CD measurement eliminates the structure distortion of DNA helix that could lead to reducing the binding affinity of EB to DNA. Therefore, the outstanding fluorescence quenching ability of lipids can be treated as an indicator of either tighter binding with DNA helix or a stronger ability to reduce the intercalation of ethidium bromide. All the synthetic lipids consist of the same DNA-binding head group, spermine, therefore the binding affinity of those lipids towards DNA should be within the similar range, which conversely emphasis the important function of alkyl chains in term of blocking access of other molecules to DNA helix structure.

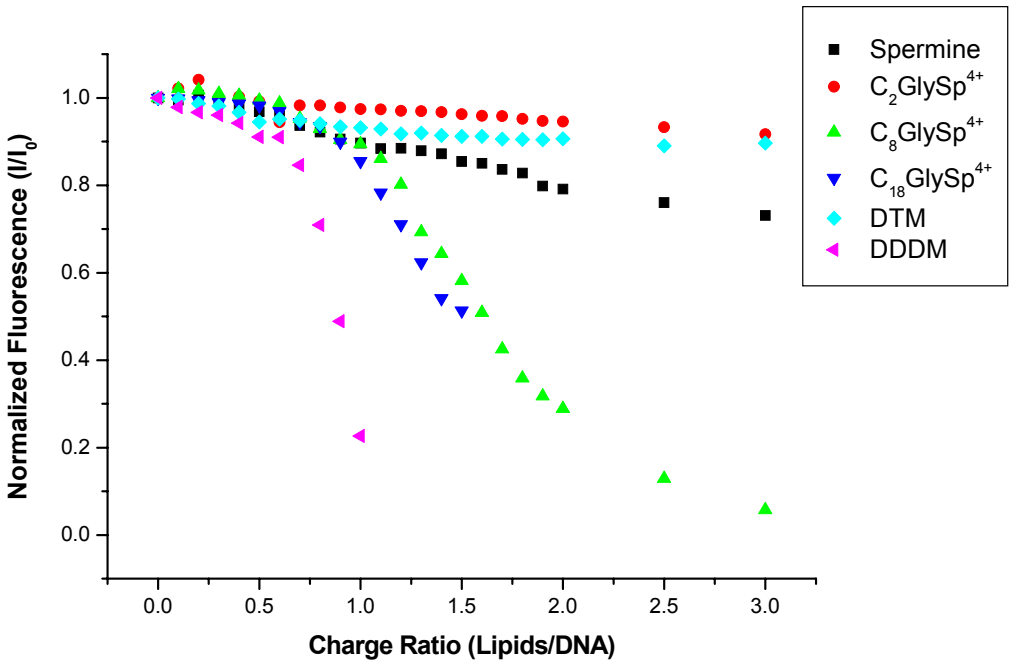

Figure III-29 Fluorescence quenching by the addition of spermine and lipids. Each sample contains 2.5 μM DNA duplex in 10 mM sodium phosphate, pH 7.0. A small aliquot of concentrated lipid solution (2 mM) was added to DNA and the spectra were recorded over the course of stable condition which is monitored by UV spectrometer.

Photo-induced cleavage in DNA-spermine and DNA-lipid Complex

Oxidative damage in DNA-lipid aggregate

Photoexcitation of anthraquinone photosensitizer creates a radical cation, a positive charged hole, in DNA helix. The radical cation can migrate through the DNA via base stacking and get trapped at certain bases which are labile to oxidative stress. 5'-GG-'3 sequence is common damaged site because the lowest oxidation potential of guanine among four bases.[48] In general 5'-G subjects to more damage than 3'-G in GG step. This is a characteristic observation with damage induced by intra-strand charge transport process. Many DNA cleavage agents, like active oxygen species, would damage the guanine base without specificity.

We examined the effect of lipids on charge transport in DNA(I) in parallel with the characterization experiments. The autoradiograms of DNA-C_8GlySp^{4+} and DNA-$C_{18}GlySp^{4+}$ were reported in Figure III-30. As the radical cation migrates through DNA helix, the cleavage is revealed at guanine sites in GG steps with the lowest oxidation potential.

The damage at the proximal and distal GG-sequence step and at an isolated G site is observed in Figure III-30 after hot piperidine treatment and revealed by gel electrophoresis analysis. The strand breakage within AQ-conjugated duplex locates mainly at the 5'-G of each GG step. The damage at 3'-G of each GG site and at isolated G site is not as significant. Those are the characteristic observation with the oxidative damage caused by photo-induced intra-strand charge transfer process. As we increased

the concentration of either C_8GlySp^{4+} or $C_{18}GlySp^{4+}$ lipid, the less damage at both GG steps was seen in the autoradiogram.

The initial irradiation experiment showed very significant effect of our synthetic lipids on inhibiting the damage at GG sites. (Figure III-30) The damage at both proximal and distal GG sites was reduced dramatically in the samples containing C_8GlySp^{4+} and $C_{18}GlySp^{4+}$ lipid. When the concentration of lipids increased above 1:4 charge ratio (135 uM), the oxidative damage was completely absent from the gel. The quantified damage analysis revealed that the damage at proximal GG sites in DNA(I) containing 1:2 charge ratio of $C_{18}GlySp^{4+}$ (63.5 uM) is 50-fold less than the oxidative cleavage observed in pure native DNA(I) samples. (Figure III-31) Whereas the samples containing C_8GlySp^{4+} showed less effect than $C_{18}GlySp^{4+}$, the damage was still significantly reduced to 10 percentage of that in pure DNA(I) sample with 137 μM C_8GlySp^{4+} (1:4 charge ratio). This finding initially gave credence to the speculation that the binding of lipid forms a hydrophobic layer surrounding the DNA helix structure which could reduce the reaction of water with radical cations. This is achieved by either loosing the binding of water molecule with phosphate backbond and bases via hydrogen bond[13-14] or reducing the access of surrounding water molecules to the helical duplex.

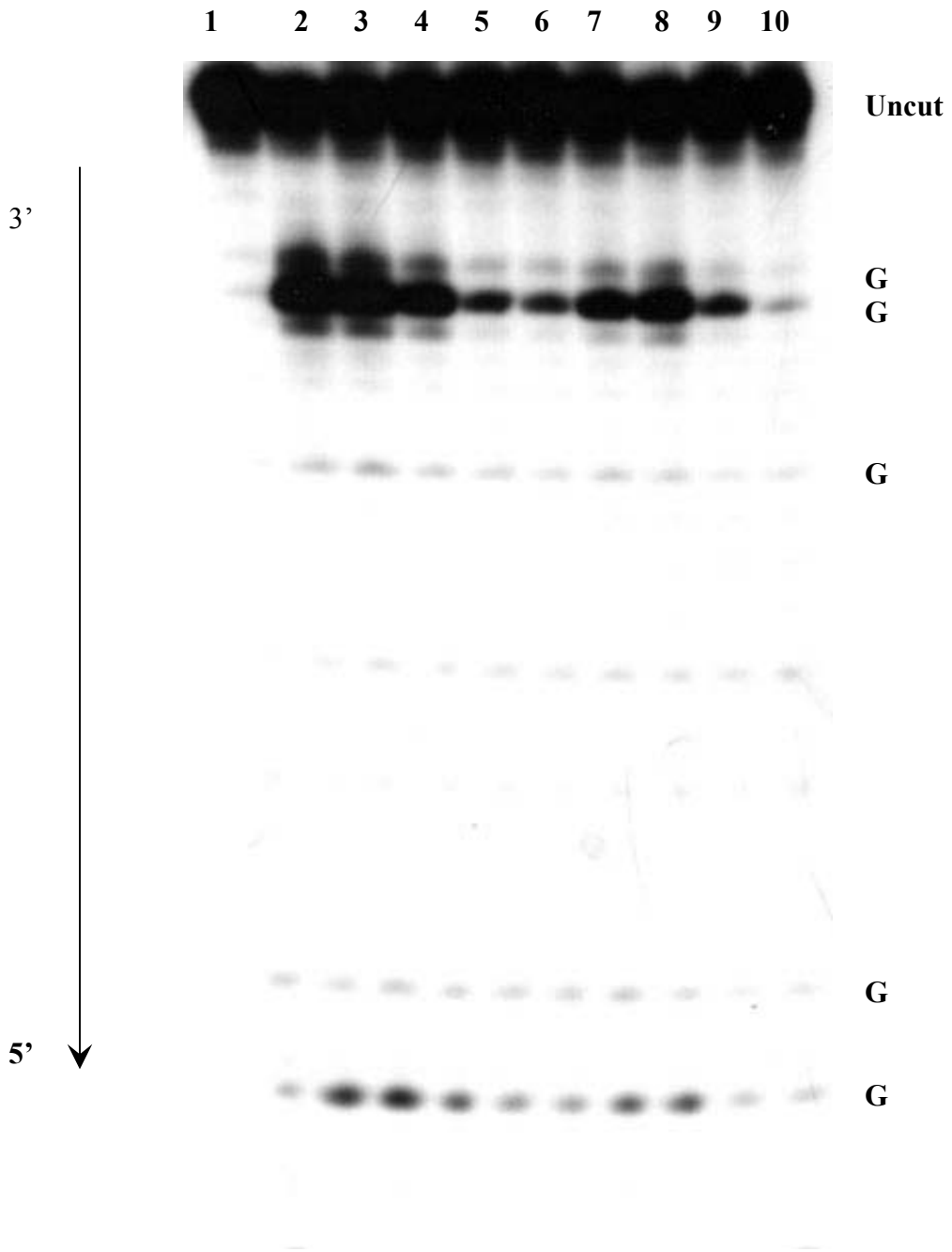

Figure III-30 Autoradiogram of DNA (I) with various concentrations of C_8GlySp^{4+} and $C_{18}GlySp^{4+}$ lipids. Lane 1 corresponds to dark control samples without irradiation. All other samples were incubated with lipids for 30 min prior to 5 min irradiation at 30 ^{o}C. Land 2-6 corresponds to DNA (I) with 0, 0.5, 1, 2, 4 charge ratio of C_8GlySp^{4+}. Lanes 8-10 corresponds to DNA(I) with 0.5, 1, 2 charge ratio of $C_{18}GlySp^{4+}$. Lane 7 contains the sample hybridized with the presence of 1:1 C_8GlySp^{4+} lipid.

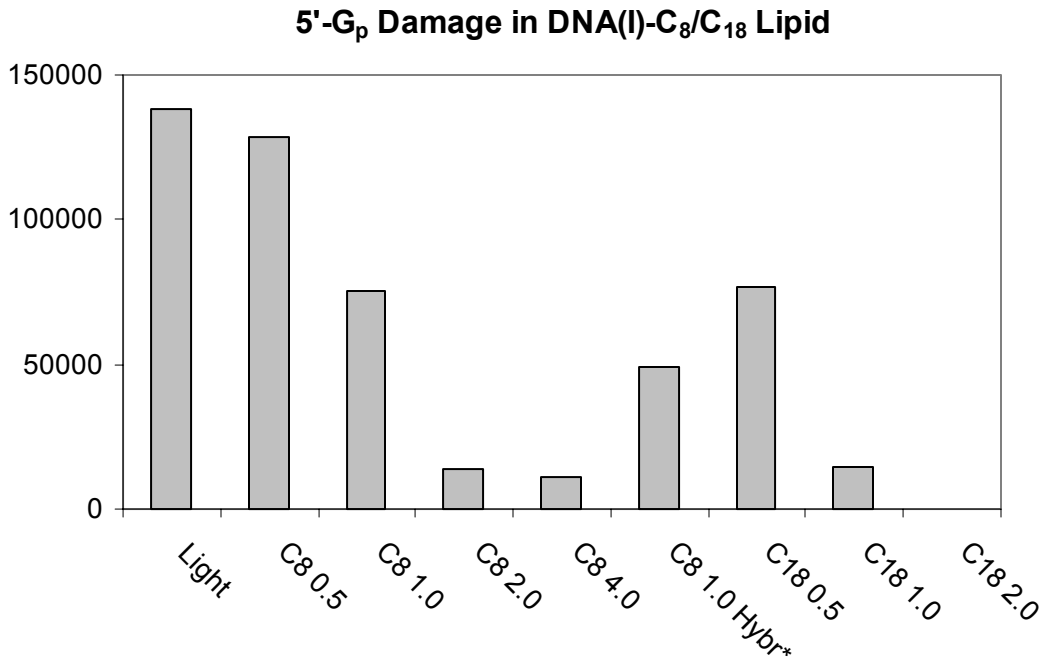

Figure III-31 The photo-induced oxidative damage at 5'-G in proximal GG sequence. Each sample contains 2.5 μM DNA duplex in 10 mM sodium phosphate pH 7.0 and lipid as indicated.

However, the complication of heterogeneous DNA samples became obvious after we examined thermal denaturation data, time dependant CD and UV-vis spectra. Our characterization experimental results indicated alternative possible explanation for the observed reduction in photo-induced oxidative damage. The thermal denaturation, UV spectra and CD spectra unveiled no evidence for stable DNA-C_{18}GlySp^{4+} and DNA-C_8GlySp^{4+} complexes at high lipids' concentration, above 1:1 charge ratio for C_{18}GlySp^{4+} and 1:2 charge ratio for C_8GlySp^{4+} respectively, in 10 mM sodium phosphate buffer, a condition under which we ran the photo-irradiation experiment on DNA-lipid samples. The further investigation using time-dependent UV and CD measurement confirmed the results acquired in previous regular experiment and clarified the borderline condition for obtaining stable DNA-lipid complexes.(Table III-3) For C_8GlySp^{4+}, the stable DNA-lipid

complex was obtained at up to 1:2 charge ratio. The distortion and decrement in CD spectra were observed for DNA-lipid complex at higher charge ratio. Time-dependent UV spectra showed the slow formation of aggregation and precipitation of DNA-lipid complex at high lipid concentration. (Figure III-17, III-22) For $C_{18}GlySp^{4+}$ the stable DNA-lipid complex was only obtained at charge ratio up to 1:1 according to CD spectra. However, even at this concentration a significant enhancement in UV spectrum was observed, which is associated with the formation of aggregate (Figure III-18, III-23)

Base on those data, DNA-lipid complexes at high lipid concentration did not maintain a stable water soluble structure. Aggregation, precipitation and conformation alteration, which causes by hydrophobic effect of lipids binding, were supported by those experiments. If the large amount of DNA duplex exists in aggregate form, the photo irradiation efficiency would be much lower due to lower exposure volume to UV light and stronger light scattering. Furthermore, we can not identify the DNA duplex conformation in such aggregate structure because of the lack of CD spectrum. There was even no convincing evident for DNA duplex structure. It is well established that charge transfer occurs through π-π stacking between base pairs.[49,50] DNA helix structure is critical for the efficiency in charge transfer, any alteration in helix may has the significant effect on charge transport[51,52] Some previous research showed that the aggregate formed between DNA and cationic lipids tend to have dehydrated structure and compact form.[4-8, 17] Therefore, any data obtained under such condition are questionable and not comparable with native DNA duplex soluble in aqueous solution. Herein, we have to perform the photoinduced oxidative damage experiment with stable and water soluble DNA-lipid complex with no or little conformation change.

If DNA-lipid complexes form aggregate and precipitate from aqueous phase, it can account for the decrease of damage. First, the excitation of AQ would be strongly less efficient in solid phase compared to that in liquid phase due to strong light scattering. The charge transport process can be drastic different in aggregate form than in normal form because the duplex are well-packed and in rigid helix formation. In polaron hopping model, the relaxation and distortion of DNA segment is helping delocalize and stabilize the radical cation and the migrating of the radical cation.[53, 54] We can not easily determine the conformation of DNA duplex, which has tremendous effect on charge transport process, in such aggregate form by the inspection of CD spectrum. Therefore the comparison between normal DNA and aggregate DNA-lipid complex would be invalid or improper at least. Too much variable prevents us from uniquely and independently interpreting the data and subsequently attributing the observation to a particular origin. As a consequence we had to restrict our experimental condition to eliminate the possible aggregation of DNA-lipid complexes so that the oxidative damage from charger transport in DNA-lipid complex can be compared with that in nature DNA duplex without any ambiguity.

The stability of DNA-lipid complex depends not only on the concentration of lipid and DNA duplex but also the salt concentration. Lipoplex formation and aggregation process accelerates in the presence of high salt concentration. Even though DNA-lipid complexes can be stabilized at higher lipid concentration by lowering the salt concentration, we can not reduce salt concentration to the extent where DNA duplex structure is not stable or denatured. It is well known that salt is crucial driving force for the annealing of DNA duplex and maintaining the structure integrity and stability of

DNA secondary helical structure. For instance, Z-form DNA only exists at high salt concentration while A-form DNA prevails under dehydrated condition and low salt. It also has strong impact on the DNA melting behavior. After experimenting with thermal denaturation of DNA(I) in various salt and lipid concentration, we decided to keep the salt condition consistent with previous photoinduced charge transport experiments in Schuster's group.

The characterization experiments elaborated above, including circular dichroism, thermal denaturation and time-dependent UV measurement, provide a tool to fully examine the stability and structure of DNA-lipid complex. Combining all the data, we were able to find the limiting concentration for each lipid to maintain a stable complex with DNA.(Table III-3) The further photoinduced charge transport in DNA-lipid complexes experiment was carried out under such stable condition to provide comparable and reliable results

Oxidative damage in stable DNA-lipid complexes

The photo-irradiation experiment was repeated under the condition where the stable soluble DNA-lipid complex presents as indicated by time dependent UV and CD spectra. The results were shown in Figure III-32.

It is undoubted that the oxidative damage at both proximal and distal GG steps had been dramatically reduced by the addition of spermine, C_2GlySp^{4+} and C_8GlySp^{4+} lipid compound. However, C_8GlySp^{4+} lipid yields more dramatic effect than the others. The only major difference between three compounds lies in the dialkyl tail group.

C_8GlySp^{4+} has two longer hydrophobic eight-carbon chains while C_2GlySp^{4+} has only two-carbon chains and spermine has none. This is the strong evidence for our hypothesis mentioned earlier.

There are three major factors contributing to the charge transport efficiency in DNA, radical cation injection, charge migration and the irreversible trapping of radical cation through the reaction with water and reactive oxygen species.

The radical cation injection is determined by the efficiency of photoexcitation of anthraquinone and the nucleotide linked to anthraquinone.[34] As observed in Figure III-11, DNA-C_8GlySp^{4+} exhibits small but distinctive baseline enhancement over the time possibly due to the light scattering by the small amount of aggregate accumulated in the solution. However, this did not affect the photoexcitation of anthraquinone in DNA-C_8GlySp^{4+} complex as shown in Figure III-33. The samples were incubated with C_8GlySp^{4+} lipid from 3 minutes up to 24 hours before the 3 minute UV irradiation. The samples were in the same condition as those in time-dependent UV measurement. No significant difference in oxidative damage between samples was observed. Since the incubation time is the only variant between samples, which is related to the amount of scattering light as described above, the influence of the scattered light on photo-excitation of anthraquinone is negligible under our experimental condition.

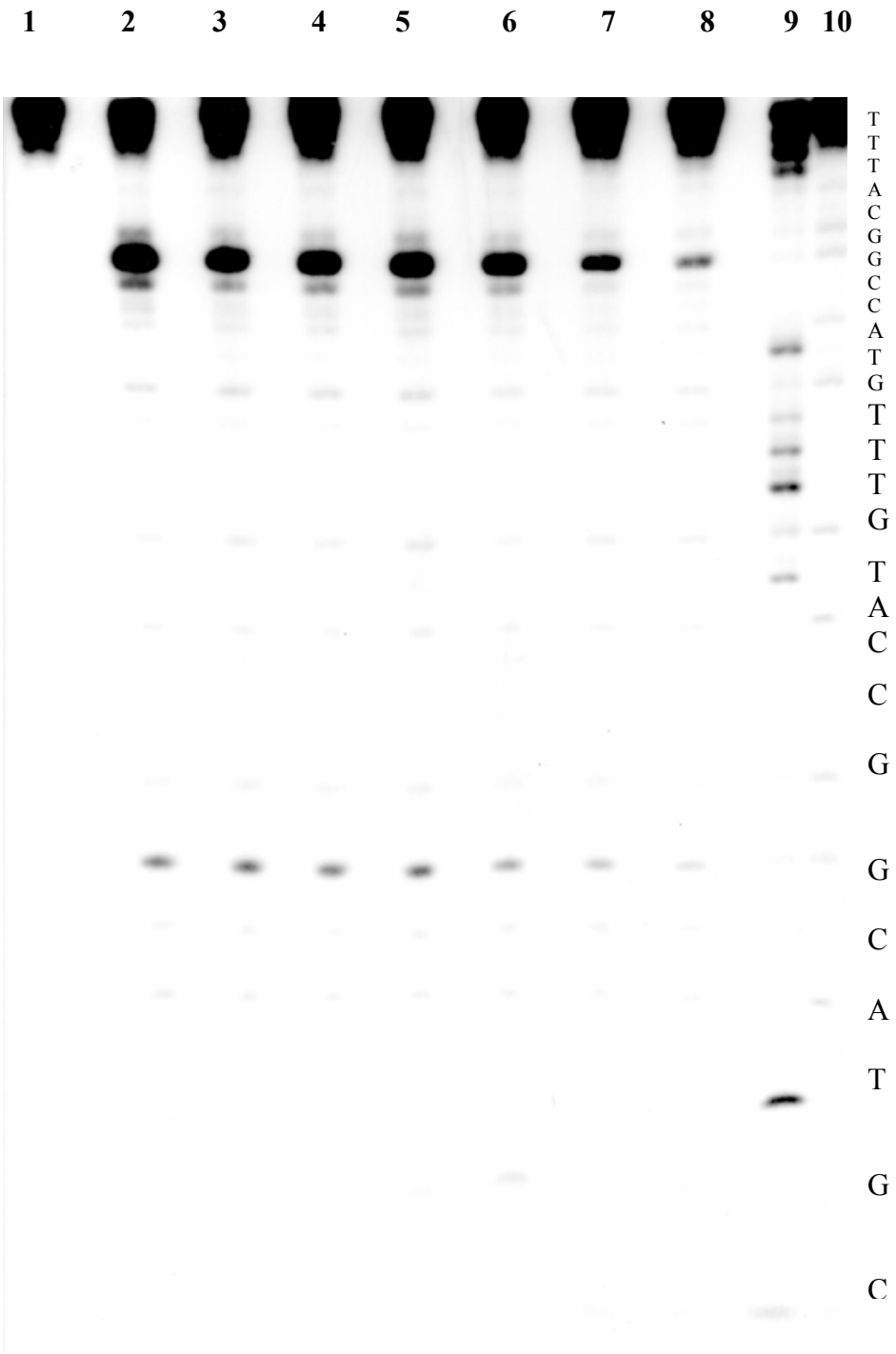

Figure III-32 Autoradiogram of a denaturing gel electrophoresis for DNA(I) with spermine, C_2GlySp^{4+} and C_8GlySp^{4+} lipids. Lanes 1 is sample w/o irradiation. Lane 2 is the sample w/o lipid. Lanes 3-8 correspond to the samples incubated with 1.0, 2.0 equivalent spermine, C_2GlySp^{4+}, C_8GlySp^{4+} lipid (charge ratio), respectively for 30 min before the 2.5 min irradiation and cleaved by treatment with hot piperidine at 90 ^{o}C for 30 min. Lane 9, 10 corresponds to Maxam-Gilbert T and A/G sequencing lanes. All samples contain 2.5 μM DNA in 10 mM sodium phosphate buffer.

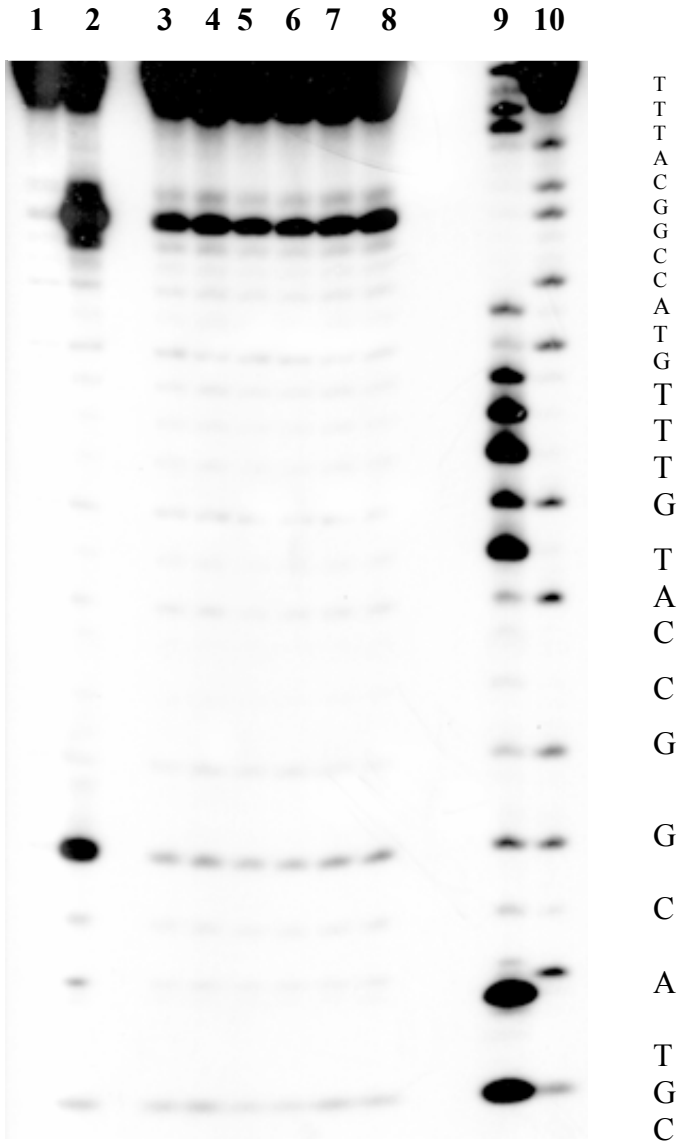

Figure III-33 Autoradiogram of a denaturing gel electrophoresis for DNA(I) with C_8GlySp^{4+} (charge ratio of 2.0) lipids at different incubation time. Lanes 1 is sample w/o irradiation. Lane 2 is the sample w/o lipid. Lanes 3-8 correspond to the samples incubated with C_8 lipid for 3 min, 30 min, 60 min, 6 hrs, 12 hrs and 24 hrs respectively before the 3 min irradiation using 8x350nm Rayonet lamps and cleaved by treatment with 1M hot piperidine at 90 ^{o}C. Lane 9 and 10 correspond to Maxam-Gilbert T and A/G sequencing lanes. All samples contain 2.5 μM DNA in 10 mM sodium phosphate buffer at pH 7.0.

Oxidative damage induced by singlet oxygen

In aqueous solution the radical cation in DNA was not only trapped by water molecules but also reactive oxygen species. Molecular oxygen ($^3O_2$) is a very important molecule in the energy metabolism of all aerobic organisms, either as terminal electron acceptor in oxidative phosphorylation or as a product of photosynthesis in cyanobacteria and the chloroplasts of plants and green algae. Even though molecular oxygen itself is not very reactive, it can give rise to the formation of reactive oxygen species (ROS) which are superoxide radicals (O_2^-), hydrogen peroxide (H_2O_2), hydroxyl radicals (OH•) and singlet oxygen ($^1O_2$).[55] These molecules are highly reactive and can damage the cell seriously by mutating the genome, disturbing the plasma membrane integrity or inactivating essential proteins.[56] The reactivity is determined by the amount and state of the electrons in the π* orbitals, which is responsible for the stability of a specific molecule. Triplet molecular oxygen has two electrons with parallel spins, one in each of its π* orbital (Figure A-4). This is the most stable state of oxygen and therefore does not oxidize spontaneously biological molecules. If a single electron is added to the ground state $^3O_2$, the electron must enter one of the π* antibonding orbitals, which destabilizes the molecule by decreasing the strength of the double bond. The resulting superoxide radical is very reactive and reduces many molecules to get rid of the extra electron and to return to the stable ground state. The addition of a second electron results in O_2^{2-} molecule with four electrons in the π* orbitals. This would destabilize the molecule completely if it would not accept two protons to form a more stable hydrogen peroxide molecule. The same is true for the $O_2^{\bullet -}$ molecule, which is protonated to form water.[56]

Instead of accepting additional electrons, molecular oxygen can be excited by absorbing energy. In this case the spin of one of the two parallel electrons in the π* orbital is reversed resulting in an electron pair with anti-parallel spins, either in the same orbital (1g O_2) or in the higher energy form with the electrons in separate orbitals ($1g^+$ O_2). This oxygen form is called singlet oxygen ($^1O_2$) and is very reactive due to its excited state.[56] The form with higher energy ($1g^+$) is very unstable and rapidly returns to the lower energy form (1 g), which is therefore the only form of $^1O_2$ with biological relevance.[57] It can be produced either chemically by redox reactions or by photosensitizers, which absorb energy from UV, visible or high-energy radiation and transfer it to ground state oxygen converting it to singlet oxygen. Thus O_2 is quenching the excited state of the photosensitizer. Many endogenous compounds can act as photosensitizers, such as flavins (FMN and FAD), porphyrins, chlorophylls, bilins, retinal, quinones, pterins and reduced pyridine nucleotides (NADH and NADPH).[58, 59] Beside these, many synthetic photosensitizers are known, of which some can successfully be used to produce elevated concentrations of singlet oxygen in a liquid media. The most prominent of them are rose Bengal, methylene blue, acridine orange and neutral red.[60] Oxidation of guanosine by singlet oxygen has been the focus of considerable interest because of its importance in cancer etiology and its cure via photodynamic therapy.[61, 62]

In our previous study, we showed that lipids effectively reduced oxidation damage by binding to DNA duplex and constructing a hydrophobic layer around DNA. The influence of lipids on oxidative damage induced by singlet oxygen was also studied using rose bengal, which generates singlet oxygen when it is irradiated with light. (Figure III-34, III-35) In our experiment, the visible light region was chosen because DNA and

AQ absorb around 260 nm and 350 nm, respectively. The irradiation with visible light can prevent the excitation of AQ such that no intramolecular charge transport would occur. The singlet oxygen reaction with guanine presents a plethora of pathways and potential products depending upon the reaction conditions and structural context, nucleoside versus double strand DNA.[63, 64] The studies showed that the primary product from guanosine in DNA duplex reacting with singlet oxygen was mainly 7,8-dihydro-8-oxo-deoxyguanosine (8-oxoG), a species that is not alkali-labile by hot piperidine treatment.[64] FPG enzymatic cleavage was carried out to reveal the damaged sites after irradiation and the results was showed in Figure III-36.

Scheme. *Mechanism Proposed for the Reaction of $^1O_2$ with the Guanine Moiety of Isolated DNA That Specifically Produces 8-OxodGuo*

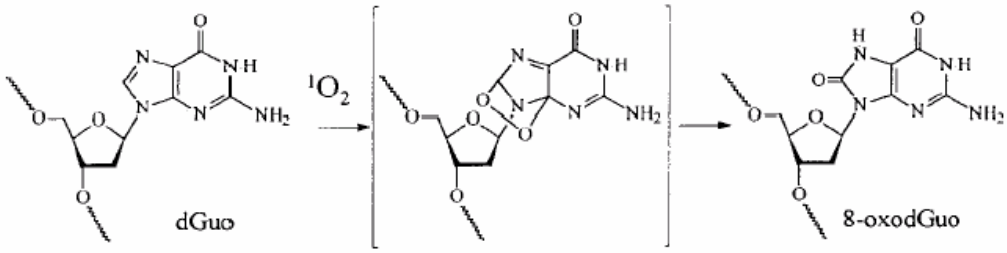

Figure III-34 Proposed mechanism for the reaction of $^1O_2$ with guanine in DNA duplex.[64]

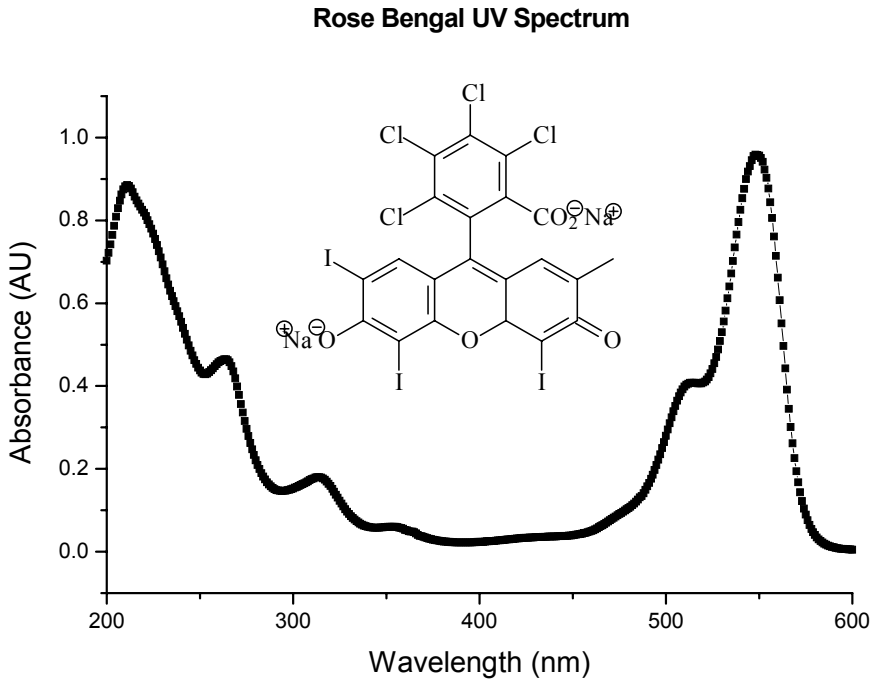

Figure III-35 UV Spectrum of Rose Bengal in 10 mM sodium phosphate at pH 7.0.

All the Gs, either in GG steps or singlet, were damage during irradiation, a characteristic symptom of oxidative damage occurred via intermolecular reaction instead of intramolecular charge transport followed by radical cation trapping through the irreversible reaction with water or oxygen species. In those reactions, singlet oxygen, generated by rose bengal, directly attacked most oxidative liable site, guanine in DNA. Therefore, the extent of damage is only determined by the reaction rate of singlet oxygen with guanine, which is controlled by the abundance of reactants and the diffusion rate. There is no obvious difference in G damage among the samples with different lipid concentration. (Figure III-36) This can be attributed to the lack of repelling force between DNA-bound lipid and singlet oxygen.

The finding in study further supports the hypothesis that hydrophobicity is the foundation of reduced oxidation damage at GG sites. The observation that lipid has no effect on singlet oxygen reaction with guanine is, at least partly, due to the impotency of holding singlet oxygen, ahydrophobic species, away from the DNA duplex.

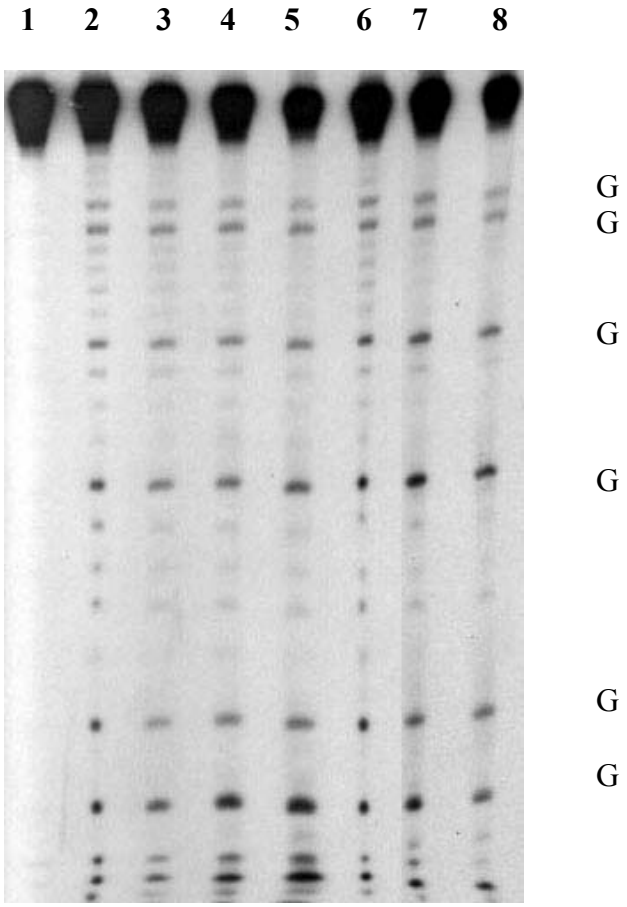

Figure III-36 Autoradiogram of a denaturing gel electrophoresis for DNA DNA(I) damaged by singlet oxygen from Rose Bengal at the presence of C_8GlySp^{4+}. Lanes 1 is sample w/o irradiation. Lane 2 is the sample w/o lipid. Lanes 3-8 correspond to the samples incubated with 0.1, 0.2, 0.5, 1.0, 1.3, 2.0 equivalent C_8 lipid before the 15 min irradiation using Oriel lamps equipped with a filter and cleaved by treatment with FPG enzyme. All samples contain 2.5 μM DNA and 10 μM rose bengal in 10 mM sodium phosphate buffer.

Investigation on the effect of lipid concentration on charge transfer in DNA

We finally carried out photo-excitation experiment in a series of samples with increasing lipid concentration from 0 to 2 charge ratio. The oxidative damage at guanine sites was quantified (both proximal and distal G) with phosphorimagery. The damage was normalized to the total damage account in the sample without lipid and plotted against the concentration of lipids (in charge ratio). The results of 5'-G at proximal distal GG sequence was shown in Figure III-37. DNA-spermine and DNA-C_2GlySp^{4+} demonstrated the similar damage pattern where the damage at 5'-G decreased with the increase in spermine or C_2GlySp^{4+} concentration, respectively. A significantly less oxidative damage was observed for C_8GlySp^{4+} when the concentration was enhanced above 0.5 charge ratio, i.e. 16.9 μM. This added protection against oxidative damage was a solid indication of hydrophobic effect from long dioctyl chains considering the structure similarity, the same binding group spermine, and difference, the length of dialkyl chains, between three compounds.

The damage at 5'-G at proximal GG sequence and distal GG sequence were compared over the series of samples (Figure III-38). The ratio between the damage at 5'-G at proximal and distal GG sequence was plotted versa the concentration of lipid. In the samples containing either spermine or C_2GlySp^{4+}, the data showed little difference in the damage ratio over the range of concentration. As stark contrast, a dramatic decrease in the ratio is evident in the presence of C_8GlySp^{4+} lipid. This is not a surprise if C_8GlySp^{4+} slowed the radical cation quenching reaction with water by limiting the access from

radical cation to water molecule. A radical cation was injected into DNA duplex upon irradiation with UV light, the injected radical cation can migrate along the DNA helix π-π stack followed by trapping at a specific labile site or back electron transfer (BET) to return to initial state. Our experiment was carried out under single hit condition where only a small amount of DNA was involve in the reaction such that every DNA molecule was subject to only one photoexcitation during the experiment. The increasing damage at the distal site can only be the consequence of two possible reasons.

First, a more efficient charge transport pathway through DNA helix. It is well established that DNA π-π stacking, especially purine bases are the major charge carrier in DNA charge transport process. The change in DNA secondary structure can disturb this well-defined extended π orbital in DNA helix and, therefore, affect the charge transport efficiency. However, the conformation change is not evident in CD spectra, which is very sensitive to any alteration in DNA secondary structure. (Figure III-19-III-21)

Second, the slower reaction rate at the first GG step allows the farther migration of the radical cation to reach, get trapped and react at distal GG step. The slower radical cation trapping rate, cooperated with the consistent charge injection and hopping rate, results in the enhanced 5'-G damage ratio at the distal GG step.

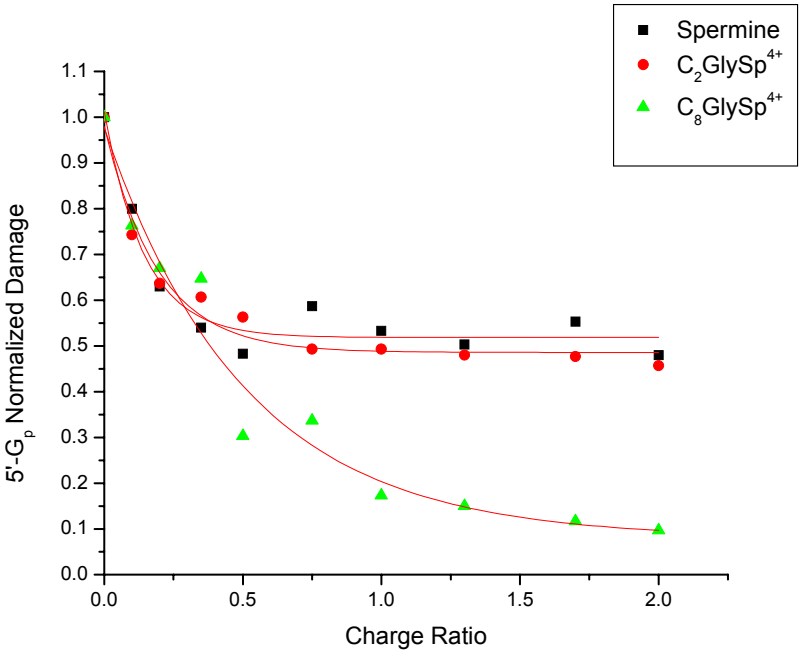

Figure III-37 Normalized proximal 5'-G_p damage in DNA at the presence of spermine, C_2GlySp^{4+} and C_8GlySp^{4+} lipid.

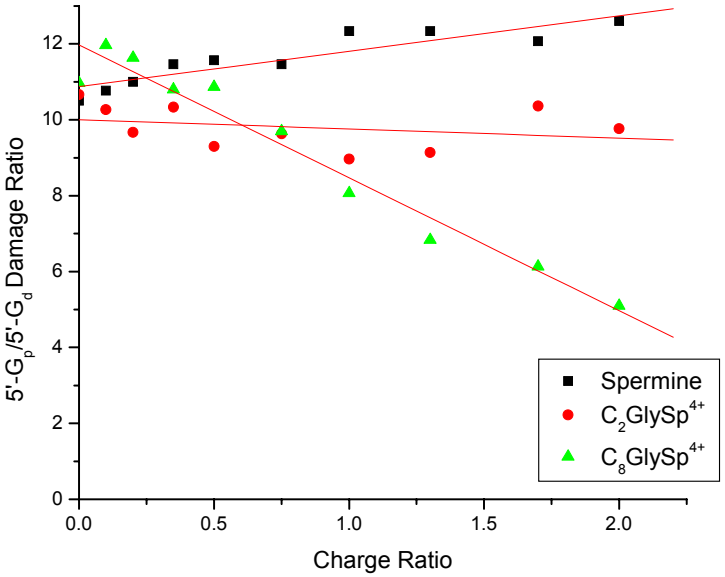

Figure III-38 Oxidation damage ratio of 5'-G_p/5'-G_d in DNA at the presence of spermine, C_2GlySp^{4+} and C_8GlySp^{4+} lipid.

Proposed mechanistic scheme for oxidative damage in DNA-lipid complex

Charge hopping mechanisms and kinetic model

DNA mediated charge transport over a wide range of distance and time regimes has been under extensive investigation.[65] After a decade of experimental and theoretical study in charge transport process, two distinct mechanisms prevail in rationalizing various features of DNA charge transport.

The superexchange-mediated tunneling mechanism, only applicable in short distance, was used to explain the deep distance dependence and fast transport process in neighboring bases. In this model the radical cations are localized on individual guanines because these have the lowest oxidation potential among four DNA bases,[48] and tunnel from guanine to guanine, either on same strand or complementary strand with some kinetic penalty, without reside on the intervening A/T bridges. A positive injection barrier for migration of guanine hole exists because of different oxidation potentials of DNA bases (G: E_{ox} ≈1.3 V, A: E_{ox}≈1.4 V). When the A/T bridge separating G "stepping stone" is longer than three bases, the tunneling through the energy barrier was found to be unrealistic by experimental data.[66-68] The occupation of higher energy Adenine Bridge is invoked to rationalize long-range charge transport between guanines. However, the charge was proposed to hop along the adenines in an essentially distance-independent fashion.

Superexchange mechanism failed to explain experimental observation of distance-dependent long distance charge transport and relatively slow radical migration rates. Recently time-resolved spectroscopic measurements have yielded results suggesting that

tunneling is not rate determining step even for short migration distance.[69-72] Lewis, Wasielewski and coworkers have assigned the fastest isoenergetic hop, from G to G through a single A bridge, rate constant that is two order magnitudes less than expected values for tunneling theory.[73, 74] The hopping rate in GTG sequence is even slower than that in GAG sequence. The time scope of charge transport is far greater than that large amplitude structural motions of DNA occurs. Those rapid motion have been shown to dramatically modulate electronic coupling between DNA bases.[75-77] Therefore, the mechanism with slower rating determining step than tunneling must be sought for charge transport in DNA.

Several charge hopping mechanisms are under extensive studies to explain the experimental findings in long distance charge transport in DNA, for instance A-hopping model by Giese and coworkers,[78] phono-assisted polaron hopping model by Schuster and coworkers [53, 54] and most recently conformationally gated hopping model by Barton and coworkers[79]. All these different views base their roots on the dynamics of DNA duplex in the time scale of the charge transport. During the process the thermally induced base fluctuations was proposed to facilitate the optimal alignment of bases [80, 81] to stabilize the charge and promote the migration of radical cations.

The phonon-assisted polaron hopping model proposed by Schuster envisions the polaron, a self-stabilized distortion of DNA sequence induced by charge injection, is the entity propagating through DNA helix, which is also gated by its nearby environments, such as water molecules and counterions to the phosphate anions of the backbone. The hopping from one site to the neighboring site is thermally activated (phonon) to overcome the energy barrier associated with self-trapping of the charge. In this model,

the number of hopping is determined by the extent of charge delocalization, size of the polaron, and the time scale of hopping is controlled by the height of energy barriers, the energy difference between polarons and bridging bases. The latter is related to the natural and number of bases involved in delocalization of charge, the low energy sites, and bases comprised the bridge barriers, the high energy sites. Consequently the rate determining step for charge migration in the model is the modulation of free energy to overcome the energy barriers, which is associated with collective motion of DNA bases and its environments during each hopping time frame.[75]

Schuster group investigated the oxidative damage induced by radical cation transport in a series of DNA with regular repeating sequences and proposed a simple kinetic model to illustrate the distance and sequence dependence observed from experimental data.[54] The model, shown in Figure III-39, takes into account of the two factors governing the charge transport rate through DNA helix, the radical cation trapping rate, k_{trap} and the radical migration rate, k_{hop}. The irreversible trapping rate is treated as constant regardless the neighboring based around GG sequence. This assumption has experimental supports and has been generally made for the analysis of relative reactivity data for radical cation in DNA. [49-50], [82-83] The k_{hop} rate was independent of directions in the DNA. In other words, the hopping rate from GG to GG across either $(A)_n$ or $(T)_n$ bridge is the same from 5' to 3' as it is from 3' to 5' which is supported by previous experimental data.[84] The kinetic model is simple yet fits into experimental results.

The model predicts different charge distribution in DNA with various sequences, revealed by oxidative cleavage on GG sites in DNA, is a consequence from different k_{ratio}, equal to k_{hop}/k_{trap}. The ratio is not only determined by intrinsic DNA characteristic but

also by its environment like solvent and counterions. However, it is important to note that overall lifetime of the radical cation ($1/k_{trap}$) is expected to be same for GG steps in native DNA because the values is solely determined by the rate of the irreversible trapping reaction with water and oxygen species.[54,84] The trapping reaction is bimolecular reaction but the concentration of the water and molecular oxygen are large and unchanging during the reaction which is included in rate constant k_{trap}, a pseudo-first-order rate constant.

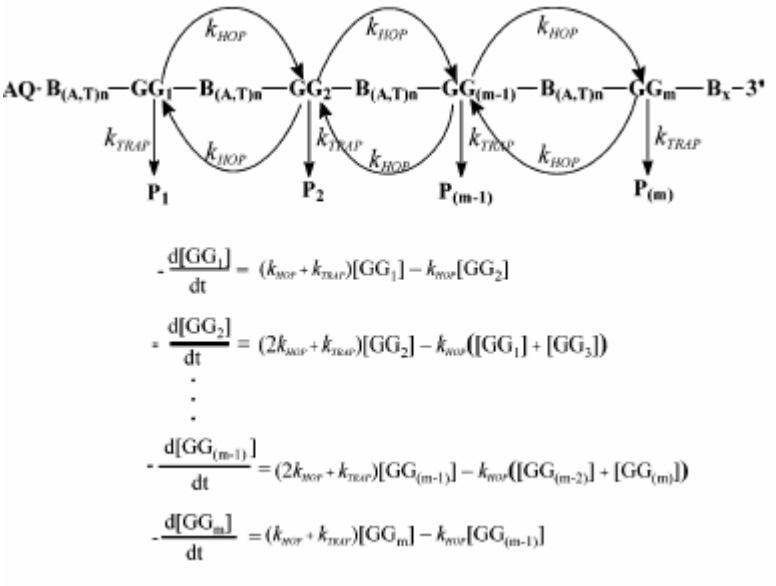

Figure 39 Kinetic model for radical cation hopping. [54]

Experimental result discussions

The irradiation of AQ-DNA in buffer solution causes reaction of the guanines at the GG steps. The amount of strand cleavage at the proximal GG step, 20 Å from the AQ-linked terminus, is 11±1 times greater than at the distal GG step, 70 Å from the AQ. (Lane 2 of Figure III-32) The relative amount of reaction at GG and GG is controlled by

the magnitude of the rate for radical cation hopping (k_{hop}) from GG to GG (and vice versa) compared with the rate for irreversible trapping (k_{trap}) of the radical cation by reaction with H_2O or O_2.[54, 84] When k_{hop} and k_{trap} are of comparable value, $K_{ratio} \approx 1$ and the amount of strand cleavage seen at GG steps falls off approximately exponentially with distance, as is the case for DNA(I). In competition with the trapping reactions that lead eventually to strand cleavage, annihilation of the radical cation by back electron transfer [53] from superoxide in solution removes the radical cation from the DNA with no net reaction.[90]

The ratio of 5'-G_p/5'-G_d in DNA without the addition of lipid and spermine is about 11. It is easy to postulate the k_{ratio} is somewhere close to 1 or smaller in native DNA used in our study based on the theoretical kinetic model described earlier. When k_{ratio} is close to 1 or smaller, the rate of hopping is comparable to rate of irreversible trapping. Consequently most of radical cations are consumed at proximal GG site before a significant population reaches the distal GG sites. The ratio 5'-G_p/5'-G_d in DNA does not significantly change at the presence of increasing amount of spermine and C_2GlySp^{4+}. For example, at a charge ratio of 2, for Sp^{4+} the amount of cleavage at proximal GG is 12 times that at distal GG step, and for C_2GlySp^{4+} the ratio is 10 times. This indicates slight change in k_{ratio}. However, when C_8GlySp^{4+} is present at a charge ratio of 2, the amount of cleavage at proximal GG is only 4 times greater than it is at distal GG. This finding reveals that in the presence of C_8GlySp^{4+} the rate of irreversible trapping of the radical cation that leads to strand cleavage decreases relative to the rate of radical cation hopping; that is, k_{ratio} increases, which results in relatively more reaction at the distal GG step. When k_{hop} and k_{trap} are proximately equal value, the distribution of radical cations among

the GG steps is determined by both thermodynamic stability on each of the GG steps and the rate of radical cation hopping, i.e. distance and energy barrier between bases.

Further evidence for the unique properties of C_8GlySp^{4+} is revealed by combining the result of the total amount of reaction at the 5'-G of the proximal GG step (Figure III-37). Addition of Sp^{4+}, C_2GlySp^{4+} or C_8GlySp^{4+} up to a charge ratio of 0.5 to the AQ-DNA solution causes the amount of cleavage at proximal GG resulting from irradiation to decrease systematically until it reaches ca. 50% of that observed in the absence of spermine. Further additions of Spermine or C_2GlySp^{4+} up to a charge ratio of 2.0 do not affect the amount of strand cleavage at proximal GG. However, the amount of strand cleavage continues to decrease with increasing amounts of C_8GlySp^{4+}, and at a charge ratio of 2.0 it is reduced to only 10% of its zero-lipid value. Clearly, radical cation hopping, trapping or annihilation in DNA are affected when the polycations, Sp^{4+}, C_2GlySp^{4+} replace Na^+, but there is an additional effect that protects the DNA oligomers from reaction observed only when the long alkyl chains of C_8GlySp^{4+} are incorporated in the polycations.

Kinetic rate constants in charge transport

The results from charge transport in DNA-lipid complexes supports the previous model and indicate the back electron transfer can play an role once the rate (k_{bet}) is comparable with k_{hop} and k_{trap}. Lewis and coworkers reported the time-resolved spectroscopic measurement of charge transport in DNA using stilbene as radical injector. In the studies, the guanine is separate from the stiblene by one or two A/T base pairs and

the life time of first-formed guanine radical cation is estimated to be 90 ps and 2 ns, respectively. The time scale is limited by the charge recombination of the radical ion pair once formed (back electron transfer process), which is expected to occur rapidly because the reaction is exothermic and not prohibited by spin conservation rules (both base radical and stilbene radical are in singlet state). Herein, any hopping process significantly slower than radical cation annihilation will not be competitive and observed subsequently. A similar experimental result was observed in charge transport that conducted with thionine. Even though G loses an electron to generate the G radical cation in the presence of photoexcited thionine, the fast BET suppress the decomposition of G radical because of lower irreversible reaction rate consuming G radical cation, i.e. $k_{bet} >> k_{trap}$. However, the integration of N^2-cyclopropylguanosine (^{cp}G), a much faster hole trapper, in DNA reveals the occurrence of charge transfer because the rapid ring opening reaction is fast enough to be competitive with BET, i.e. $k_{bet} <\approx k_{trap}$.(ref 92, 93)

In such cases the back electron transfer plays the deterministic role in charge transfer process. On the other hand, the excited anthraquinone in singlet state, formed upon UV irradiation, undergoes rapid intersystem crossing (ISC) yielding anthraquinone radical in triplet state, which remove an electron from neighboring purine base to form AQ radical cation. Molecular oxygen in solution will remove an electron from AQ radical cation and no charge annihilation will occur. Therefore the long distance charge transport occurs and the life time of radical cation is restricted by the irreversible trapping and quenching reaction (k_{trap}). Even though there is no report of direct determination of k_{trap}, Giese and coworker deduced that its value is in the order of $6x\ 10^4\ s^{-1}$at pH 7.0 by analysis of kinetic data in combination with product yield.[85] The slow rate constant

permits the long distance migration that could not be observed in Lewis's time-resolved spectroscopic system. Based on k_{trap} and k_{ratio} value from previous experiments Schuster calculated the hopping rate constant in long distance charge transport from GG to GG sequence separated by $(A/T)_n$ bridges. The value of k_{hop} ranges from 10^6 to 10^4 s^{-1} as the length of $(A/T)_n$ bridge increase, which indicated the slow radical cation migration rate with the life time between 0.1 μs and 15 μs.[54]

Recently Majima and coworkers reported a first direct observation of the hole transfer through double-helical DNA using time-resolved transient measurement. They concluded that the hole transfer process over long distance in DNA occurs at the apparent rate constants of $1.2x10^4$- $5.7x10^7$ in the time scale of microsecond to milliseconds.[86] The experimental results perfectly match the estimated value from Schuster based on k_{trap} and k_{ratio} values. This is a much longer time scale than that required for large-amplitude motions of DNA and its water and counterions environment.[75] This supports the notion that ions and water molecule 'gate' the dynamics of radical cation.[77, 87] Any factors that influence the distribution of ions and water molecule surrounding DNA and the interaction between them should have an impact on the radical cation migration and quenching.

Kinetic model with back electron transfer effect

After all, we integrate the rate of back electron transfer (k_{bet}) into kinetic model to fully understand observed reduced oxidative damage in both GG step in DNA-lipid complexes. Barton and coworkers recently reported that BET can be a critical factor in

rationalizing the various sequence dependent damage pattern from different research group using different photo-oxidants. When GG step is so close to photooxidant that k_{bet} is comparable to k_{trap} and k_{hop}, reverse damage pattern was reported, the photocleaveage is more intense at GG sequence distal to photooxidants than that proximal to photooxidants.

Recent theoretical investigations have suggested that the dynamics of the DNA environment, particularly the water molecules, may modulate the relative redox potential of DNA bases.[91] Thermal movements of the water molecules significantly dominate the variation of hole state energy. This fluctuation in radical cation state energy is significant even at the absence of counterions in the case of DNA with methylphosphate in backbone.

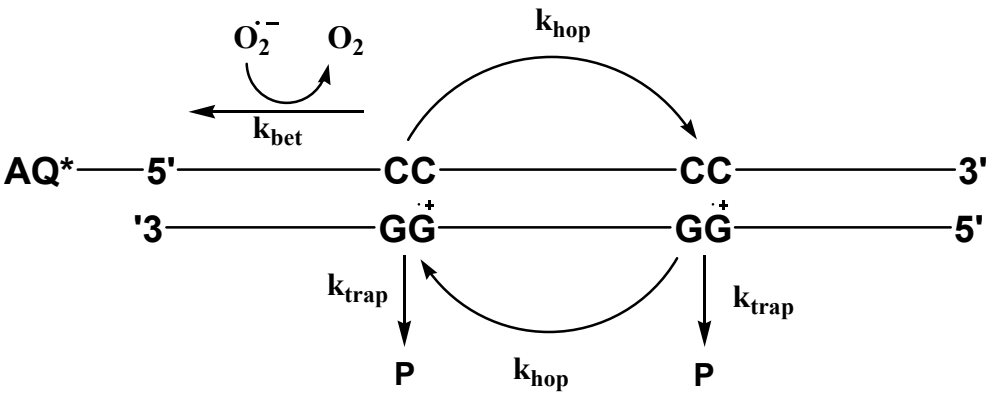

Figure III-40 Kinetic model for the charge hopping and annihilation mechanism

Higher damage ratio at distal GG site was observed in the samples containing C_8GlySp^{4+} lipid. This can be attributed to the smaller value of k_{ratio} such that radical cation population can distribute along DNA sequence evenly.

Mechanism of water reaction with guanine radical

The ratio of the proximal GG/ distal GG sequence depends not only upon the charge transfer but also upon the water trapping reaction rate [54, 85] as described earlier. Some researches have been done to address how water quenching reaction affects k_{trap}. This water trapping of a guanine radical cation should change if the reaction conditions are modified. For example, Giese and coworkers observed that the water trapping of the guanine radical cation $G^{\bullet+}$, which competes with the hole transfer to GGG, is more efficient at pH 7.0 than at pH 5.0, which can be explained by an increase of the water's nucleophilicity.

The deprotonation of guanine radical without base pair yields guanosyl radical, which is a much poorer oxidant than a guanine radical cation, and therefore slows down the charge transport. In perfectly paired G:C base pairs the proton transfer from $G^{\bullet+}$ to water is too slow to compete with the hole transfer because the protons are fixed between the heterocyclic bases (Figure III-40).[88] A substitution of guanine with 3'-methyl guanine eliminates deprotonation and enhances the charge transfer efficiency.

Theoretical molecular dynamic calculation by Schuster indicated that phosphate may play a role in modulate the reaction of phosphate with water molecule. Energy barrier limits the reaction rate between water molecule and guanine radical cation. The phosphate on the DNA backbond can interact with H_2O through hydrogen bonding and lower the ΔG to accelerate the water quenching reaction. A substitution of phosphate with methyl phosphate backbone effectively quenches the strand cleavage (lower k_{trap}) at

guanine bases containing methylated phosphate without significantly alter the damage at the distal sites (no change in k_{hop}).

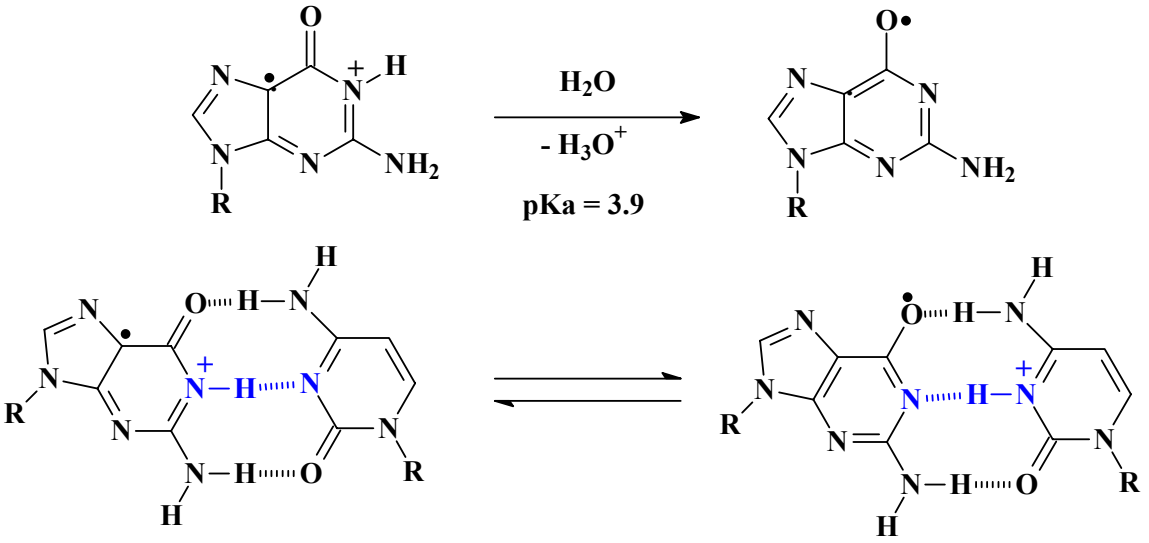

Figure III-41 Deprotonation of Guanine radical with and without complimentary bases.[89]

As described earlier, the binding of Sp^{4+} and lipid slows down the radical cation trapping and quenching rate hereby reduces the oxidative damage at GG sites. The mechanism of the reduced reaction rate at GG steps can not be interpreted accurately from our experimental data. This is attributable to several reasons. The binding of our synthetic lipid toward DNA is not well defined in our experiments. A plethora of experimental and theoretical researches have tried to elucidate the binding affinity and sites of spermine on DNA duplex. Electrostatic interaction with negative charged phosphate backbond was commonly considered as a major driving fore for the interaction.[13, 14] However, the polyamine binding sites in DNA have been observed within both the minor and major groove of DNA,[95-97] slightly favoring the minor groove

rich in (A/T) track as shown in experimental study.[98] Theoretical molecular simulation suggested that spermine possibly had binding locations to major groove of GC-rich duplexes[99] and to minor groove of AT-rich duplexes.[13, 100] Recent molecular dynamic simulation indicates that the presence of spermine makes significant influence on the DNA hydration and on the interaction of the sodium ions with DNA. Water molecules were pushed out of the minor groove by spermine which displayed a high presence in the minor groove and competing with sodium ion in binding to DNA phosphate and minor groove.[101] In such case, when the spermine replaces the sodium ion to neutralize phosphate anion, the ion-gated modulation would be affected as the consequence of energetic reconfiguration of excited radical cation orbital. Native B-form DNA maintains a well-hydrated minor groove. The groove binding of spermine can lead to the redistribution of ions and waters residing the grooves and possibly closely associated with nucleobases through hydrogen bonding. Those microenvironments of DNA have been shown to modulate the nucloebases' oxidation potential significantly.[94] Spermine may act as a ligand to alter the distribution of sodium ion and water molecules along the backbone and grooves that subsequently changes the charge hopping and quenching rate.

Because all synthetic lipids have a spermine core as binding group for DNA, It is reasonable to postulate that individual lipid would bind to DNA in the similar mode as spermine does. C_8GlySp^{4+}, additionally, has the ability to form a dense hydrophobic layer surrounding the DNA duplexes, comparing to either spermine or C_2GlySp^{4+}. The experimental results from singlet oxygen reaction with DNA rule out the effect of lipid on reducing the reaction with oxygen species. Thus, the added hydrophobic layer from C_8GlySp^{4+} becomes the apparent factor to block guanine radical cation reaction with the

water to reduce k_{trap}. The slower reaction at proximal GG not only gives radical cation more chance to hopping to next GG steps, yielding lower 5'-G_p/5'-G_d ratio but also make BET, slower rate constant in AQ-conjugate system, competitive. The latter could occur through charge recombination with excited AQ^* or the removal of an electron from superoxide ($O_2\bullet^-$) in bulk media, affording no net reaction at GG sites.

Summary and Perspectives

Since the determination of the molecular structure of DNA by Watson and Crick, the ability of the base pairs to support charge transport through π-stack array has been conclusively delineated by numerous investigation. Studies revealed that charge transport process occurs over remarkable distance at relative fast rate with shallow dependence on distance. Additional investigations have found it to be exquisitely sensitive to perturbation in the π-stack, oxidation potential of radical traps and solvation environments. DNA binding protein, mismatches or bulges in the base pairs has all been found to attenuate charge transport. The wealth of experiment evidence provoked the shift in the charge transfer field from whether it occurs towards ruminations about the mechanism of the process. The work described in this dissertation commenced in this highly intellectual controversial environment.

During this time, a super-exchange model that described DNA charge transport as that of hopping among easily oxidizable guanine steps and tunneling through higher energy adenine/thymine steps was being touted as a dominant mechanism. However, this mechanism did not appear to elucidate the slower rates of charge transport observed over

a range of distances or the shallow dependence on distance. An investigation utilizing 5'-covalented linked anthraquinone assemblies and varying lengths of A/T sequences in Schuster's group does not show marked decreases in oxidative damage yield, as would be expected for increasing the number of tunneling steps, but hints at a mechanism that is far more complicated than the proposed model of single nucleotide tunneling. A phonon-assisted polaron hopping model, in which charge is injected into extended, transiently formed base distortion to stabilize the charge and the hopping occurs adiabatically, has been proposed as an alternative DNA CT mechanism and is more encompassing in describing experimental data. A kinetic scheme based on the model provides accurate estimation of hopping rate in long distance charge transport. The competition between charge hopping rate (k_{hop}) and charge trapping rate (k_{trap}) is deterministic in the observed oxidative damage at labile guanine sites due to charge transport. In order to investigate the factors that affects charge trapping rate we developed a system in which DNA is coated with lipid to form a hydrophobic environment.

DNA-lipid complexes naturally occur in biological systems and have been widely applied to facilitate the gene transfection through cell membrane. The lipids with various lengths of hydrophobic alkyl chains (C_2, C_8 and C_{18}) and a spermine core binding group were synthesized and their complexes with a 27-mer DNA were characterized by spectroscopic methods. Hydrophobic aggregate formation is evident at high lipid concentration and carefully avoided in UV-irradiation experiment to ensure the stable complex formation in aqueous solution and the valid comparison between native DNA and DNA-lipid complexes. The aggregation effect was attributed to the association of complexes at high concentration due to the hydrophobic effect. The fluorescence

quenching assay indicates the strong affinity of spermine and lipids to DNA, in which the intercalating ethidium bromide was replaced and excluded from DNA duplexes. The oxidative damage at GG sequences at either proximal or distal sites was dramatically reduced with no indication of DNA π-stack disturbance. The lipid with longer dialkyl chain, C_8GlySp^{4+}, demonstrates stronger ability to quench the reaction but enhance the distal/proximal damage ratio at GG sites, compared to spermine and C_2GlySp^{4+}. Since the amount and ratio of photocleavage is related to the radical cation hopping and the subsequent reaction with water and oxygen species, this led us to consider the factors that may explain the experimental observation. Circular dichroism spectra provide no evidence for the conformational transformation induced by binding of either spermine or lipids, which undermines the significant alteration π stacking in base pairs. Singlet oxygen ($^1O_2$), created by irradiation of rose bengal, damage the DNA guanine site in dramatic different pattern from that of photoexcitation of anthraquinone. The yield of oxidative damage is independent of the presence of spermine and synthetic lipids, thus indicating the reaction rate with oxygen species is unaffected in DNA-lipid complexes. We attribute the effect of lipids on reducing oxidative damage at GG sites to theirs ability to change microenvironment around DNA by replacing the counterions associated with phosphates backbone and weaken the hydration spine along minor and major groove as well as the backbone. The longer dialkyl chain in C_8GlySp^{4+} acts as an additional hydrophobic shield from bulk aqueous media providing extra protection from the water quenching of radical cation. The overall slower radical trapping rate makes back electron transfer (BET) to anthraquinone or superoxide ($O_2^{\bullet-}$) a competitive pathway leading to no net reaction.

With the burgeoning interest in the use of DNA in the field of microelectronics and the creation of effective biological sensors, it has become increasingly imperative to comprehend the mechanism(s) of DNA charge transport and those factors that attenuate the process. The work described in this project provides insight into a salient parameter that reduces the oxidative damage induced by charge transport and hence enhances the ability of DNA to support charge transport to the distal sites. Many crucial questions remain to be answered. Is there the relevance of the phenomenon to living systems and biological implications? How can we directly observe the charge transport through DNA without creating the strand cleavage? What is the detailed mechanism of the quenching of guanine radical by water molecule? Is it possible to create the high efficient DNA nanowire if the trapping and quenching reaction is completely eliminated? Only further study will elucidate the answers to these and other questions. It is essential to thoroughly investigate and understand the various factors governing the DNA charge transport process such that an accurate and general mechanism(s) can be formulated.

References

1. Behr, J.-P.; Demeneix, B.; Loefeler, J.-P.; Perez-Mutul, J. *Proc. Natl. Acad. Sci. USA.* 1989, 86, 6982-6986

2. Felgner, P. L.; Gadek, T. R.; Holm, M.; Roman, R.; Chan, H. W.; Wenz, M.; Northrop, J. P.; Ringold, G. M.; Danielsen, M. *Proc. Natl. Acad. Sci. U.S.A.* 1987, 84, 7413-7417

3. Gershon, H.; Ghirlando, R.; Guttman, S. B.; Minsky, A., *Biochemistry* 1993, 32, 7143-7151

4. Rädler, J. O.; Koltover, I.; Salditt, T.; Safinya, C. R. *Science* 1997, 275, 810-814

5. Rädler, J. O.; Koltover, I.; Jamieson, A.; Salditt, T.; Safinya, C. R. *Langmuir* 1998, 14, 4272-4283

6. Lasic, D. D.; Strey, H.; Stuart, M. C. A.; Podgornik, R.; Frederik, P. M. *J. Am. Chem. Soc.* 1997, 832-833

7. Gustafsson, J.; Arvidson, G; Karlsson, G.; Almgren, M. *Biochim. Biophys. Acta* 1995, 1235, 305-312

8. Battersby, B. J.; Grimm, R.; Huebner, S.; Cevc, G. *Biochim. Biophys. Acta* 1998, 1372, 379-383

9. Templeton, N. S.; Lasic, D. D.; Frederik. P. M.; Strey, H. H.; Roberts, D. D.; Pavlakis, G. N. *Nat. Biotechnol.* 1997, 15, 647-652.

10. Dauty, E.; Remy, J.-S.; Blessing, T.; Behr, J.-P. *J. Am. Chem. Soc.* 2001, 1239227-9234

11.Koltover, I.; Salditt, T.; Rädler, J. O.; Safinya, C. R. *Science*, 1998, 281, 78-81

12. Sternberg, B.; Sorgi, F. L.; Huang, L. *FEBS Lett.* 1994, 356, 361-366.

13. Feurstein, B. G.; Pattabiraman, N.; Marton, L. J. *Proc. Natl. Acad. Sci. USA* 1986, 83, 5948-4952

14. Hou, M. H.; Lin, S. B; Yuan, J. M.; Lin, W. C.; Wang, A. H.; Kan. L.-S. *Nucleic Acids. Res.* 2001, 29, 5121-5218

15. Behr, J. P. *J. Chem. Soc., Commun.* 1989, 101-103

16. Bergeron, R. J.; Garlich, J. R. *Synthesis* 1984, 782-784

17. Remy J. S.; Sirlin, C; Vierling, P.; Behr, J. P. *Bioconjugate Chem*. 1994, 5 (6), 647-654

18. Siegel, C. S.; Lee, E. R.; Harris, D. J.; *US Patent 5912239*, 1997

19. Cain, B. F.; Baguley, B. C.; Denny, W. A. *J. Med. Chem.* 1978, 21, 658.

20. Delcros, J.-G.; Sturkenboom, M. C. J.M.; Basu, H. S.; Shaffer, R. H.; Szollosi, J.; Feuerstein, B. G.; Marton, L. *J. Biochem. J.* 1993, 291, 269

21. Stewart, K. D.; Gray, T. A. *J. Phys. Org. Chem.* 1992, 5, 461

22. Lasic, D. D. *Liposomes in Gene Delivery*, CRC Press, 1997

23. Sheehan, J. C; Preston, J.; Cruickshank, P. A., *J. Amer. Chem. Soc.* 1965, 87, 11, 2492-2493

24. Izdebski, J.; Orlowaska, A., *Peptides* 1989, 16-18

25. Yamada, S.; Kasai, Y.; Shioiri, T., *Tetrahedron Lett.* 1973, 18, 1595-1598

26. Shioiri T.; Ninomiya K., Yamada, S., *J. Amer. Chem. Soc.* 1972, 94, 17, 6203-6205

27. Castro, B.; Oormoy, J. R.; Evin G.; Selve, C.; *Tetrahedron Lett.* 1975, 14, 1219-1222

28. Paul, R.; Anderson, G. W., *J. Amer. Chem. Soc.* 1960, 82, 4596-4600

29. Ho, G. J.; Emerson, K. M.; Mathre, D. J.; Shuman, R. F.; Grabowski, E. J. J., *J. Org. Chem.* 1995, 60, 3569-3570

30. Sartor, V., Henderson, P. T.; Schuster, G. B.; *J. Am. Chem. Soc.* 1999, 121, 11027-11033.

31. Gasper, S. M.; Schuster, G. B. *J. Am. Chem. Soc.* 1997, 119, 12762-12771

32. Kawai, K., Kimura, T., Kawabata, K.; Tojo, S.; Majima, T.; *J. Phys. Chem. B*. 107, 12838-12841

33. Kawai, K., Takada, T.; Tojo, S.; Majima, T. *Tetrahedron Lett.* 2002, 43, 89-91.

34. Sanii, L.; Schuster, G. B. *J. Am. Chem. Soc.* 2000, 122, 11545-11546

35. Du H., Fuh R. C. A.; Li J. Z.; Corkan L. A.; Lindsey J. S. *Photochem. Photobio.* 1998, 68, 141-142

36. Pontitus, B. W.; Berg, P. *Proc. Natl. Acad. Sci. USA* 1991, 88, 8237-8241

37. Drew, H. R.; Dickerson, R. E. *J. Mol. Biol.* 1981, 151, 535-556

38. Dickerson, R. E., Drew, H. R., Conner, B. N.; Wing, R. M.; Fratini, A. V.; Lopka, M. L. *Science* 1982, 216, 475-484

39. Hanlson, S.; Brudno, S.; Wu, T. T.; Wolf, B. *Biochemistry* 1975, 14, 1648

40. Girod, J. C.; Johnson, W. C. Jr.; Huntington, S. K.; Maestre, M. F. *Biochemistry* 1973, 12, 5092.

41. Wiethoff, C. M.; Gill, M. L.; Koe, G. S.; Koe, J. G.; Middaugh, C. R. *J. Biol. Chem.* 2002, 277, 44980-44987

42. Vijayanathan, V.; Thomas, T.; Shirahata, A.; Thomas, T. *J. Biochemistry* 2001, 40, 13644-13651

43. Critical micelle concentration (cmc) is unknown for those compounds. However, the cmc of a similar compound is about 150 μM reported in literature which is roughly fit with our experimental observation

44. Nelson, J. W.; Tinoco, I. *Biochemistry* 1985, 24, 6416-6421

45. Henderson, P. Dissertation, Georgia Institute of Technology, Atlanta, GA, 1998

46. Heller D.P., Greenstock C. L. *Biophys. Chem.* 1994, 50, 305-12

47. Patterson, S. E.; Coxn, J. M; Strekowski, L. *Bioorg. Med. Chem.* 1997, 5, 227-281

48. Steenken, S.; Jovanovic S. V. *J. Am. Chem. Soc.* 1997, 119, 617-619

49. Schuster, G. B. *Acc. Chem. Res.* 2000, 33, 253-260

50. Giese, B. *Acc. Chem. Res.* 2000, 33, 631-636

51. Giese, B, Wessely, S. *Angew, Chem. Int. Ed.* 2000, 39, 3490-3495

52. Boone, E.; Schuster, G. B Nucleic Acids Res. 2002, 30, 830-837

53. Henderson, P. T.; Jones, D.; Hampikian, G.; Kan, Y. Z.; Schuster, G. B.; *Proc. Natl. Acad. Sci. U. S. A.* 1999, 96, 8353-8358

54. Liu, C.-S.; Hernandez, R; Schuster, G. B; *J. Am. Chem. Soc.* 2004, 126, 2877-2884

55. Halliwell, B.; Gutteridge, J. M. C., Free radicals in biology and medicine. 1st ed. Oxford science publications. 1985, Oxford; New York: Clarendon Press; Oxford University Press. xii, 346

56. Pitari G.; Dupre S.; Spirito A.; Antonini G; Amicarelli F. *Adv Exp Med Biol.* 2000, 483, 157-162

57. Briviba, K., L.-O. Klotz, and H. Sies, *Biol. Chem.* 1997, 378, 1259-1265.

58. Neverov, K.V., et al*., Biochemistry Moscow*1996, 61, 1149-1155.

59. Ryter, S.W.; Tyrrell, R. M. *Free Radical Biol. Med* 1998, 24, 1520-1534

60. Kochevar, I.E.; Redmond, R. W., *Methods Enzymol.* 2000, 319: p. 20-8.

61. Ravanat, J.-L.: Cadet, J. *Chem. Res. Toxicol.* 1995, 8, 379-388

62. Ahmed, N.; Mukhtar, H. *Methods Enzymol.* 2000, 319, 342-358

63. Ye, Y.; Muller, J. G.; Luo, W; Mayne, C. L.; Shallop, A. J.; Jones, R. A.; Burrows, C. J. *J. Am. Chem. Soc.* 2003, 125, 13926-13927

64. a) Ravanat, J.-L.; Saint-Pierre, C.; Di Mascio, P.; Martinez, G. R.; Medeiros, M. H. G.; Cadet, J. *Helv, Chim. Acta* 2001, 84, 3702-3709 b) b) Ravanat, J. L.; Sauvaigo, S.; Caillat, S.; Martinez, G. R.; Medeiros, M. H. G.; Di Mascio P.; Favier, A.; Cadet, J. *Biol. Chem.* 2004, 385, 17-20

65. Schuster, G. B.; Editor *Top. Curr. Chem.* 236, 237

66. Giese, B.; Amaudrut, J.; Kohler, A.; Sporman, M.; Wessely, S. *Nature* 2001, 412, 318-320

67. Sartor, V.; Boone, E.; Schuster, G. B. *J. Phys. Chem. B* 2001, 105, 11057-11059.

68. Williams, T. T.; Odom, D. T.; Barton, J. K. *J. Am. Chem. Soc.* 2000, 122, 9048-9049

69. Lewis, F. D.; Liu, J.; Zou, X.; Hayes, R. T.; Wasielewski, M. R. *J. Am. Chem. Soc.* 2003, 125, 4850-4861.

70. Kawai, K.; Tkada, T.; Tojo, S.; Ichinose, N. M. T. *J. Am. Chem. Soc.* 2001, 123, 126880-12689

71. Shafirovich, V.; Dourandin, A.; Huang, W. D.; Luneva, N. P.; Geacintov, N. E.; *J. Phys. Chem. B* 1999, 103, 10924-10933

72. Takada, T, Kawai, K, Fujitsuka, M; Majima, T.; *Proc. Natl. Acad. Sci. U. S. A*. 2004, 101, 14002-14006

73. Bixon, M.; Giese, B.; Wessely, S. langenbacher, T.; Michel-Beyerle, M. E.; Jortner, J. *Proc. Natl. Acad. Sci. U. S. A.* 1999, 96, 11713-11716

74. Zhang, H.-Y,; Li, X.-Q.; Han, P.; Yu, X.; Yan, Y.-L. *J. Chem. Phys.* 2002, 117

75. Beveridge, D. L.; McConnel, K. J. *Curr. Opin. Struc. Biol.* 2000, 10, 182-196

76. Voityuk, A. A.; Siriwong, K.; Rosch, N. *Phys. Chem. Chem. Phys.* 2001, 3, 5421-5425

77. Troisi, A.; Giorgio Orlandi, G. *J. Phys. Chem. B* 2002, 106, 2093-2101

78. Meggers, E., Micheal-Beyerle, M. E.; Giese, B. *J. Am. Chem. Soc.* 1998, 120, 12950-12955

79. O'Neill, M. A.; Barton, J. K. *J. Am. Chem. Soc.* 2004; 126; 11471-11483

80. D'Orsogna, M. r.; Rudnick, *J. Phys. Rev. E* 2002, 66 artno041904

81. Bruinsma, R.; Cruner, G.; D;Orsogna, M. R.; Rudnick, J. *Phys. Rev. Lett.* 2000, 85, 4393-4396

82. Kino, K.; Saito, I.; Sugiyama, H. *J. Am. Chem. Soc.* 1998, 120, 7373-7374

83. Nunez, M.; Hall, D. B.; Barton, J. K. *Chem. Biol.* 1999, 6, 85-97

84. Liu, C.-S.; Schuster, G. B *J. Am. Chem. Soc.* 2003, 125, 6098-6102

85. Giese, B; Spichtly, M. *Chem. Phys. Chem*. 2000, 1, 195-198

86. Takada, T.; Kawai, K.; Fujitsuka, M.; Majima, T.; *Proc. Natl. Acad. Sci. USA* 2004, 101, 14002-14006

87. Barnett, R. N.; Cleveland, C. L.; Joy, A.; Landman, U.; Schuster, G. B. *Science* 2001, 294, 56-571

88. Giese B.; Wessely S.*; Chem Comm.* 2001, 2108

89. Giese, B, *Top. Curr. Chem.* 236, 27-44

90. Shafirovich, V.; SERMACS meeting, Atlanta, 2003, private communication

91. Voityuk, A. A.; Siriwong, K,; Rosch, N. *Angew, Chem. Int. Ed.* 2004, 43, 624-627

92. Dohno, C.; Stemp, E. D. A.; Barton, J. K. *J. Am. Chem. Soc.* 2003, 125, 9586-9587

93. Williams, T. T; Dohno, C.; Stemp, E. D. A.; Barton, J. K.; *J. Am. Chem. Soc.* 2004, 126,8148-8158

94. Barnett, R. N.; Cleveland, C. L.; Landman, U.; Boone, E; Kanvah, S.; Schuster, G. B. *J. Phys. Chem. B* 2003, 107, 3525-3537

95. Egli, M.; Tetreshkov, V.; Teplova, M.; Minasov, G.; Joachimiak, A.; snishvili, R.; Weeks, C. M.; Miller, R.; Maier, M. A.; An, H.; Dan Cook, P.; Manoharan, M. *Biopolymer* 1998, 48, 234-252

96. Shui, X.; McFail-Isom, L.; Hu, G. G., Williams, L. D. *Biochemistry* 1998, 37, 8341-8355

97. Tari, L. W., Secco, A. S., *Nucleic Acids Res.* 1995, 23, 2065-2073

98. Schmid, N.; Behr, J.-P. *Biochemistry* 1991, 30, 4357-4361

99. Feuerstein, B. G.; Pattabiraman, N.; Marton, L. J., *Nucleic Acids. Res.*1990, 18, 1271-1282

100. Zakrzewska, K.; Pullman, B. *Biopolymer* 1986, 25, 375-392

101. Korolev, N.; Lyubartsev, A. P.; Laaksonen, A.; Nordenskiöld, L.; *Biophysical J.* 2002, 82, 2860-2875

PART II

CHARGE TRANSFER IN DNA CONTAINING MODIFIED GUANINE BASES: STERIC AND ENERGERIC CONTROL OF REACTIVITY

CHAPTER I

INTRODUCTION

Charge Transfer in DNA

One-electron oxidation of guanine base is a common cause of damage in DNA. In many studies damage sites far away from initial oxidation site have been reported. How the electron or charge transfer through the DNA duplex structure to reach the damage site is still under debate.[1] Two mechanisms, namely coherent superexchange for short-distance transport [2,3] and hole [4] or polaron [5] multi-step hopping for long-range transport are evoked to describe this observation.[6] Experimentally, it is becoming clear that long-range hole transfer requires intermediate guanines and also adenines, to a lesser extent, to function as temporary charge carrieres.[7,8] Much research has been done to investigate the mechanism of charge transfer in DNA. Photosensitizers, for instance anthraquinone derivatives,[9,10] riboflavin,[11, 12] and napthalimides,[13] are often used in such research to intensify the damage so that the mechanism can be studied. A unique feature of the cleavage is that it predominates at the 5'-G of the GG sequence, with a ratio of approximately 5:1 to 11:1. Selective guanine reactivity is not unique to charge transfer processes. It has been observed in many systems involving singlet oxygen,[14] hydroxyl radical,[15] superoxide [16] and other alkylating agents such as dimethyl sulfide and piperidine formate (Maxam and Gilbert sequencing reagents for G and A+G, respectively).[17] However, these reagents showed no particular selectivity in 5'-GG-3'

steps. One electron transfer from DNA base to photosensitizer, resulting in radical cation, may be the first step in DNA cleavage in these systems. In this process the base serves as electron donors, while photosensitizer acts as excited state oxidants.

$$P^* + B \longrightarrow P^{\bullet -} + B^{\bullet +}$$

DNA's unique secondary structure, i.e. stacking and overlapping of the π electrons of the DAN bases, provides a path for efficient electron/charge transfer over long distances. The oxidative damage at GG steps due to charge transfer as far as 180 Å away has been reported by Schuster and Henderson.[18]

Anthraquinone derivatives are one of such kind of intercalating photosensitizer. It has been well studied and proven to be very effective initiator of charge transfer in duplex DNA.[9, 10, 19, 20] The excitation wavelength of the anthraquinone at 334 nm is far apart from DNA absorption band at 260 nm, which makes selective excitation feasible. After photoexcitation, several competing reactions will carry on leading to either quenching the excited AQ and base pair or charge transfer in DNA (Figure I-1). Previous work by Schuster has demonstrated that the fast cation hole transfer process, less than 20 ps, effectively precludes reaction by other pathway.[21] The slow back electron transfer (BET), 200 ps, and fast intersystem crossing from singlet state to triplet state, less than 20 ps, attribute to the stable radical anion of triplet state AQ, in which BET is prohibited due to the same spin direction on both AQ and base's unpaired electron. Oxygen further removes the electron from DNA helix and leaves the radical cation which undergoes either quenching by superoxide ($O_2^{\bullet -}$) to reproduce AQ and oxygen or hole trapping and

migration. The latter will subsequently cause the damage of base far from radical cation injection site via irreversible reaction with water and oxygen.

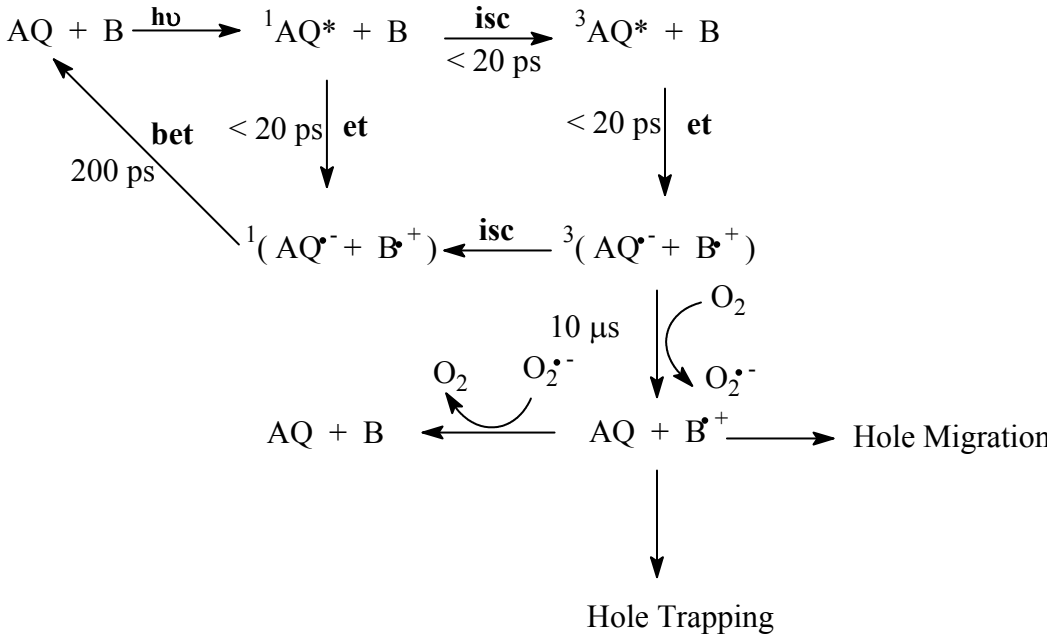

Figure I-1 The mechanism of anthraquinone photoexcitations (Armitage, B. *Chem. Rev.* 1998, 98, 1188)

Formation and Reaction of Guanine Radical Cation

Guanine is the predominate target of oxidation damage in long distance charge transfer in DNA because of its lowest one electron oxidation potential, i.e. 1.29 V at pH 7.0, in four natural bases, shown in Table I-1,[22, 23] The oxidation potential of the nucleoside guanosine has been studied extensively by Steenken.[24, 25] It has been observed that the reduction potential is highly pH dependent because of the rapid deprotonation of the corresponding radical cation at neutral or basic pH. However, the oxidation potential

of guanine in a DNA helix is very likely to be different from that of an isolated nucleoside due to base stacking and surrounding solvent environment. It has been proposed that $G^{\bullet+}$ ($pK_a = 3.9$)[25] formed in duplex DNA has more cation character than an isolated G due to proton transfer to N^3 of cytosine which has slightly higher pK_a (4.3) than $G^{\bullet+}$ and result in a small equilibrium constant $K_{eq} = 2.5$. This also affects the oxidation potential of guanine in charge transfer.

Table I-1 Oxidation potentials of the DNA bases at pH 7.0.

	Guanosine	**Adenosine**	**Cytidine**	**Thymidine**
E^0 (V)[a]	1.29	1.42	1.6	1.7

In aqueous solution, guanosine has several pathways to produce the final oxidation product. After guanine loses one electron to form radical cation, it subsequently loses hydrogen. Following addition of oxygen, CO_2 and formamide quickly fragment from the ring structure and lead to the observed product imidazolone and oxazolone.[26] The second pathway involves the addition of H_2O to the guanine radical which followed by loss of hydrogens and one more electron, resulting in the formation of 8-oxoG, a predominately product of G radical cation quenching in DNA duplex. 8-oxoG can also be formed through the reaction with singlet oxygen or hydroxyl radical (Figure 5).[24, 27, 28] Both imidazolone and oxazolone are piperidine labile species whereas the 8-oxoG is the good target of enzymatic cleavage by formamidopyrimidine glycosolase (FPG). On the

other hand 8-oxoG is resistant to the cleavage by hot piperidine treatment. A rough estimation of ratio of 8-oxoG product to other products from irradiation damage can be obtained using these two complimentary measurements. In the oxidation process of guanosine, addition of H_2O is preferred in duplex DNA, but deprotonation and reaction with O_2 are preferred in nucleosides.

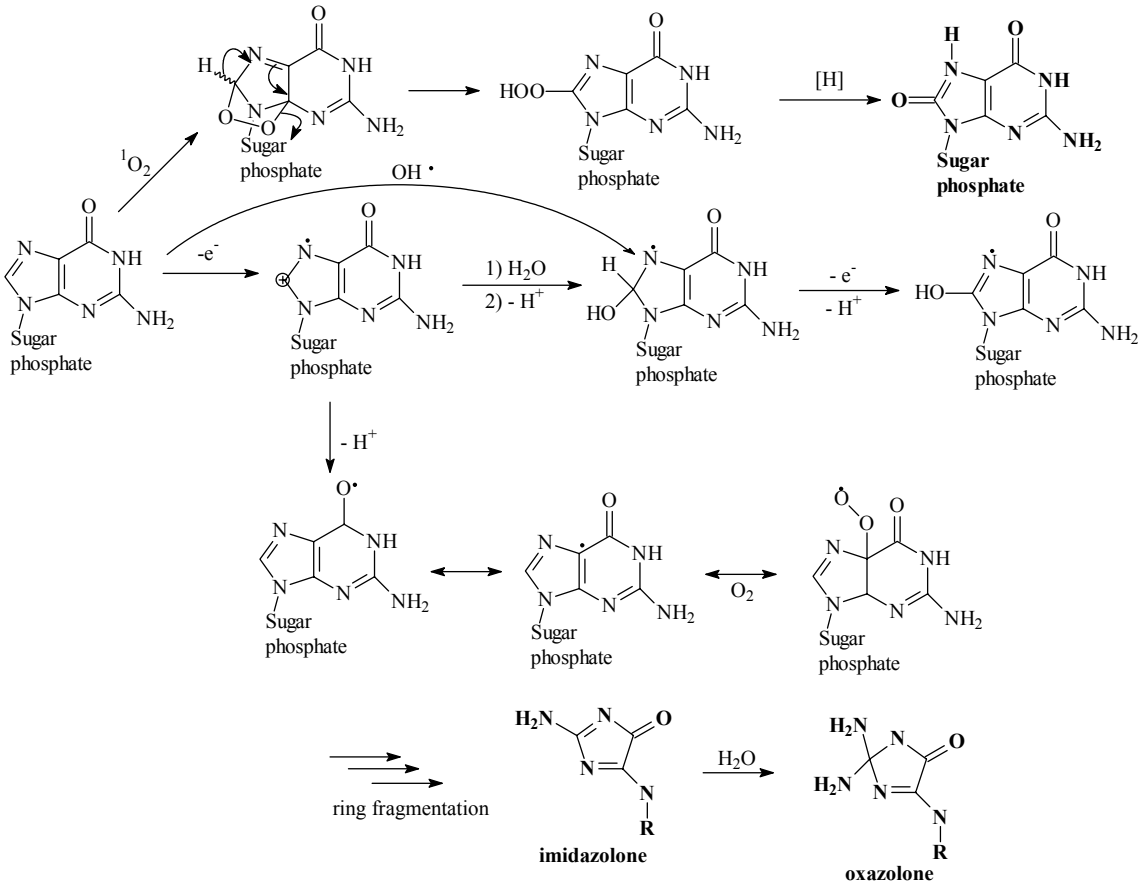

Figure I-2 Oxidation of deoxyguanosine

As early as 1985 Rubin and coworkers had found the reactivity of guanine toward photo-oxidation was sequence dependent.[29] Guanines located on the 5'-side of at least one other purine, especially a G, are strongly preferred over all the other cleavage sites.

Sugiyama and Saito have applied *ab initio* molecular orbital calculation on G, XG sites and showed that GG site has the lowest ionization potential, shown in Table 3, among the 10 possible stacked bases examined. They concluded the π-stacking effect of the purines in which the HOMO resides predominately on the 5'-G in a purine stack, thus the electron should be kinetically removed from the 5'-G of the sequence.[30] Further studies revealed that 5'-GGG-3' is a more effective trap in hole migration than 5'-GG-3' due to its low ionization potential of 6.34 V.[31-33] Selectivity in guanine damage of triple G segment is highly sequence-dependent [11, 34-36] which is attributed to different stability of neutral radicals (5'-XGGGX-3')$^{\bullet}$ according to *ab initio* molecular orbital calculations by Saito group.[37] It is shown that 5'-TGG$^{\bullet}$G-3' has lower energy than 5'-TG$^{\bullet}$GG-3' which causes observed more damage in the middle guanine. On the other hand the G_1 orbital in 5'-CG_1G_2G-3' radical is delocalized as opposite to G_2 which is essentially localized on middle guanine which was ascribed to stacking interaction with 5'-side G of the opposite strand. This explains the favorable reactivity on G_1 over G_2.

Prat et al. also performed the similar *ab initio* calculation and suggested that the origin of the GG stacking effect lies in the favorable orientation of N7 of the 3'-G compared to the site of oxidation of the 5'-G. In particular, the N7 is aligned, in B-DNA, beneath carbonyl group of the 5'-G.[38]

These theoretical calculations were also supported by other kinetic experimental studies in electrochemistry.[39, 40] Thus the observed order of reactivity of G sequences is G**GG**G > G**GG** > G**G** > A**G** > T**G** ≈ C**G**. Experimentally a guanine radical cation is the implied intermediate because of the observed products.

Table I-2 Ionization potential of stacked guanosines

Sequence	**I.P. (eV)[a]**	**E^0 (V vs. NHE)[b]**
3'-GGGG-5'	6.98	0.57
3'-G**G**G-5'	7.07	0.64
3'-G**G**-5'	7.28	0.82
3'-A**G**-5'	7.51	1.00
3'-C**G**-5'	7.68	1.15
3'-T**G**-5'	7.69	1.16
G	7.75	1.20

[a] From Reference 30

[b] Calculated from IP data using E^0=0.827xI.P. – 5.20 (adjusted for V vs. NHE)

Inquiry into the Modified Guanines

Guanine is the oxidation damage target of one electron transfer in DNA. Therefore modified guanine species or analogues are of great interest to investigate the various aspects of mechanisms of charge transfer in DNA, such as effect of oxidation potential, selectivity and efficiency of transport.

Several researches have demonstrated that 8-methyl guanine (8-MeG), a product of methyl radical attack on guanine residue, is one of product of DNA base free radical damage, both in vivo and vitro.[26, 41-43] A detectable level of 8-MeG was observed in liver and stomach of rat treated with t-butyl hydroperoxide (t-BOOH) whose behavior is very likely to be shared by cumene hydroperoxide, consumed 7 billion pounds per year in United States.[42] 8-MeG has been identified as mutagenic lesion, which is capable of generating G-C and G-T transversions and deletion in vitro.[44] 8-MedG is able to form base pairs with dG and dA in *syn* conformation(Figure 6). It has been shown that DNA duplex containing 8-MedG:dG and 8-MedG:dA is thermodynamically more stable than corresponding duplex with dG:dG and dG:dA. This fact presents a threat to the genomic fidelity.

Both 8-MeG and 8-bromoguanine (8-BrG) are known to stabilize Z-form DNA. It was showed 8-MeG acquires syn/C3'-endo conformation [45, 46] to pair with cytidine residue which is in anti/C2'-endo conformation. In such structure the hydrophobic 8-methyl group is located in the periphery of the helix and prominently exposed to the solvent region.(Figure I-3)

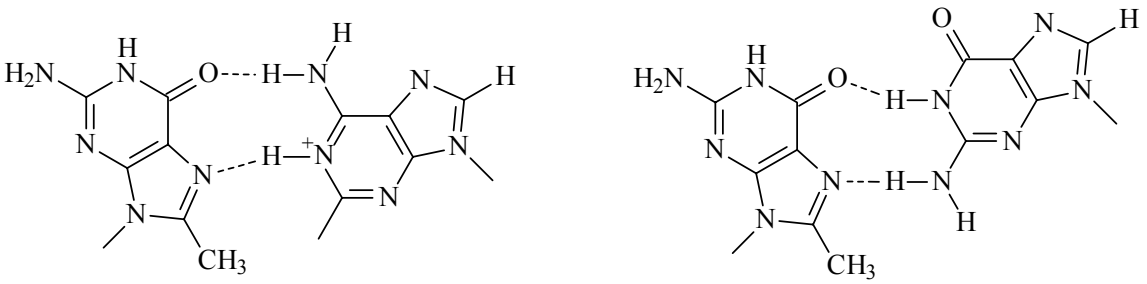

Figure I-3 Structures of 8-MedG:dG and 8-MedG:dA base pairing.

One interesting feature of 8-MeG and 8-BrG is that their E_{ox} bracket that of guanine,[47] which makes them good candidates to investigate the effect of oxidation potential and structure on the electron transfer in DNA. This research focuses on the synthesis of 8-methylguanine and incorporation of modified guanosine moiety to DNA sequences to study the electronic and steric effect on charge transport in DNA duplex.

CHAPTER II

EXPERIMENTAL SECTION

General Methods

^{1}H and ^{13}C NMR spectra were recorded on a Varian 300 MHz Spectrometer. Radioactively labeled isotope [γ-^{32}P] ATP was purchased from Amersham Bioscience. Synthetic oligonucleotides (gel filtration grade) were obtained either commercially from Midland Certified Reagent Company or were synthesized on an Applied Biosystem DNA synthesizer and were, therein, purified by reverse-phase HPLC. Terminally-linked anthraquinone oligonucleotide and oligonucleotide containing modified bases (G_m or G_{br}) were synthesized in the second way mentioned above. The mass of each oligonucleotide was determined by matrix assisted laser desorption ionization time-of-flight (MALDI-TOF) mass spectrometry. The extinction coefficients of the oligonucleotides were calculated using nearest-neighbor values, and the absorbance was measured at 260 nm. Anthraquinone-modified oligonucleotide solution concentrations were determined in same way except that an anthraquinone was replaced with adenine in the extinction coefficient determination. UV melting and cooling curves were recorded on a Cary 1E spectrophotometer equipped with a multi-cell block, temperature controller and sample transport accessory. The buffer used for all DNA experiments (Gel PAGE, CD and T_m) was 10 mM sodium phosphate at pH 7.0.

UV Thermal Denaturation

2.5 μM solutions of various oligonucleotides in 10 mM phosphate buffer, pH 7.0, were prepared. The samples were placed in cuvettes (1.5 mL capacity. 1.0 cm path length) and sealed with tape to prevent evaporation of water during heating/cooling cycles. Melting curves were obtained by monitoring the UV absorbance at 260 nm as the temperature was ramped from ~90 ºC to 20 ºC at a rate of 0.5 ºC /min. Data obtained for cooling process was found to be same as that obtained from heating. Data was exported to origin 3.78 where first derivative curves were obtained. The melting temperatures (T_m) were determined as the maxima of the first derivative plot of absorbance versus temperature.

Cleavage Analysis by Radiolabeling and PAGE

DNA oligomers were radiolabeled at 5'-end using [γ-^{32}P] ATP and T4 Polynucleotide kinase. The labeling was performed according to the standard procedures. Radiolabeled DNA was purified by 20% PAGE. The DNA band was excised from the gel, eluted overnight and ethanol-precipitated in the presence of 1 μL glycogen. The sample for irradiation were prepared by hybridizing a mixture of "cold" (unlabeled) and radiolabeled oligonucleotide (5 μL) to a total volume of 20 uL each in 10 mM sodium phosphate, pH 7.0. Hybridization was achieved by heating the sample up to 90 ºC for 5 min, followed by slow cooling to room temperature over the course of 6 hours or overnight. Samples were irradiated in microcentrifuge tubes in a Rayonet photoreactor (Southern New England Ultraviolet Company, Barnsford, CT) equipped with 8X 350 nm lamps. After irradiation,

the sample were precipitated once with cold absolute ethanol with presence of 1ul glycogen, washed twice with 80% ethanol, dried and treated with piperidine at 90 ºC for 30 min (samples with G_{br} were treated at 70 ºC for 30 min). After evaporation of piperidine, drying and suspension in denaturing loading buffer, samples (3000 cpm) were electrophoresed on a 20 % 19:1 acrylamide:bisacryamide gel containing 7 M urea. The gels were dried and the cleavage sites were visualized by autoradiography.

FPG Enzymatic Digestion

1 ml FPG enzyme and 10 µL standard buffer solution containing 50 mM TrisHCl (pH 7.5), 2 mM EDTA, 70 mM NaCl were incubated with 5 µM DNA at 37 ºC for 1 hour. FPG enzyme was killed by heating at 70 ºC for 30 minutes and followed by ethanol precipitation at -20 ºC. The samples were analyzed by 20% gel as described above.

Circular Dichroism

CD spectra were recorded on Jasco-720 instrument. 5 accumulations were collected for each sample. Solutions were prepared containing 2.5 µM DNA duplex in 10 mM sodium phosphate buffer (pH 7.0). Spectrums were recorded from 200 to 350 nm.

8-methylguanosinephosphoramidite Synthesis

The figure II-1 was followed in synthesis of 8-methylguanosinephosphoramidite.

^{2}N-isobutyryl-8-methyl-2'-deoxyguanosine (2). ^{2}N-isobutyryl deoxyguanosine (**1**) (1 g, 3.8 mmol) was added to an ice-cold solution of $FeSO_4.7H_2O$ (6.7 g, 22 mmol) in 160 mL 1N H_2SO_4 with stirring. Add 100 ml aqueous solution containing 6ml *tert*-Butyl hydroperoxide (70 %) dropwise during 10 min. Keep solution under 0 ºC stirring for 1h. Aqueous saturated KOH solution was then added to neutralize the mixture to pH 7.0. The reaction mixture was filtered and the residue was washed with MeOH. Remove H_2O from aqueous phase and wash residue with MeOH. Combine the organic phase. The crude product was applied to silica gel column chromatography and eluted with CH_2Cl_2:MeOH (9:1) to yield ^{2}N-isobutryl-8-methyl-2'-deoxyguanosine (512 mg, 49%). 1H NMR (Me_2SO-d_6) o 1.13 (d, 6H, $C(CH_3)_2$), 2.06-2.15 (m, 1H, 2'-Hb), 2.51(s, 3H, 8-CH_3), 2.75-2.86(m, 2H, 2'-Ha and $CH(CH_3)_2$), 3.52-3.60(m, 2H, 5'-CH_2), 3.78(m, 1H, 4'-H), 4,84(t, 1H 5'-OH), 5.28(d, 1H, 3'-OH), 6.26(t, 1H, 1'-H).

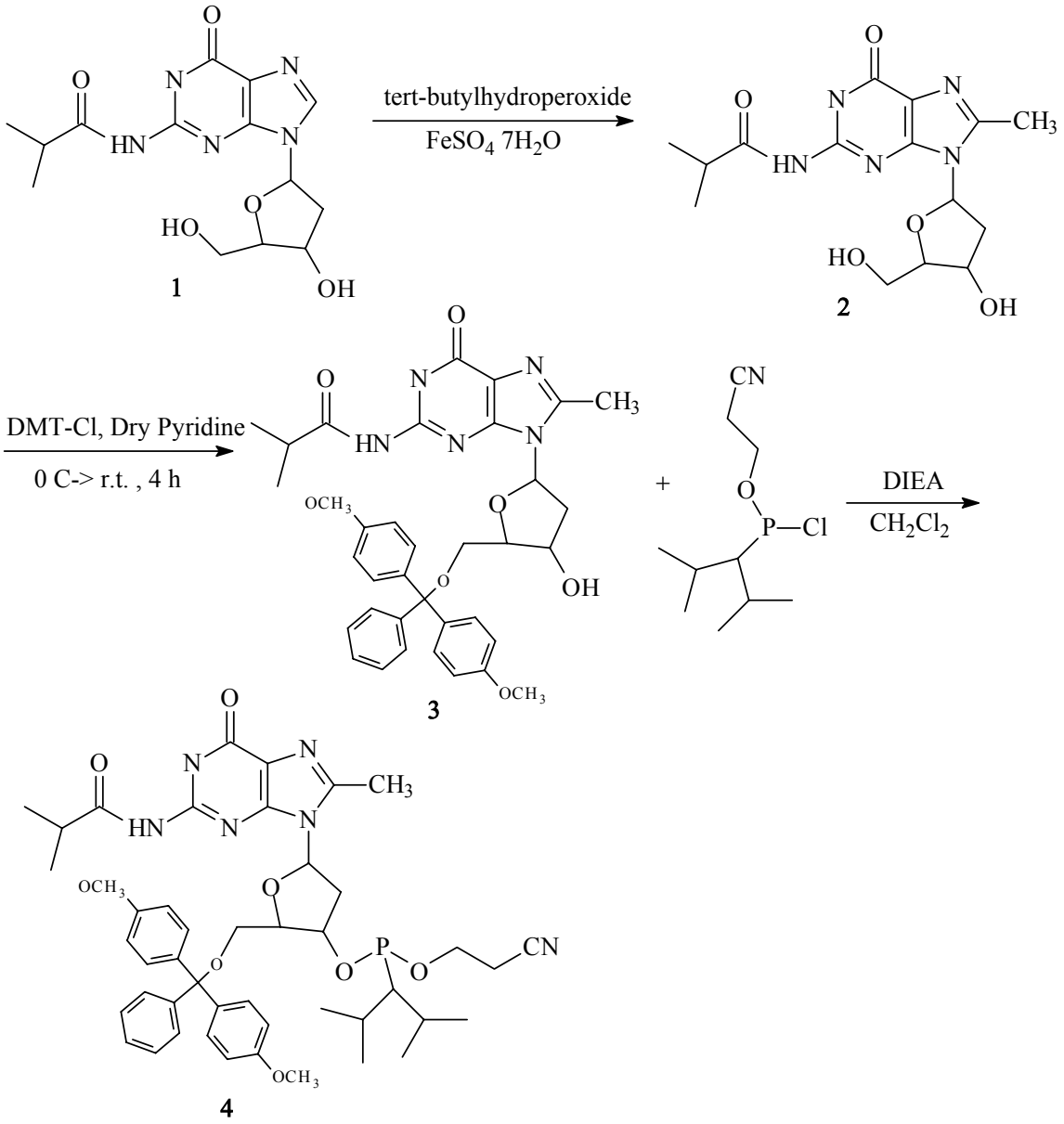

Figure II-1 Synthesis of 8-methylguanosine phosphoramidite

5'-O-(4, 4'-Dimethyloxytrityl)-^{2}N-isobutyryl-8-methyl-2'-deoxyguanosine (3). After N^2-isobutyryl-8-Methyl-2'-deoxyguanosine (2, 250 mg, 0.71 mmol) was coevaporated with dry pyridine (10 mL) twice under vacuum pump. It was suspended in 5 ml of dry pyridine when 4, 4'-Dimethyoxytrytyl chloride (95%, 304 mg, 0.85 mmol), triethylamine (138 μL, 0.99 mmol) were added to the solution and the mixture was stirred at room temperature for 2.5h. After 5 ml H_2O was added, the product was extracted with diethyl ether (3X20 mL). The combined organic extracts were dried over $MgSO_4$, filtered and concentrated at reduced pressure. The crude product was purified on silica gel column chromatography and eluted with CH_2Cl_2:MeOH (19:1) yielded **3** 381 mg (82%). 1H-NMR (Me_2SO-d_6) o 1.11 and 1.12 (each d, each 3H, $C(CH_3)_2$), 2.20 (m, 1H, 2'-H), 2.48 (s, 3H, 8-CH_3), 2,73 (m, 1H, C*H*$(CH_3)_2$), 2.99 (m, 1H, 2'-H), 3.08-3.38 (m, 2H, 5'-CH_2), 3.70 and 3.71 (each s, each 3H, O-CH_3), 3.96 (m, 1H, 4'-H), 4.45 (m, 1H, 3'-H), 5.24 (d, 1H, J = 4.9 2'-OH), 6.28 (t, 1H, J = 7.0Hz, 1'-H), 6.72-7.31 (m, 13H, phenyl of trityl), 11.3 and 12.0 (each brs, each 1H, 1-NH and 2-NH), m/z 352(M+H)+

3'-O-[(2-Cyanoethyoxy)(diisopropylamino)phosphino]-5'-O-(4,4'-dimethyoxytrityl)-^{2}N-isobutyryl-8-methyl-2'-deoxyguanosine (4). N^2- and 5'-O-diprotected 8-methyl-2'-deoxyguanosine (3, 120 mg, 0.19 mmol) was dried over P_2O_5. After compound 3 was coevaporated with dry CH_2Cl_2-Benzene, CH_2Cl_2(1 mL), diisopropylethylamine (60 μL, 0.43 mmol, 2.3 equiv mol), and 2-cyanoethyl N, N-diisopropylchlorophosphoramidite (60 μL, 0.27 mmol, 2.4 equiv mol) were added, and the mixture was stirred at room temperature for 30 min. Formation of the product was monitored by TLC (silica gel, CH_2Cl_2/MeOH = 19/1, R_f values of product(R/S) were 0.40 and 0.51 and that of **3** was

0.18). After solvent was removed by evaporation, 6 mL of dry tetrahydrofuran-benzene(1:4) was added and the mixture was stirred for 10 min. The precipitate was removed by filtration and evaporated to remove the solvent. Coevaporation of residue with dry benzene yields **4** 155 mg (98%). Without further purification, the product was dried under vacuum pump overnight and used for subsequent oligodexoynucleotide synthesis.

Anthraquinone-oligonucleotide Conjugate Synthesis

DNA sequence synthesis was performed on the solid phase synthesis following standard conditions, using cyanophsophoramidite monomer. The resin was thoroughly washed before the conjugate was ready to be coupled to the AQ monomer. The cartridge (containing resin) was removed from the synthesizer. The AQ-phosphoramidite monomer was dissolved in 500 μL of dry CH_3CN solution containing 0.1 M tetrazole. The monomer was taken into the cartridge by a syringe. Once the reason was complete, the monomer solution was removed from the cartridge by pressure injection. The cartridge was placed back onto the synthesizer and the automated sequence was allowed to resume. The coupling efficiency was quantified by measuring the UV-absorption and the trityl cation released and comparing it to that of the pervious and subsequent step.

Removal of the oligomer from the solid support and subsequent purification by reverse phase HPLC proceed as usual. Dr. Nadia Bogusiavsky in Biology department performed solid phase synthesis and HPLC purification. The dried and purified

conjugates showed a light yellow color. Analytical HPLC, UV-vis and MALDI-TOF were used to determine the purity and identity of the conjugate.

Chapter III

RESULTS

UV Melting Experiment of DNA sequences

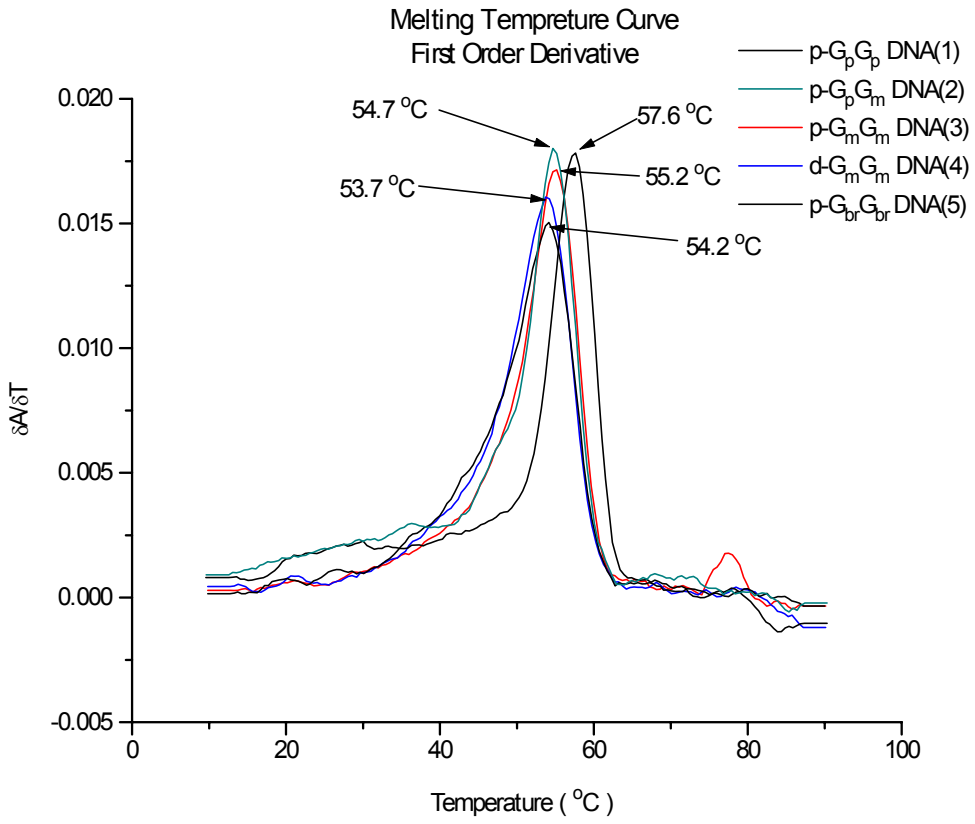

Figure III-1 Melting temperature curves of DNA duplexes (DNA 1- 5)

From melting temperature curves (Figure III-1, B-2, B-3) we can see there are few changes in melting temperatures (Table III-1) in each series, which is an indication

of the conservation of DNA secondary structure within DNA sequences containing modified guanine bases.

Table III-1 T_m data of all DNA sequences

DNA Sequence	**T_m (^oC)**
DNA(1)	57.6
DNA(2)	54.7
DNA(3)	55.2
DNA(4)	53.7
DNA(5)	54.2
DNA(6)	57.7
DNA(7)	56.1
DNA(8)	57.5
DNA(9)	55.7
DNA(10)	60.1
DNA(11)	61.2
DNA(12)	60.1

CD Spectrum of DNA Sequences

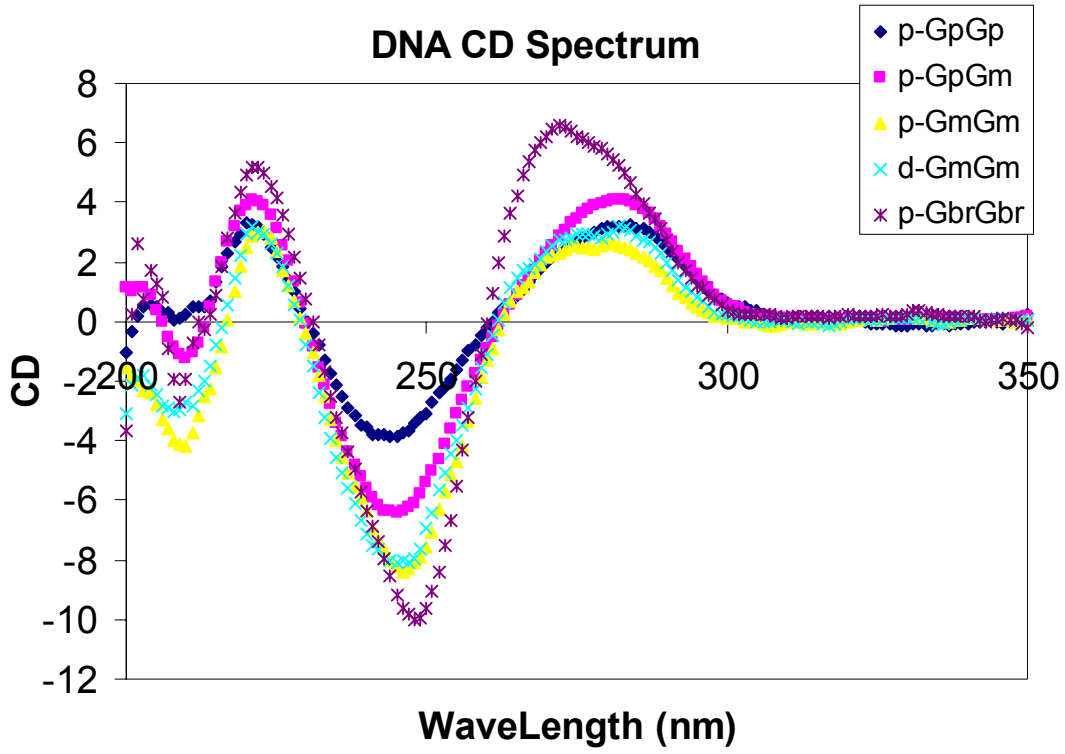

Figure III-2 CD spectrum of DNA duplexes

A slight shift in DNA containing 8-BrG at 270 nm was observed. (Figure III-2, B-4, B-5) An increase of signal at 240-250 nm region was obtained in DNA strands containing modified guanine. However all the sequences still pertain the B-form (or B-like) DNA structures.

G_mG and GG Comparison

The following duplexed DNA sequences were synthesized and studied to determine the reaction of G_m comparing to the normal G and the effect of oxidation potential on reactivity. The proximal and distal GG step damage were measured by radioactivity imaging. Two GG steps are presented in bold text to emphasize the key sequence differences and monitoring part between the duplexes.

3'-TTTAC**G_pG_p**CCATGTTTGTACC**G_dG_d**CATGC-5' **DNA(1)**

3'-TTTAC**G_pG_m**CCATGTTTGTACC**G_dG_d**CATGC-5' **DNA(2)**

Figure III-3 DNA sequences studied in G_m and G full duplex comparison

After irradiation at average temperature around 30 ºC, the duplexes were treated with hot piperidine (90 ºC) and then analyzed by PAGE and autoradiography. When irradiated for identical time, the cleavage efficiency of duplex DNA(1) at proximal GG step is much higher than that of duplex DNA(2). The distal GG step is undetectable for DNA(1). One the other hand ratio of 3'-G over 5'-G damage is significant higher in DNA(1) than in DNA(2) as shown in Figure 13. Oxidation potential of G_m was reported as a.k.a. 0.5 v lower than that of G. it's was postulated that it was lower oxidation potential causing G_m more easily oxidized and damaged.

G_mG_m and GG Doublet Comparison

In order to further evaluate the effect of G_m on charge transfer through DNA, the following two duplexes were designed, two Gs in proximal GG step in DNA(3) and two Gs in distal GG step in DNA(4) were substituted by G_m. Would two G_m further lower the oxidation potential and cause more damage on GG step?

3'-TTTAC**G_pG_p**CCATGTTTGTACC**G_dG_d**CATGC-5' **DNA(1)**

3'-TTTAC**G_mG_m**CCATGTTTGTACC**G_dG_d**CATGC-5' **DNA(3)**

3'-TTTAC**G_pG_p**CCATGTTTGTACC**G_mG_m**CATGC-5' **DNA(4)**

Figure III-4 DNA sequences studied in two G_m experiment

Duplex were irradiated for 5 min at 30 ºC. After being subjected to piperidine treatment and then analyzed by PAGE and autoradiography, there is even more noteworthy difference between those two modified G containing duplexes and normal DNA duplex. DNA(3), with two G_m in proximal step, had significantly high damage in both G_m while the damage in distal GG step was not detectable. DNA(4), with two G_m in distal step, had more damage in distal than that in normal strand. One interesting observation is that both G_m in GG step showed similar damage. In other words 5'-G selectivity in normal DNA sequence was absent.(Figure III-5)

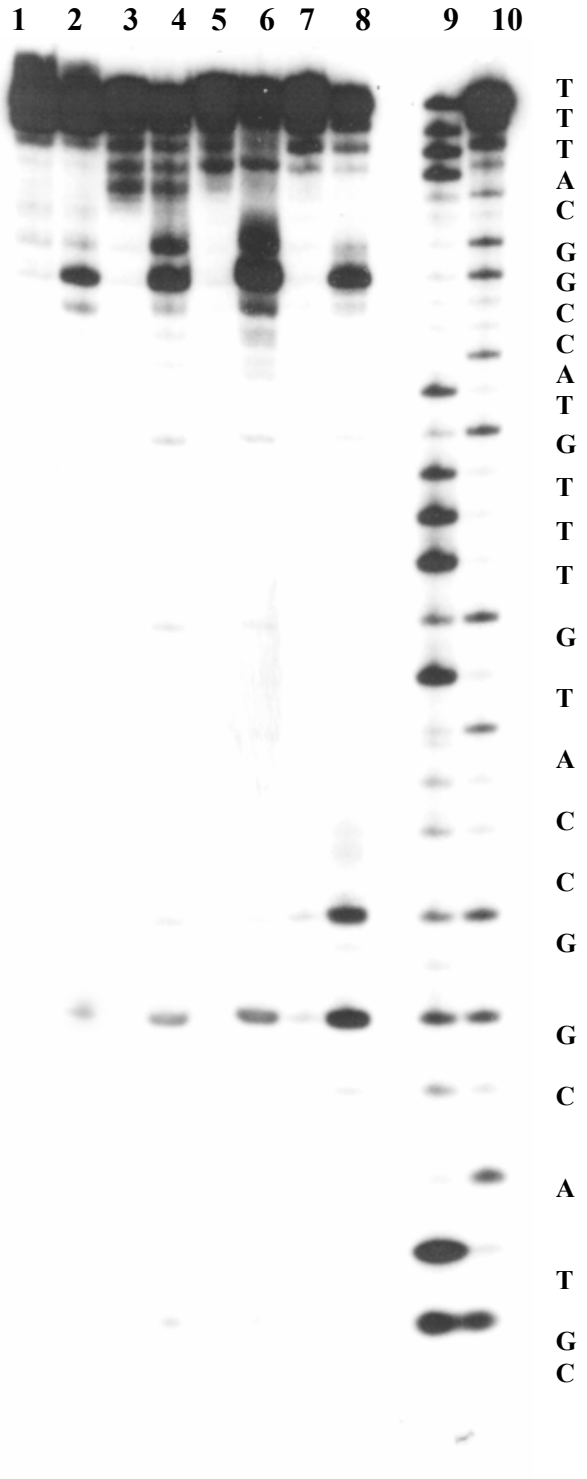

Figure III-5 Autoradiograms of a denaturing gel electrophoresis for 5'-32P-labeled DNA(1)(Lane 1, 2), DNA(2)(Lane 3, 4), DNA(3)(Lane 5, 6), DNA(4) (Lane 7, 8). The first lane in each sample is dark control (without irradiation but with hot piperidine treatment) while the second lane is irradiation sample. Lane 9, 10 are T and G Maxam-Gilbert sequencing lane for DNA(1). All samples are irradiated at 350 nm for 5 min, followed by piperidine treatment at 90 °C for 30 min.

There is no doubt that incorporated G_m in GG step cause significant more damage. Two G_m may even lower the oxidation potential at GG step and cause more damage than those in GG step containing single G_m. However, if this effect is thermodynamic or steric is still unclear. Whether oxidation potential of G_m itself is good enough to induce the more damage or it is the "well-known GG step effect" is next question to investigate.

Isolated AG_m and TG_m Full Duplex Comparison

Every duplex we have studied so far has G_m incorporated into GG step. Whether this effect stems from special configuration of GG step or from oxidation potential of guanine is still unknown. If latter is true, it would be expected that isolated G_m in duplex would cause more damage than normal isolated G too. Four more duplexes were designed to test this proposal (Figure III-6)

3'-TTTA**G_pG_p**CCATGTTTGTACC**G_dG_d**CATGC-5' **DNA(1)**

3'-TTTA**A_pG_p**CCATGTTTGTACC**G_dG_d**CATGC-5' **DNA(6)**

3'-TTTA**A_pG_m**CCATGTTTGTACC**G_dG_d**CATGC-5' **DNA(7)**

3'-TTTA**T_pG_p**CCATGTTTGTACC**G_dG_d**CATGC-5' **DNA(8)**

3'-TTTA**T_pG_m**CCATGTTTGTACC**G_dG_d**CATGC-5' **DNA(9)**

Figure III-6 DNA sequences studied in the A G_m and T G_m duplex comparison.

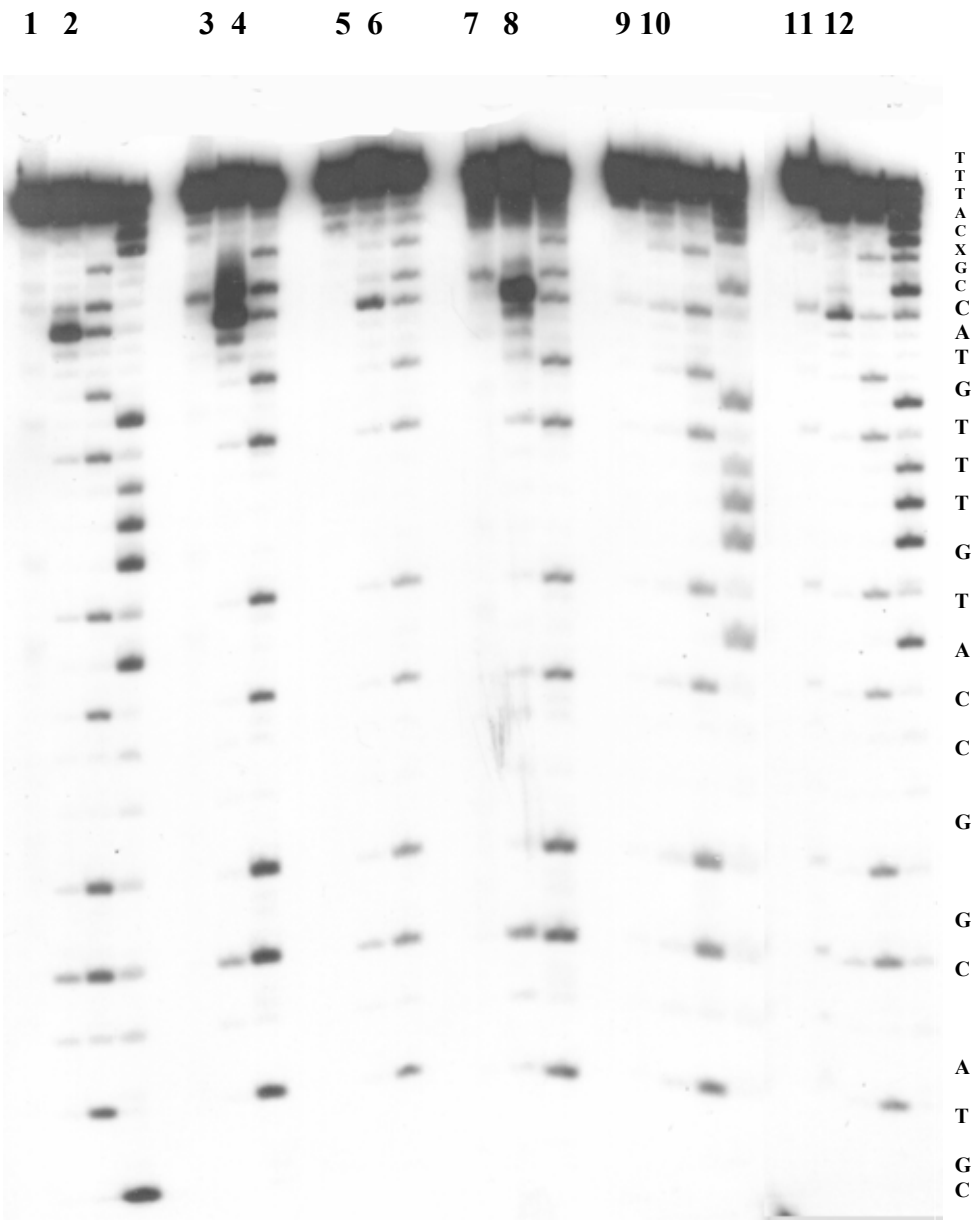

Figure III-7 Autoradiograms of a denaturing gel electrophoresis for 5'-32P-labeled DNA(1)(Lane 1, 2), DNA(2) (Lane 3, 4), DNA(6)(Lane 5, 6), DNA(7)(Lane 7, 8), DNA(8) (Lane 9, 10), DNA(9)(Lane 11, 12). The first lane in each sample is dark control (without irradiation but with hot piperidine treatment) while the second lane is irradiation sample. The others are Maxam-Gilbert T and G sequencing lanes. All samples are irradiated at 350 nm for 5 min, followed by piperidine treatment at 90 °C for 30 min.

Note that the DNA(7) has A_mG at the same position as GG step in DNA(1) and DNA(9) has TG_m at same position as proximal GG step in DNA(1). Other than these there is no difference in other base sequences. These four new duplexes were irradiated for longer time, i.e. 15 min, than for DNA(1) but under the same condition used previously. The cleavage efficiency of G_m containing strands was proved to be higher than those of duplexes containing normal G.(Figure III-7)

G_{br} and G Full Duplex Comparison

In order to investigate more thermodynamic effect of base on charge transfer on DNA, G_{br} (8-BrG), with higher oxidation potential ($\Delta E^0 = 0.06$ v) than normal G, was linked into to proximal GG step in DNA. If the damage at GG step is controlled by thermodynamic effect, it should be expected that damage at $G_{br}G_{br}$ step will be smaller than normal GG and G_mG_m. Note the proximal and distal GG steps were shown in bold text.

3'-TTTAC **G_p G_p** CCATGTTTGTACC**$G_d$$G_d$**CATGC-5' **DNA(1)**

3'-TTTAC **$G_{br}$$G_{br}$**CCATGTTTGTACC**$G_d$$G_d$**CATGC-5' **DNA(5)**

Figure III-8 DNA sequences studied in G_{br} duplex comparison

Following the irradiation, the G_{br} containing duplex was treated with piperidine and then analyzed by PAGE and autoradiography. The efficiency of proximal $G_{br}G_{br}$ step

in G_{br} containing duplex was much reduced compared to normal GG step. Note that in this experiment, the G_{br} duplex was subjected to piperidine treatment at 70 ºC., instead of 90 ºC due to significant damage to G_{br} by hot piperidine at 90 ^{o}C. A further experiment showed that treatment at 70 ºC could reflect the similar damage as treatment at 90 ºC caused by irradiation but would not lead to overwhelming damage to non-irradiated G_{br}. (Figure III-10)

DNA with Triple G Step Comparison

Several earlier researches showed that triple G (GGG) step is a much deeper trap (E^0= 0.64v much lower than calculated E^0 of GG) than GG for radical cation migrating through the DNA duplex.[13, 31, 37] What is the effect of G_m compared to GGG is an interesting question since the difference in E^0 between G_m and G is smaller than that between GGG and G. Therefore we synthesized the DNA sequences containing a GG, GGG and GG_mG sequence between the other two GG steps. (Figure III-9)

3'-TCACT$\mathbf{G_pG_p}$CTT	$\mathbf{G_pG_p}$	TTC$\mathbf{G_dG_d}$TGCAT-5'	**DNA(10)**
3'-TCACT$\mathbf{G_pG_p}$CTT	**GGG**	TTC$\mathbf{G_dG_d}$TGCAT-5'	**DNA(11)**
3'-TCACT$\mathbf{G_pG_p}$CTT	$\mathbf{GG_mG}$	TTC$\mathbf{G_dG_d}$TGCAT-5'	**DNA(12)**

Figure III-9 DNA sequences studied in triple G duplex comparison

Following the 15 min irradiation, the duplexes were treated with piperidine and then analyzed by PAGE and autoradiography. The efficiency of proximal GG step in triple G containing duplex was much reduced compared to normal GG step. DNA(10) has

three GG steps. It is used as a comparison with DNA(11) and DNA(12). DNA(11) showed little difference from DNA(10) except that there was more damage in the middle G in G triplet. On the other hand, damage at both proximal and distal GG step was significantly reduced in DNA(12) and an increase of damage at 5'-G of the G triplet was observed. (Figure III-10)

Radioactivity Counts Results

All the sequences of DNA studied are listed in Table III-2. The corresponding phosphorimagery count results are shown in Table III-3.

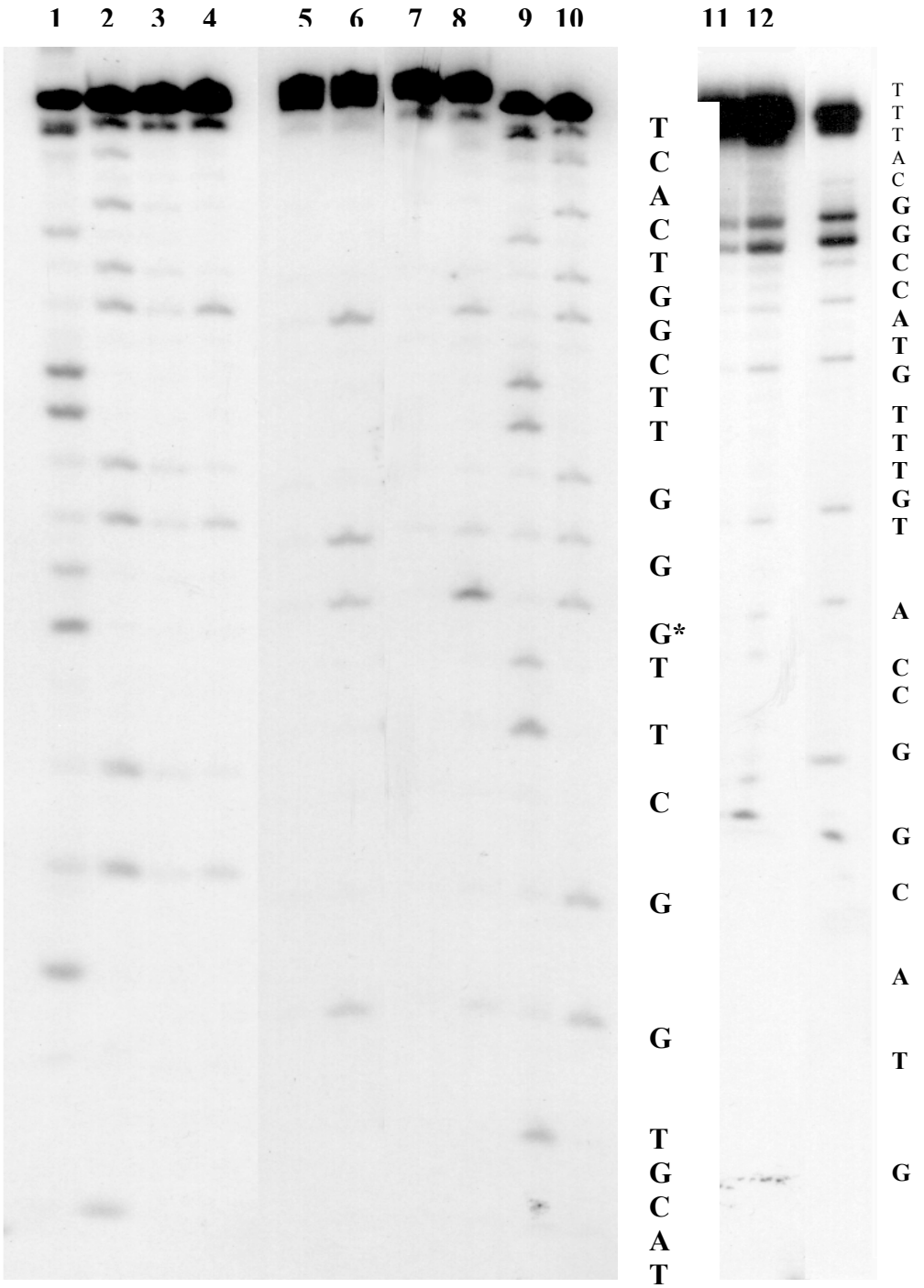

Figure III-10 Autoradiograms of a denaturing gel electrophoresis for 5'-32P-labeled DNA(10)(Lane 3, 4), DNA(11)(Lane 5, 6), DNA(12)(Lane 7, 8), DNA(5) (Lane 11,12). The first lane in each sample is dark control (without irradiation but with hot piperidine treatment) while the second lane is irradiation sample. The others are Maxam-Gilbert T and G sequencing lanes. All samples are irradiated at 350nm for 15 min, followed by piperidine treatment at 90 °C (DNA(10)-(12)) or 70 °C (DNA(5) for 30 min.

Table III-2 The sequences of DNA in experiment

AQ-DNA(I)	5′-AQ-	A	A	A	T	G	C	C	G	G	T	A	C	A	A	A	C	A	T	G	G	C	C	G	T	A	C	G	-3′
DNA(1)	3′-	T	T	T	A	C	G_P	G_P	C	C	A	T	G	T	T	T	G	T	A	C	C	G	G	C	A	T	G	C	-5′
DNA(2)	3′-	T	T	T	A	C	G	G_m	C	C	A	T	G	T	T	T	G	T	A	C	C	G	G	C	A	T	G	C	-5′
DNA(3)	3′-	T	T	T	A	C	G_m	G_m	C	C	A	T	G	T	T	T	G	T	A	C	C	G	G	C	A	T	G	C	-5′
DNA(4)	3′-	T	T	T	A	C	G	G	C	C	A	T	G	T	T	T	G	T	A	C	C	G_m	G_m	C	A	T	G	C	-5′
DNA(5)	3′-	T	T	T	A	C	G_B	G_B	C	C	A	T	G	T	T	T	G	T	A	C	C	G	G	C	A	T	G	C	-5′
AQ-DNA(I)	5′-AQ-	A	A	A	T	G	Z	C	G	G	T	A	C	A	A	A	C	A	T	G	G	C	C	G	T	A	C	G	-3′
DNA(6/8)	3′-	T	T	T	A	C	X	G	C	C	A	T	G	T	T	T	G	T	A	C	C	G	G	C	A	T	G	C	-5′
DNA(7/9)	3′-	T	T	T	A	C	Y	G	C	C	A	T	G	T	T	T	G	T	A	C	C	G	G	C	A	T	G	C	-5′
AQ-DNA(IV)	5′-AQ-	A	G	T	G	A	C	C	G	A	A	C	C	A	A	G	C	C	A	C	G	T	A						-3′
DNA(10)	3′-	T	C	A	C	T	G_p	G_p	C	T	T	G	G	T	T	C	G	G	T	G	C	A	T						-5′
AQ-DNA(V)	5′-AQ-	A	G	T	G	A	C	C	G	A	A	C	C	C	A	A	G	C	C	A	C	G	T	A					-3′
DNA(11)	3′-	T	C	A	C	T	G	G	C	T	T	G	G	G	T	T	C	G	G	T	G	C	A	T					-5′
DNA(12)	3′-	T	C	A	C	T	G	G	C	T	T	G	G_m	G	T	T	C	G	G	T	G	C	A	T					-5′

Table III-3 Efficiency of strand cleavage in DNA oligomers measured by PAGE and phosphorimagery

.

DNA	3'-Gp	5'-Gp	5'-Gp /3'-Gp	3'-Gd	5'-Gd	3'-G_c	m-G_c	5'-G_c	Gp/Gd [b]
DNA(1)	6,500	57,00	9	1,400	3,500				10
DNA(2)	30,000	94,000	7.4	5,00	1,200				70
DNA(3)	101,000	180,000	1.8	<100	770				>100
DNA(4)	23,000	172,000	7.4	74,000	124,000				1.4
DNA(5)	9,600	14,500	1.5	1,200	4,600				4.2
DNA(6)	NA	10,300		900	2,000				5
DNA(7)	NA	61,000		520	5,100				11
DNA(8)	NA	1,200		1,000	700				1
DNA(9)	NA	7,000		80	150				37
DNA(10)	1,100	13,800	13	500	6,400	500	NA	7,000	2.2
DNA(11)	860	14,200	16	2,000	10,700	950	12,400	9,000	1.3
DAN(12)	1,300	6.800	5.2			500	2,400	20,500	3.0

a. The data are the number of counts measured at the indicated base by phosphorimagery For instance, 3'-G_p refers to the 3'-G in the proximal GG step of DNA oligomers 1-12. The number of counts is proportional to the amount of damage of strand cleavage at the nucleotide.

b. The ratio of the number of counts at two sites, as indicated, which is a measure of the relative yield of radical cation reactions at those locations, subsequently resulting in the strand damages.

CHAPTER IV

DISCUSSIONS

In normal DNA duplexes, long distance charge transfer was visualized up to about 22 base pairs from the AQ as alkali labile damage at G_{22}, although the intensity of damage is reduced at the distal GG step. Several theoretical calculations have reported the IP of G is highly dependent on the flanking sequences and stacked Gs, such as G in doublet (GG) and triplet (GGG) possessing much lower IPs than that of single G (Table I-2).[13, 31, 30, 41] In principle, it should be possible to trap the radical cation by introduction of a residue with an oxidation potential known to be lower than that of the natural DNA bases. On the order hand, a residue with higher oxidation potential than that of the natural base should lead to less trapping of radical cations, i.e. less damage at that residue. Those residues should cause little distortion to the DNA structure in order to preserve the original overall π-stack, which is critical for charger transfer study and comparison with original DNA duplex. 8-MeG and 8-BrG, shown in Figure IV-1, are two promising candidates.

The proposed chemical decomposition of guanine radical cation has been described in Figure I-2. A reasonable postulation induced from this mechanism is that 8-methyl guanine, which has a methyl group blocking C8 position of guanine, will eliminate the pathway through the intermediate radical species to yield 8-oxoguanosine. It's well known that 8-oxoguanosine is not susceptible to hot piperidine treatment and gives cleavage at this position. However, it can undergo other routes to produce

piperidine liable products. This can enhance the damage shown under piperidine treatment. In addition 8-methyl guanosine has lower oxidation potential than normal guanosine. It is supposed to be more easily oxidized thermodynamically.

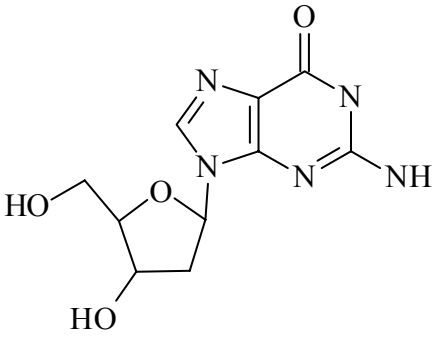

2'-deoxyguanosine

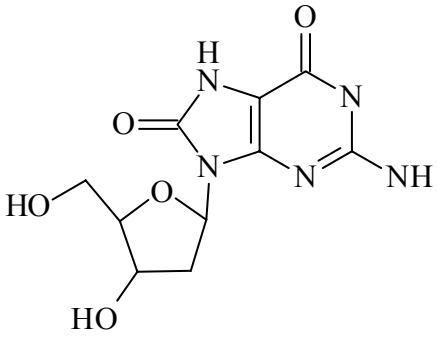

8-oxo-7,8-dihydro-2'-deoxyguanosin

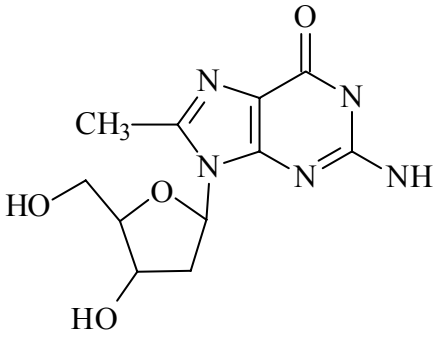

8-methyl-2'-deoxyguanosine

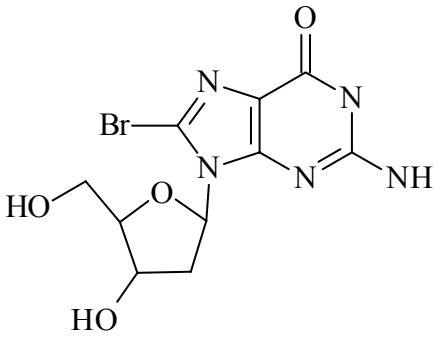

8-bromo-2'-deoxyguanosine

Figure IV-1 Guanosine and 8-MeG, 8-BrG and 8-oxoG derivatives.

Several studies[49, 50] on 8-oxoG (Figure IV-1) containing duplex supported the formation of hydrogen bonds between 8-oxoG and C. Similarly it is quite reasonable to predict that 8-MeG and 8-BrG can form hydrogen bonds with C (Part I Figure I-2). Both the CD (Figure III-1) and the melting temperature data (Figure III-2) indicate that there is little difference between normal DNA duplex and DNA duplexes containing 8-

methylguanosine and 8-bromoguanosine. It suggests that 8-MeG and 8-BrG are able to from Watson-Crick base pair with C and preserve the overall duplex structure with minor structural change localized around modified guanosine.

One electron oxidation of DNA has been studies extensively. The primary damage site in DNA duplex is G_n(n = 2, 3) which has been attribute to lower oxidation potential of G in G_n based on theoretical calculation.[30,31,37,38,48] Most calculations indicate that IP of G in a G_n(n = 2, 3) sequence is much lower than that of isolated G (Table IV-1)

Table IV-1 The IP differences between isolated G and that of G_n

	G in GG	**G in GGG**
ΔIP (V)	-0.5	-0.7

Recently, Ratner and coworkers incorporated these estimates into analysis of charge hopping in DNA.[51] The experimental finding is not totally in agreement with the calculation.

Here we examine the effect of E_{ox} and structure on the transport and reactions of radical cation in duplex DNA. In our experiments radical cation introduced at 5'-terminus of AQ-DNA(I) migrate through the proximal GG step in normal duplex and cause the damage at the distal GG step. After introducing one 8-MeG at 5'-position of proximal GG Step it significantly reduced the damage at distal GG step and more strikingly cause more damage at 3'-G in proximal GG step. One more step further, we found more

efficient charge transfer in DNA duplex with two 8-MeGs in proximal GG step. No detectable strand cleavage can be observed at distal GG step and no significant difference between two 3'- and 5'-MeG. Apparently, two factors, electronic or steric, have to be considered for the difference between normal GG and G_m containing strands. From thermodynamic perspective, 8-MeG has lower oxidation potential than normal G while 8-BrG has higher oxidation potential. Comparing the experimental data between DNA(3), two G_m in proximal GG step, and DNA(5), two G_{br} in proximal GG step, we saw tremendous impact of oxidation potential on the oxidation damage at the modified GG site and charge transport to the distal GG step.

Table IV-2 Oxidation Potential of 8-substituted Guanosine Derivatives

	$\mathbf{G_m}$	**G**	$\mathbf{G_{br}}$
$E_{p/2}$(V vs. AgCl)	1.16	1.28	1.34

G_n has been proposed to be a deep trap of charge transfer both experimentally [32,52] and theoretically.[13,30,31,37,48] Ratner and coworkers contributed the difference between GG and GGG to relaxation which is around 30 times faster in GGG than that in GG. Saito and coworkers claim the base stacking effect and stability of neutral radical play an important role in controlling the oxidative damage. In our experiment, there is significant difference in the efficiency of proximal GG strand cleavage. The normal DNA (1) gives the cleavage at both the proximal and distal GG steps. We have more distal damage when we have two G_m in distal GG step while keeping proximal GG with normal G. On the

other hand, there is little perturbation of damage at proximal GG observed for sequence containing GGG step. This demonstrates that GGG is not a very deep trap as many calculations indicated, which is also supported by other studies on different synthetic DNA system.[52]

In DNA(5) 3'- and 5'-G_{br} has similar efficiency which indicates the change in structure also influences the relative reactivity of two GG in GG step. Results from the others G_m containing strands also yielded the similar observation.

Overall, G_m, even with relative modest lower E_{ox} difference compared to normal G, is clearly a deeper trap for radical cation migration in DNA than G triplet and introduction of either modified guanine (G_m or G_{br}) reduced the selectivity of 5'-G over 3'-G, which is commonly observed in normal GG step. Electronic properties of the substituted guanines affect transport of the radical cation and steric effects influence the relative amounts of reaction at the 3'- and 5'-guanines. Most calculations only consider the effect of geometry (many from crystal structure) and base stacking. Studies have shown that radical cation introduction on DNA structure, solvent (H_2O in aqueous solution) organization and distribution and association of counter ion around DNA significantly attributes to DNA structure and charge transport in DNA.[53-55] We have to take into account flexible DNA secondary structure and environment at transition state structure to give more accurate estimation on IP of guanine radical in DNA charge transport process.

One surprising phenomena observed in this studies is that incorporation of either modified nucleobases cause the loss of selectivity of 5'-G in GG step. Prat et al. proposed that stacking orientation of the 3'-G on 5'-G lower the oxidation potential of 5'-guanine.

If this proposal holds, we should obtain different geometry in 5'-GG_m-3' and 5'-GG_{br}-3' stacking with similar *ab initio* calculation. We can further include counter ions and H_2O into calculation model to explore the effect of solvent environment on the charge transfer in DNA.

APPENDIX A

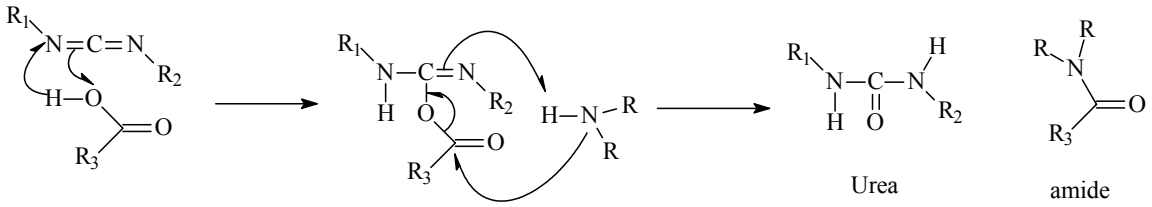

Figure A-1 The mechanism for DCC coupling reaction

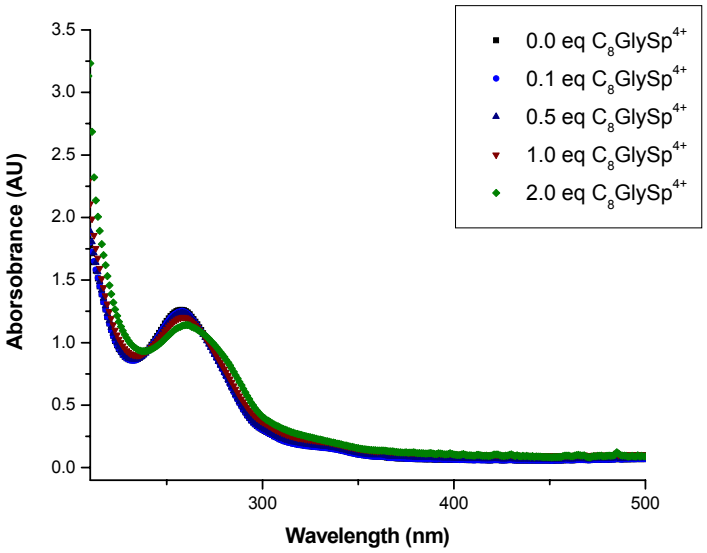

Figure A-2 UV spectra of DNA(I)-EB-C_8GlySp^{4+}. The sample contains 2.5 μM DNA(I) duplex, 5 μM Ethidium Bromide in 10 mM sodium phosphate at pH 7.0. C_8GlySp^{4+} was titrated into DNA solution in small aliquot and incubated for 15 min before the measurement.

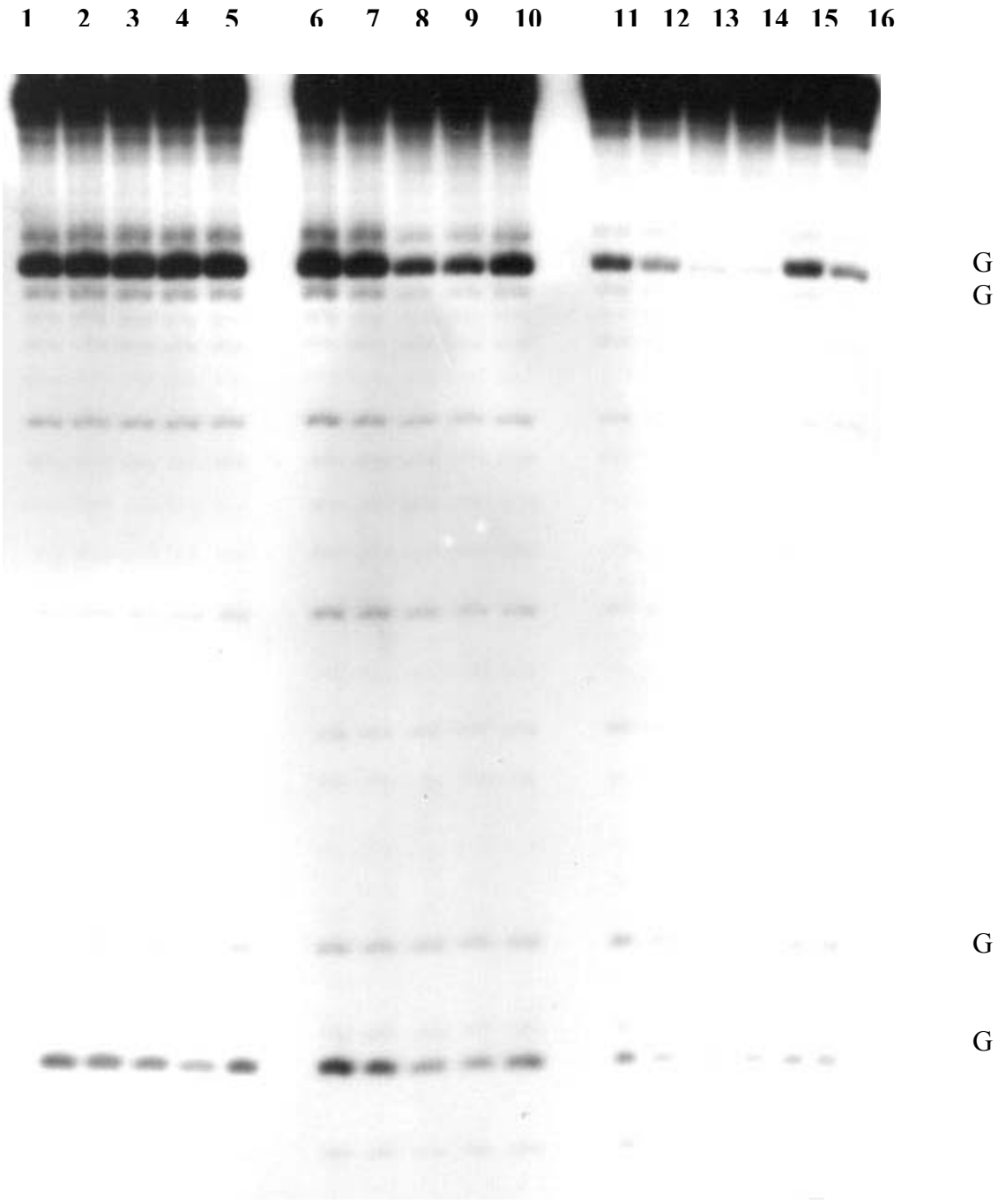

Figure A-3 Autoradiograms of a denaturing gel electrophoresis for DNA(I) with C_2GlySp^{4+}, C_8GlySp^{4+}, $C_{18}GlySp^{4+}$ lipid. Lanes 1-4, 6-9, 11-14 correspond to the samples incubated with 0.5, 1.0, 1.5, 2.0 equivalent C_2GlySp^{4+}, C_8GlySp^{4+}, $C_{18}GlySp^{4+}$ lipid (charge ratio), respectively. Lane 5, 10, 15 correspond to the samples hybridized with 1 equivalent C_2GlySp^{4+}, C_8GlySp^{4+}, C_8GlySp^{4+} lipid respectively. All samples was incubated for 30 min before the 2.5 min irradiation using 8x350nm Rayonet lamps and cleaved by treatment with 1M hot piperidine at 90 ^{o}C. All samples contain 2.5 uM DNA in 10 mM NaPi buffer.

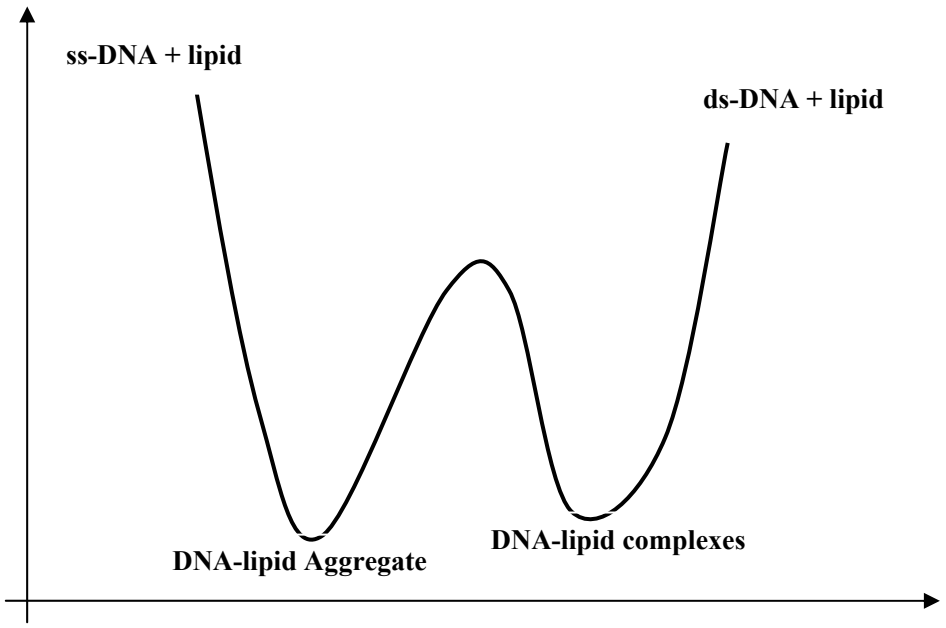

Figure A-4 Scheme for the formation energy of DNA-lipid complexes via two different routes.

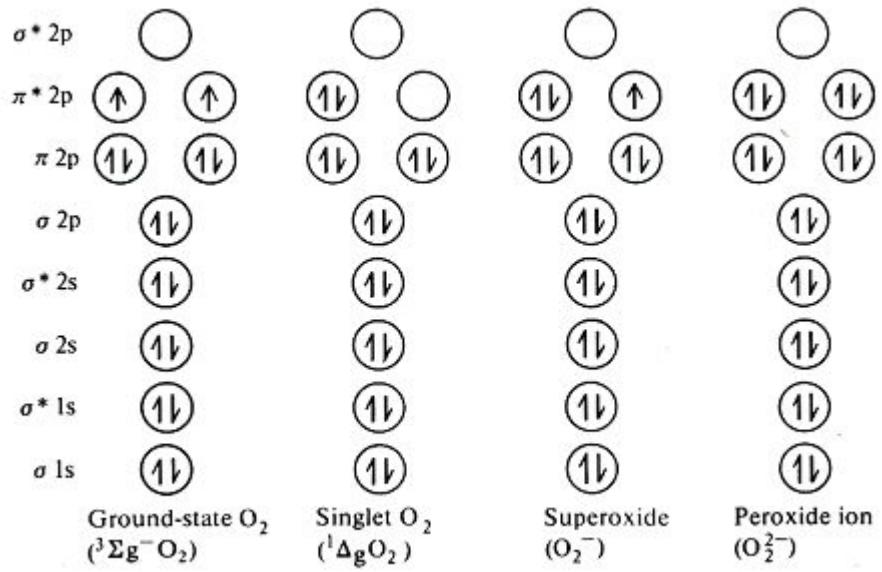

Figure A-5 Electron configuration of active oxygen species.

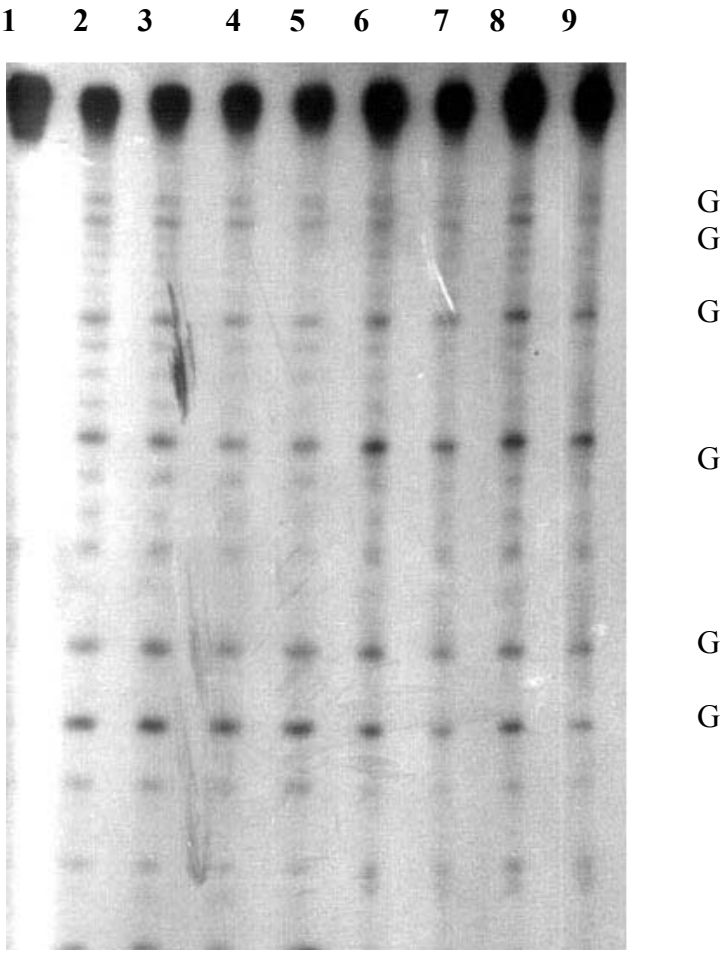

Figure A-6 Autoradiogram of a denaturing gel electrophoresis for DNA(I) damaged by singlet oxygen from Rose Bengal at the presence of spermine. Lanes 1 is sample w/o irradiation. Lane 2 is the sample w/o lipid. Lanes 3-8 correspond to the samples incubated with 0.1, 0.2, 0.5, 1.0, 1.3, 1.7, 2.0 equivalent spermine before 15 min irradiation using Oriel lamp and cleaved by treatment with FPG enzyme. All samples contain 2.5 μM DNA in 10 mM sodium phosphate buffer.

G
G

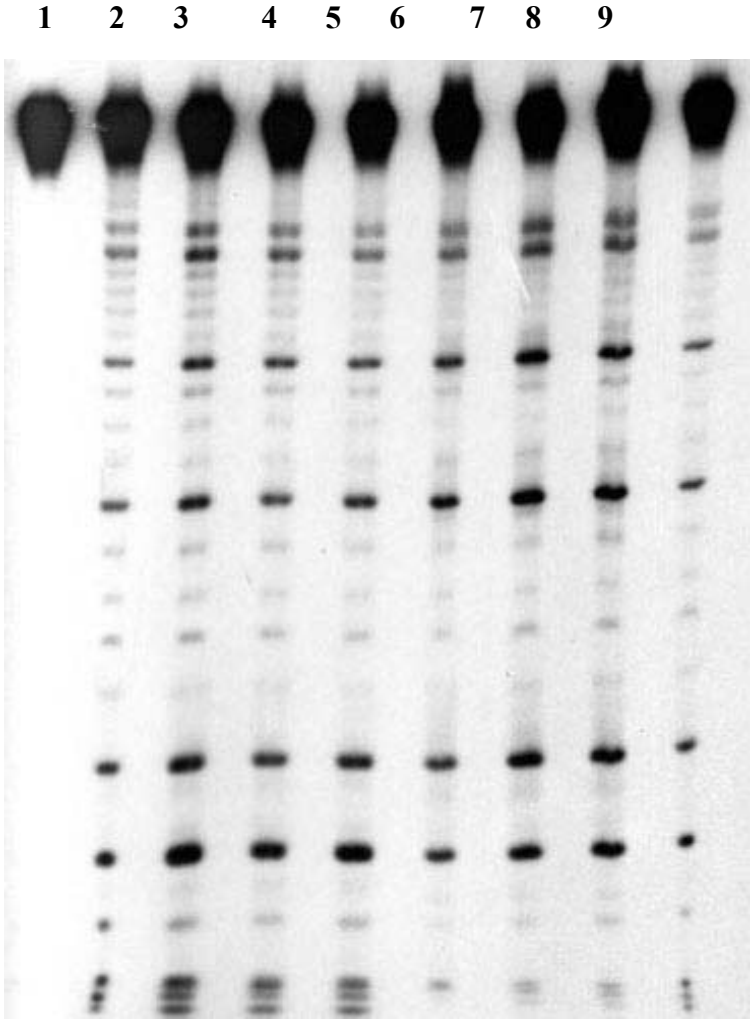

Figure A-7 Autoradiogram of a denaturing gel electrophoresis for DNA(I) damaged by singlet oxygen from Rose Bengal at the presence of C_2GlySp^{4+}. Lanes 1 is sample w/o irradiation. Lane 2 is the sample w/o lipid. Lanes 3-8 correspond to the samples incubated with 0.1, 0.2, 0.5, 1.0, 1.3, 1.7, 2.0 equivalent C_2GlySp^{4+} before 15 min irradiation using Oriel lamp and cleaved by treatment with FPG enzyme. All samples contain 2.5 μM DNA in 10 mM sodium phosphate buffer.

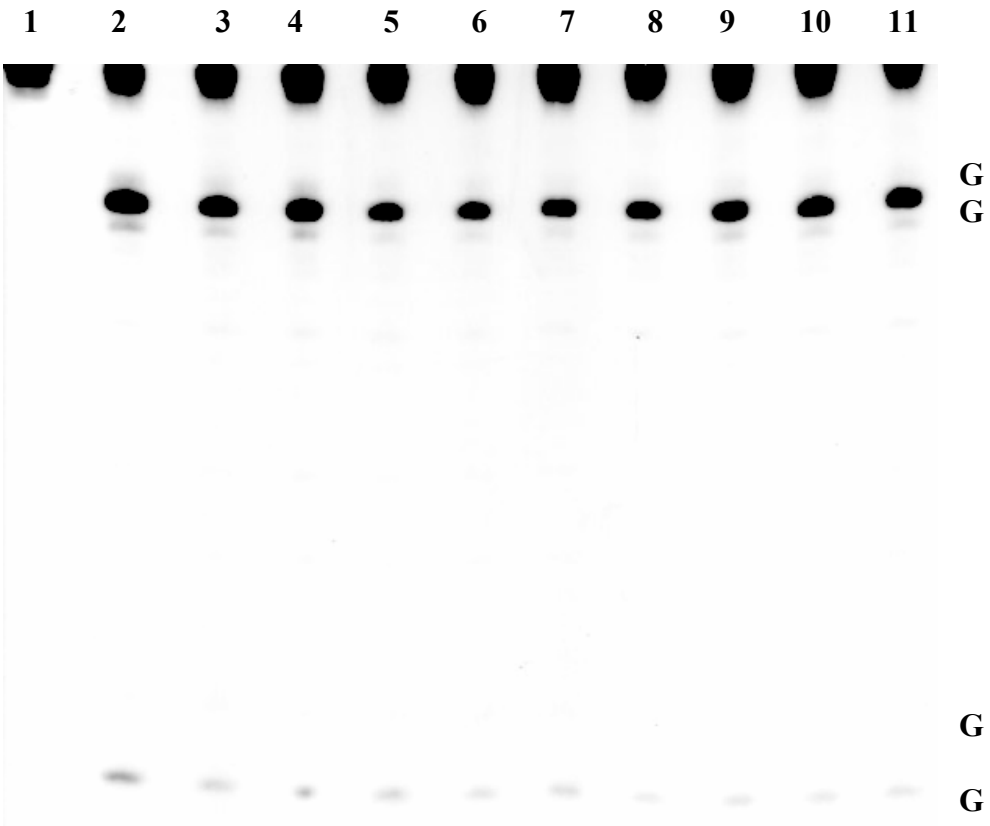

Figure A-8 Autoradiogram of a denaturing gel electrophoresis for DNA(I) at various concentration of spermine. Lanes 1 is sample w/o irradiation. Lane 2 is the sample w/o lipid. Lanes 3-11 correspond to the samples incubated with 0.1, 0.2, 0.35, 0.5, 0.75, 1.0, 1.3, 1.7, 2.0 equivalent spermine for 30 min before the irradiation for 2.5 min using 8x350nm Rayonet lamps and cleaved by treatment with 1M hot piperidine at 90 ^{o}C. All samples contain 5 uM DNA in 10 mM sodium phosphate buffer.

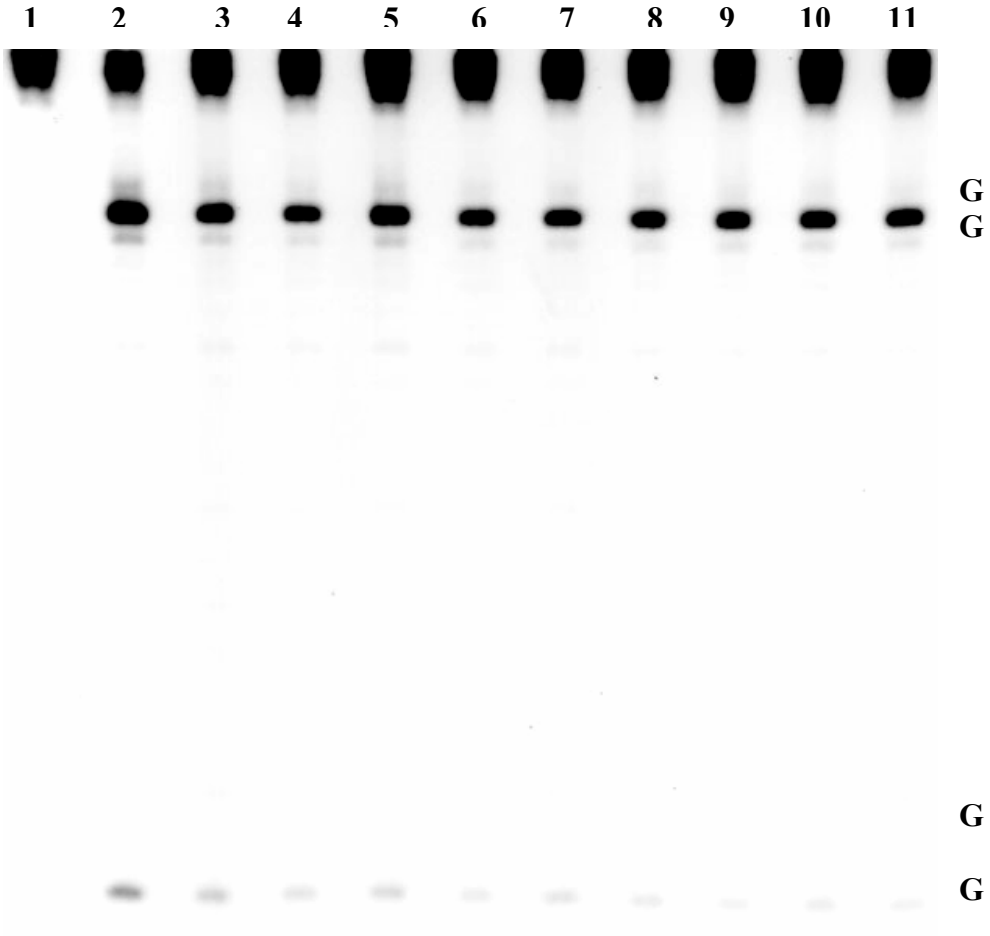

Figure A-9 Autoradiogram of a denaturing gel electrophoresis for DNA(I) at various concentration of C_2GlySp^{4+} lipid. Lanes 1 is sample w/o irradiation. Lane 2 is the sample w/o lipid. Lanes 3-11 correspond to the samples incubated with 0.1, 0.2, 0.35, 0.5, 0.75, 1.0, 1.3, 1.7, 2.0 equivalent C_2GlySp^{4+} lipid (charge ratio) for 30 min before the irradiation for 2.5 min using 8x350nm Rayonet lamps and cleaved by treatment with 1M hot piperidine at 90 ^{o}C. All samples contain 5 uM DNA in 10 mM sodium phosphate buffer.

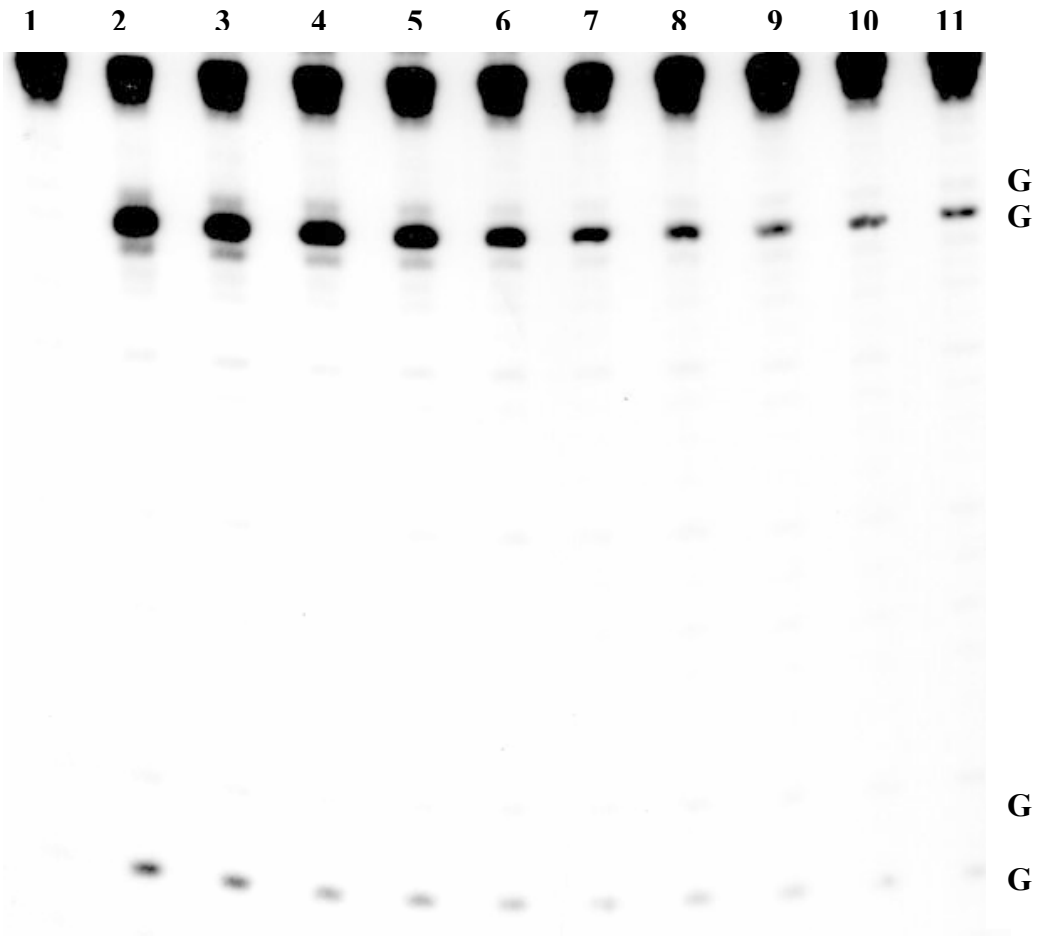

Figure A-10 Autoradiogram of a denaturing gel electrophoresis for DNA(I) at various concentration of C_2GlySp^{4+} lipid. Lanes 1 is sample w/o irradiation. Lane 2 is the sample w/o lipid. Lanes 3-11 correspond to the samples incubated with 0.1, 0.2, 0.35, 0.5, 0.75, 1.0, 1.3, 1.7, 2.0 equivalent C_8GlySp^{4+} lipid (charge ratio) for 30 min before the 2.5 min irradiation using 8x350nm Rayonet lamps and cleaved by treatment with 1M hot piperidine at 90 ^{o}C. All samples contain 5 uM DNA in 10 mM sodium phosphate buffer.

Table A-1 Normalized proximal 5'-G_p DNA(I) damage at the presence of spermine, C_2GlySp^{4+} and C_8GlySp^{4+} lipid

Charge Ratio	Spermine	C_2GlySp^{4+}	C_8GlySp^{4+}
0.0	1.00	1.00	1.00
0.1	0.80	0.74	0.76
0.2	0.63	0.64	0.67
0.35	0.54	0.61	0.65
0.50	0.48	0.56	0.30
0.75	0.59	0.49	0.34
1.0	0.53	0.49	0.17
1.3	0.50	0.48	0.15
1.7	0.55	0.48	0.12
2.0	0.48	0.46	0.10

Table A-2 Oxidation damage ratio of 5'-G_p/5'G_d in DNA(I) at the presence of spermine, C_2GlySp^{4+} and C_8GlySp^{4+}.

Charge Ratio	Spermine	C_2GlySp^{4+}	C_8GlySp^{4+}
0.0	10.5	10.7	11.0
0.1	10.8	10..3	12.0
0.2	11.0	9.7	11.6
0.35	11.5	10.3	10.8
0.5	11.6	9.3	10.9
0.75	11.5	9.6	9.7
1.0	12.3	9.0	8.1
1.3	12.3	9.1	6.8
1.7	12.1	10.4	6.1
2.0	12.6	9.8	5.1

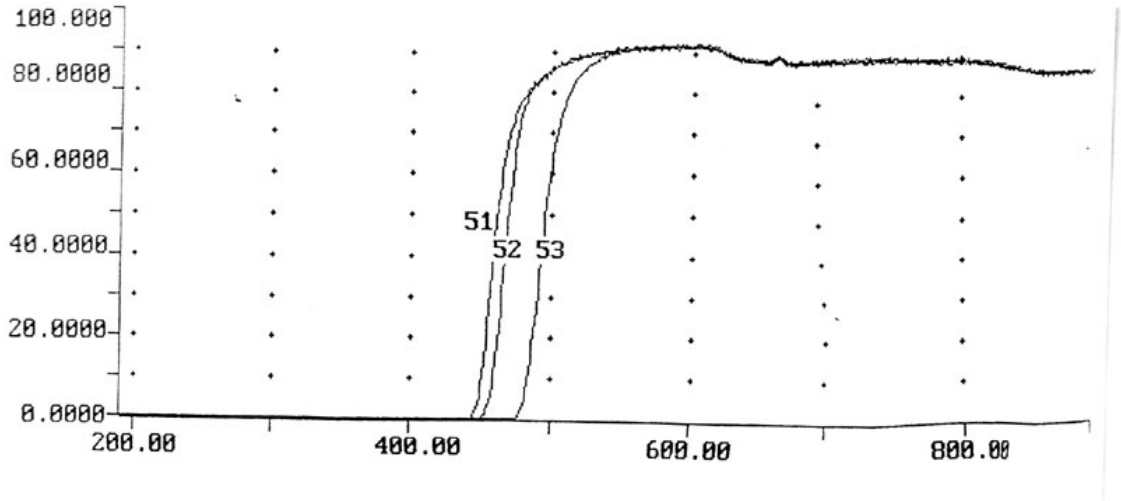

Figure A-11 UV transmittance profile of the filter 51 used for Rose Bengal experiment

APPENDIX B

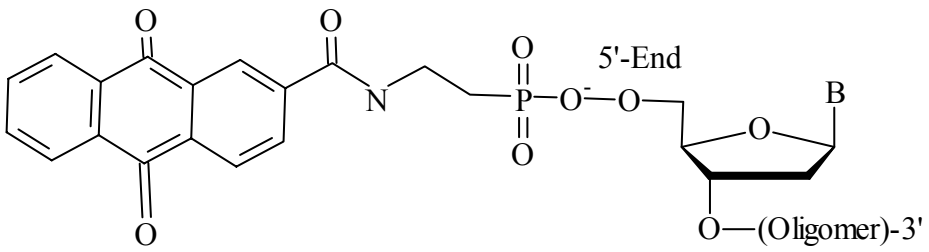

Figure B-1 Anthraquinone 5'-linked DNA

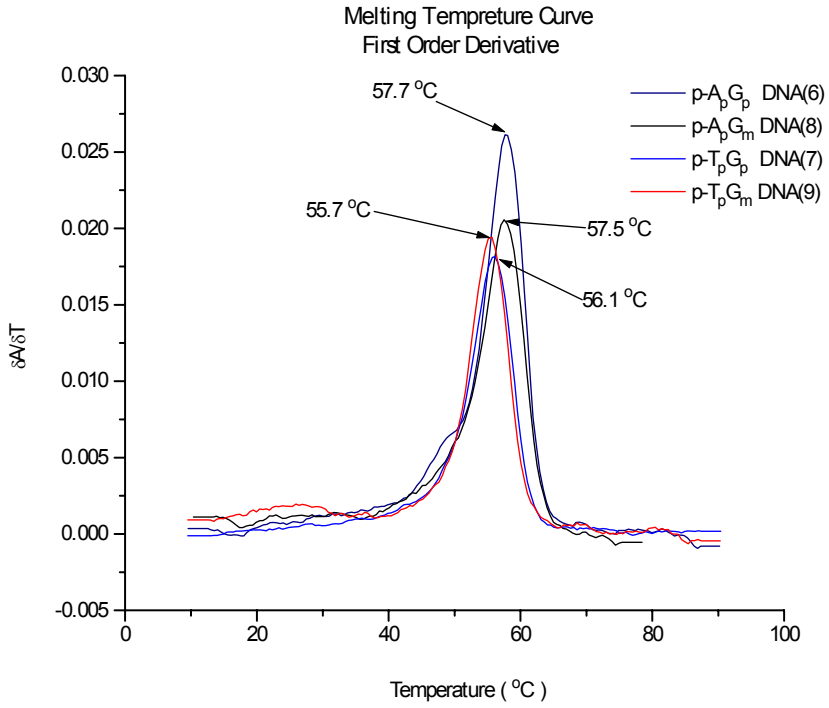

Figure B-2 T_m Experiment of DNA Sequences 6-9.

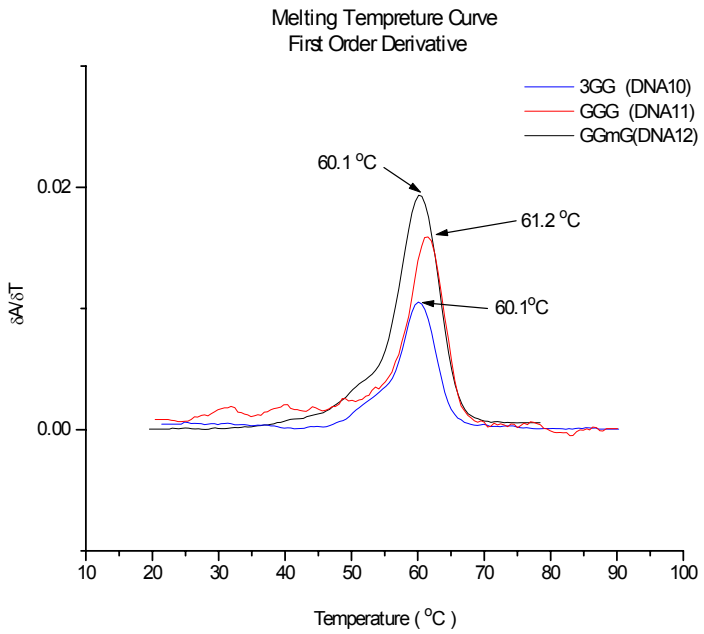

Figure B-3 T_m experiment of DNA sequences 10-12.

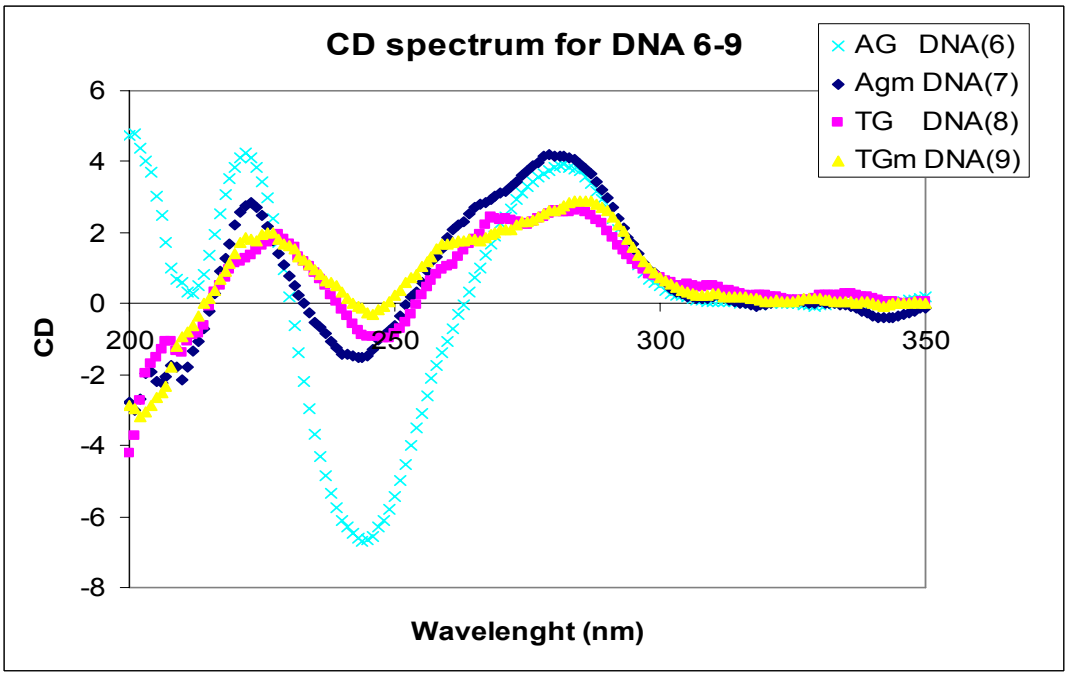

Figure B-4 CD spectra of DNA sequence 6-9

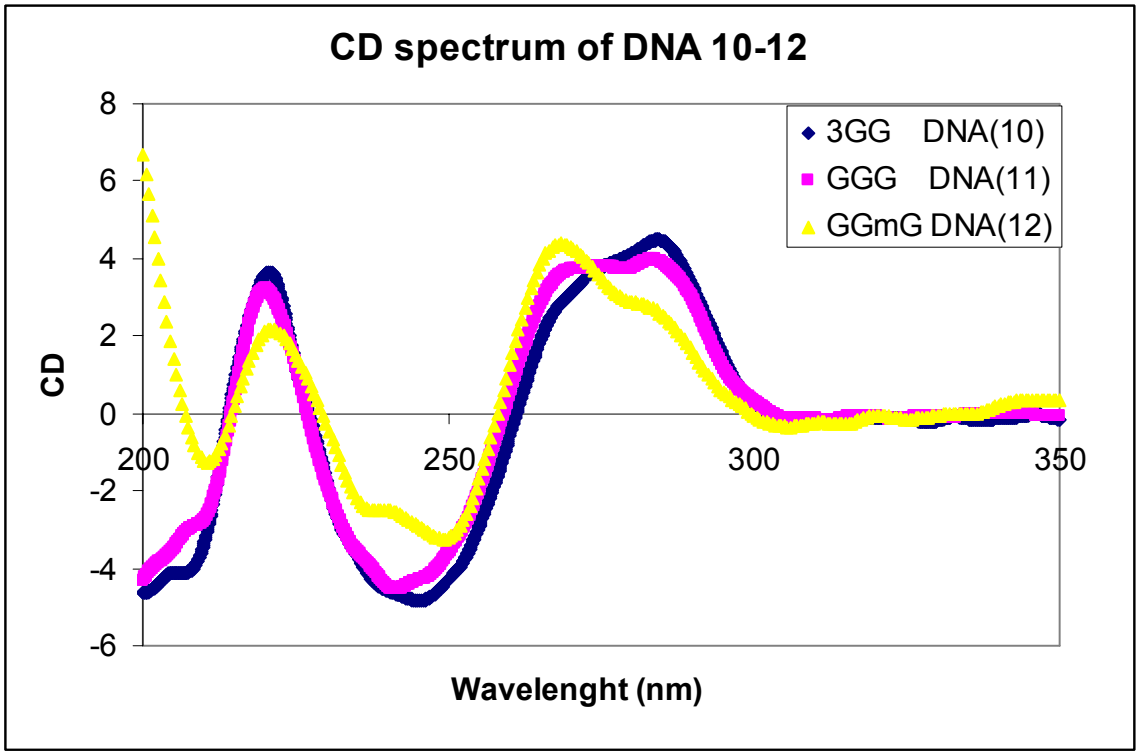

Figure B-5 CD spectra of DNA sequence 10-12

REFERENCES

1. Schuster, G. B.; Editor *Top. Curr. Chem.* 236, 237

2. S. O. Kelly, R. E. Holmlin, E. D. A. Stemp, J. K. Barton, *J. Am. Chem. Soc.* 1997, 119, 9861-9870

3. J. Jortner, M. Bixon, T. Langenbacher, M. E. Michel-Beyerle, *Proc. Natl. Acad. Sci. USA* 1998, 95, 12 759-12 765

4. B. Giese, *Acc. Chem. Res.* 2000, 33, 631-636.

5. G. B. Schuster, *Acc. Chem. Res.* 2000, 33, 253-260.

6. Grozema F. C; Berlin Y. A., Siebbeles L.D.A.; *J. Amer. Chem. Soc.* 2000, 122 , 10903-10909.

7. Sartor V., Boone E; Schuster GB, *J. Phys. Chem. B.* 2001, 105, 11057-11059

8. Giese, B.; Biland A.; *Chem. Commun.* 2002, 667-672

9. Ly, D.; Kan, Y.; Armiage, B.; Schuster, G. B. *J. Am. Chem. Soc.* 1996, 118, 8747-8748.

10. Berslin, D. T.; Schuster, G. B. *J. Am. Chem. Soc.* 1996, 118, 2311-2319.

11. Ito, K.; Inoue, S.; Yamamoto, K.; Kawanishi, S. *J. Biol. Chem.* 1993, 268, 13221-13227.

12. Kasai, H.; Yamaizumi, Z.; Berger, M.; Cadet, J. *J. Am. Chem. Soc.* 1992, 114, 9692-9694.

13. Saito, I.; Takayama, M.; Sugiyama, H.; Nakatani, K.; Tsuchida, A.; Yamamoto, M. *J. Am. Chem. Soc.* 1995, 117, 6406-6407.

14. Devasagayam, T. P. A.; Steenken, S.; Obendorf, M. S. W.; Schulz, W. A.; Sies, H. *Biochemistry* 1991, 30, 6283-6289

15. MacGregor, R. B. J. Anal. *Biochemistry* 1992, 204-324.

16. Boon, P. J.; Cullis, P. M.; Symons, M. C. R.; Wren, B. W. *J. Chem. Soc. Perkin Trans,* 2 1984, 1393-1399

17. Maxam, A. M.; Gilbert, W. Methods in Enzymology, V. *Nucleic Acids Pt. I*; Academic Press: New York, 1980.

18. Henderson P. T., Jones D., Hampikian G., Kan Y. Z., Schuster G. B.; *Proc Natl. Acad. Sci.* 1999, 96, 8353-8358

19. Gaspar, S. M.; Schuster, G. B. *J. Am. Chem. Soc*. 1997, 119, 12762-

20. Sanii, L.; Schuster, G. B *J. Am. Chem. Soc.* 2000, 122, 11545-11546

21. Armitage, B.; Yu, C.; Devadoss, C.; Schuster, G. B. *J. Am. Chem. Soc.* 1994, 116, 9847

22. Jovanovich, S. V.; Smimic, M. G. *J. of Phy. Chem.* 1986, 90, 974-979.

23. Steenken, S.; Jovanovich, S. V.*; J. Am. Chem. Soc.* 1997, 119, 617-618.

24. Steeken, S. *Chem. Rev.* 1989, 89, 503-530.

25. Steeken, S. *Free Rad. Res. Comms*. 1992, 16, 349-379

26. Hix S.; Augusto O.; *Chem-Biol. Interact.* Apr. 1 1999, 118 (2): 141-149

27. Cadet, J.; Berger, M.; Buchko, G. W.; Joshi, P. C.; Raoul, S.; Ravanat, J.; L. *J. Am. Chem. Soc.* 1994, 116, 7403-7404.

28. Cadet, J.; Berger, M.; Decarroz, C.; Mouret, J.-F.; van Lier, J. E.; Wagner, J. R.; *J. Chim. Phys.* 1991, 88, 1021-1022

29. Budowsky, E. I.; Kovalsky, O. I.; Yakovlev, D. Y.; Simukova, N. A.; Rubin, L. B. *FEBS Lett.* 1985, 188, 155-158.

30. Sugiyama, H.; Saito, I. *J. Am. Chem. Soc.* 1996, 118, 7063-7068.

31. Saito, I.; Nakamura, T.; Nakatani, k.; Yoshioka, Y.; Yamaguchi, K.; Sugiyama, H.; *J. Am. Chem. Soc.* 1998, 120, 12686-12687.

32. Meggers, E.; Michea-Beyerle, M. E.; Giese, B. *J. Am. Chem. Soc.* 1998, 120, 12905-12915

33. Spassky, A.; Angelov, D.; *Biochemistry* 1997, 36, 6571

34. Ito, K.; Kwanishi, S.; *Biochemistry* 1997, 36, 1774

35. Hall. D. B.; Holmin, R. E.; Barton, J. K.; *Nature* 1996, 382, 731

36. Arkin, M. R.; Stemp, E. D. E.; Pulver, S. C.; Barton, J. K., *Chem. Biol.* 1997, 4, 389

37. Yoshioka, Y.; Kitagawa, Y.; Takano, Y.; Yamaguchi, K.; Nakamura, T.; Saito, I. *J. Am. Chem. Soc.* 1999, 121, 8712-8719.

38. Prat, F.; Houk, K. N.; Fotte, C. S. *J. Amer. Chem. Soc.* 1998, 120, 845-846.

39. Sistare, M. F.; Codden S. J.; Heimlich, G.; Thorp, H. H. J. *Am. Chem. Soc.* 2000, 122, 4742-4749

40. Yang, I. V.; Thorp, H. H. *Inorg. Chem.* 2001, 40, 1690-1697.

41. Hix S., Morais M. D., Augusto O. *Free Radical Biol. Med.* 1995, 19, 293-301

42. Hix S.; Kadiiska M. B.; Mason R. P.; Augusto O. *Chem. Res. Toxicol.* OCT 2000, 13, 1056-1064

43. Netto, L. E. S.; Ramakrishna N. V. S.; Kolar C.; Cavalieri, E. L. Valieri, E. L; Rorgan, E. G.; Lawson, T. A.; Augusto, O. *J. Biol. Chem.* 1992, 267, 21524-21527

44. Kohda K.; Tsunomoto H.; Minoura Y.; Tanabe K.; Shibutani S.; *Chem. Res. Toxicol.*, 1996, 9, 1278-1284

45. Sugiyama H, Kawai K, Matsunaga A, Fujimoto K, Saito I, Robinson H, Wang A. H. J., *Nucleic Acids Res*. 1996, 24, 1272-1278

46. Van Lier, J. J. C.; Smits, M. T.; Buck, H. M.; *Eur. J. Biochem.* 1983, 55-62

47. Sheu, C.; Foote, C. S.; *J. Org. Chem.* 1995, 60, 4498-4503

48. Nakatani, K.; Dohno C.; Saito I.; *J. Am. Chem. Soc.* 2000, 122, 5893-5894

49. Oda, Y.; Uesugi, S.; Ikehara, M.; Nishimura, S.; Kawase, Y.; Ishikawa, H.; Inoue, H.; Ohtsuka, E. *Nucleic Acids Res.* 1991, 19, 1407-1412.

50. Lipscomb, L. A.; Peek, M. E.; Morningstar, M. L.; Verghis, S. M.; Miller, E. M.; Rich, A.; Essigmann, J. M.; Williams, L. D. Proc *Natl. Acad. Sci. U.S.A.* 1995, 92, 719-723

51. Berlin, Y. A.; Burin, A. L.; Ratner, M. A; *J. Am. Chem. Soc.* 2001, 123, 260-268.

52. Giese, G; Wessely, S.; Spormann, M.; Lindemann, U.; Meggers, E.; Michel-Beyerle, M. E. *Angew. Chem. Int. Ed.* 1999, 38, 996-998.

53. Lewis F. D.; Letsinger R. L.; Wasielewski M.R.; *Acc. Chem. Res.* 2001, 34, 159-170

54. Basko, D. M.; Conwell, E. M., *Phys. Rev. Lett.* 2002, 88 (9),

55. Barnett R. N.; Cleveland C. L.; Joy A.; Landman, U.; Schuster G. B., *Science* 294, 567-571.

56. Jackson N. M.; Hill M. G.; *Curr. Opin. in Chem. Biol.* 2001, 5, 209-215